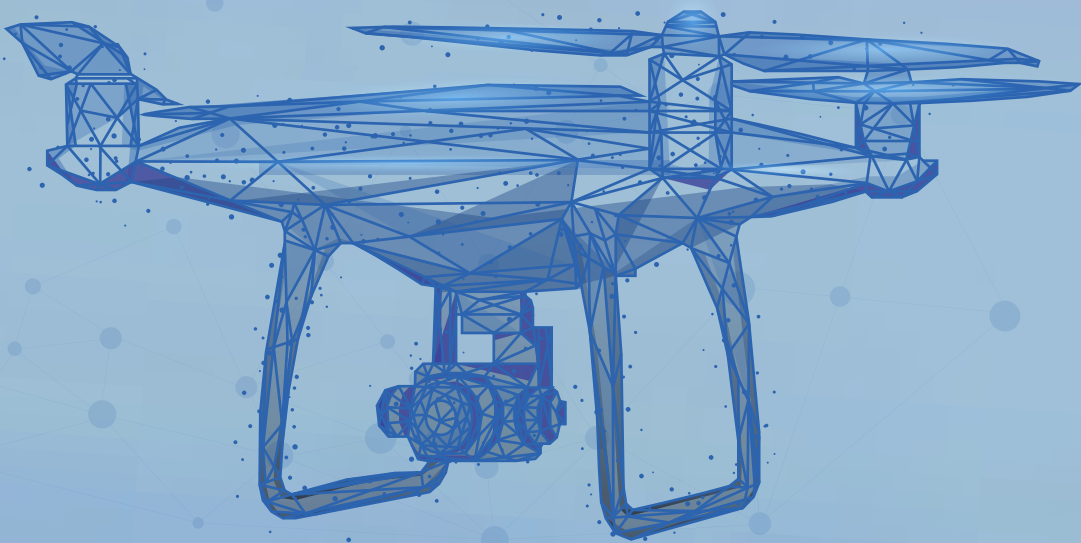




International  
**Journal of Aviation**  
Science and Technology

**Volume 5, Issue 2, December 2024**



e-ISSN: 2687-525X



[www.sares.org](http://www.sares.org)



# International Journal of Aviation Science and Technology



## Owner

International Sustainable Aviation and Energy Society (SARES)

## Privilege Owner

T. Hikmet Karakoç

Eskisehir Technical University, Turkiye

[hkarakoc@eskisehir.edu.tr](mailto:hkarakoc@eskisehir.edu.tr)

## Honorary Editor in Chief

Max F. Platzer

University of California, USA

[maximilian.platzer@gmail.com](mailto:maximilian.platzer@gmail.com)

## Editor in Chief

T. Hikmet Karakoç

Eskisehir Technical University, Turkiye

[hkarakoc@eskisehir.edu.tr](mailto:hkarakoc@eskisehir.edu.tr)

## Co-Editor

Alper Dalkıran

Suleyman Demirel University, Turkiye

[alperdalkiran@sdu.edu.tr](mailto:alperdalkiran@sdu.edu.tr)

## Section – Editors

Pouria Ahmedi

University of Illinois, USA [pouryaahmadi81@gmail.com](mailto:pouryaahmadi81@gmail.com)

Patti J. Clark

Embry-Riddle Ae. University, USA [clark092@erau.edu](mailto:clark092@erau.edu)

Raj Das

RMIT University, Australia [raj.das@rmit.edu.au](mailto:raj.das@rmit.edu.au)

Chingiz Hajiyev

Istanbul Technical University, Turkiye [cingiz@itu.edu.tr](mailto:cingiz@itu.edu.tr)

Soledad Le Clainche

Universidad Politécnicade Mad., Spain [soledad.leclainche@upm.es](mailto:soledad.leclainche@upm.es)

Ionna Pagoni

University of Aegean, Greece [ipagoni@aegean.gr](mailto:ipagoni@aegean.gr)

Publisher : SARES  
International Sustainable Aviation and Energy Research Society  
Licence holder : Prof. Dr. T. Hikmet Karakoç (President, SARES)  
Address : Research and Application Center of Civil Aviation, Research Centers  
Building, Technical University, Eskisehir, Turkiye

e-ISSN : 2687-525X  
DOI : [10.23890/IJAST](https://doi.org/10.23890/IJAST)  
web : [www.ijast.org](http://www.ijast.org)  
submission : [DergiPark-IJAST](http://DergiPark-IJAST)  
e-mail : [ijast@saes.org](mailto:ijast@saes.org)  
Copyright : SARES Society

IJAST is published with the contribution of “Research and Application Center of Civil Aviation, Eskisehir Technical University”



## Language Editor

**Martin Zorrilla**

Purdue University, US, [martin.zorrilla@mail.concordia.ca](mailto:martin.zorrilla@mail.concordia.ca)

## Editorial Board

**Ramesh K. Agarwal**

Washington University, USA [rka@wustl.edu](mailto:rka@wustl.edu)

**Pouria Ahmedi**

University of Illinois, USA [pouryaahmadi81@gmail.com](mailto:pouryaahmadi81@gmail.com)

**Hikmat Asadov**

National Aerospace Agency, Azerbaijan [asadzade@rambler.ru](mailto:asadzade@rambler.ru)

**Ruxandra Mihaela Botéz**

Université du Québec, Canada [ruxandra.botez@etsmtl.ca](mailto:ruxandra.botez@etsmtl.ca)

**Elbrus Caferov**

Istanbul Technical University, Türkiye [cafer@itu.edu.tr](mailto:cafer@itu.edu.tr)

**Patti J. Clark**

Embry-Riddle Ae. University, USA [clark092@erau.edu](mailto:clark092@erau.edu)

**Raj Das**

RMIT University, Australia [raj.das@rmit.edu.au](mailto:raj.das@rmit.edu.au)

**Rao Korrai Deerga**

Vasavi College of Engineering, India [korraidrao@yahoo.com](mailto:korraidrao@yahoo.com)

**Umut Durak**

German Aerospace Center, Germany [umut.durak@dlr.de](mailto:umut.durak@dlr.de)

**Marina Efthymiou**

Dublin City University, Ireland [marina.efthymiou@dcu.ie](mailto:marina.efthymiou@dcu.ie)

**Vincenzo Fasone**

Università Kore di Enna, Italy [vincenzo.fasone@unikore.it](mailto:vincenzo.fasone@unikore.it)

**Akhil Garg**

Huazhong University of Sci. and Tech. [garg.mechanical@gmail.com](mailto:garg.mechanical@gmail.com)

**Chingiz Hajiyev**

Istanbul Technical University, Türkiye [cingiz@itu.edu.tr](mailto:cingiz@itu.edu.tr)

**Jae-Hung Han**

Korea Advanced Institute of Sci. Tech., Korea [jaehunghan@kaist.edu](mailto:jaehunghan@kaist.edu)

**Gopalan Jagadeesh**

Indian Institute of Science, India [jagadeeshgopalan@gmail.com](mailto:jagadeeshgopalan@gmail.com)

**Kyriakos I. Kourousis**

University of Limerick, Ireland [kyriakos.kourousis@ul.ie](mailto:kyriakos.kourousis@ul.ie)

**Soledad Le Clainche**

Universidad Politécnica de Mad., Spain [soledad.leclainche@upm.es](mailto:soledad.leclainche@upm.es)

**Luiz A Horta Nogueira**

Federal University of Itajubá, Brasil [lahortanog@gmail.com](mailto:lahortanog@gmail.com)

**Ionna Pagoni**

University of Aegean, Greece [ipagoni@aegean.gr](mailto:ipagoni@aegean.gr)

**Marco Raiola**

University Carlos III de Madrid, Spain [mraiola@ing.uc3m.es](mailto:mraiola@ing.uc3m.es)

**Mohammad Mehdi Rashidi**

Tongji University, China [mm\\_rashidi@yahoo.com](mailto:mm_rashidi@yahoo.com)

**Ethirajan Rathakrishnan**

Indian Institute of Technology, India [erath@iitk.ac.in](mailto:erath@iitk.ac.in)

**Daniel Rohacs**

University of Tech. & Econ., Hungary [drohacs@vrht.bme.hu](mailto:drohacs@vrht.bme.hu)

**Yevgeny Somov**

Samara State Technical University, Russia [e\\_somov@mail.ru](mailto:e_somov@mail.ru)

**Jelena Svorcan**

University of Belgrade, Serbia [jsvorcan@mas.bg.ac.rs](mailto:jsvorcan@mas.bg.ac.rs)

**Kateryna Synylo**

National Aviation University, Ukraine [synyka@googlemail.com](mailto:synyka@googlemail.com)

**David Sziroczak**

University of Tech. & Econ., Hungary [dsziroczak@gmail.com](mailto:dsziroczak@gmail.com)

**John Kian Tan**

Northumbria University, England [k.tan@northumbria.ac.uk](mailto:k.tan@northumbria.ac.uk)

**Nadir Yilmaz**

Howard University, USA [nadir.yilmaz@howard.edu](mailto:nadir.yilmaz@howard.edu)

**Oleksander Zaporozhets**

National Aviation University, Ukraine [zap@nau.edu.ua](mailto:zap@nau.edu.ua)

## Editorial Office

**Mustafa Azer**

Eskişehir Technical University, Türkiye [mustafaazerr@gmail.com](mailto:mustafaazerr@gmail.com)

**Benginur Kaplan**

Eskişehir Technical University, Türkiye [benginurkaplan@gmail.com](mailto:benginurkaplan@gmail.com)

**Elif Karakılıç**

Eskişehir Technical University, Türkiye [ekarakilic26@gmail.com](mailto:ekarakilic26@gmail.com)

**Özge Küçükkör**

Eskişehir Technical University, Türkiye [ozgekucukkor123@gmail.com](mailto:ozgekucukkor123@gmail.com)

**Murathan Pekacar**

Eskişehir Technical University, Türkiye [murathanpekacar@gmail.com](mailto:murathanpekacar@gmail.com)

## Index

	<b>Title</b>	<b>Start Page</b>	<b>Finish Page</b>
1	Utilizing Mel-Frequency Cepstral Coefficients for Acoustic Diagnostics of Damaged UAV Propellers <a href="#">Bahadir Cinoglu, Umut Durak, T. Hikmet Karakoc</a>	79	89
2	An Empirical Analysis on The Use of Sustainable Fuels in The Aviation Industry <a href="#">Yaşar Köse, Emre Oğuzhan Polat</a>	90	100
3	Aerodynamic Investigation of Fixed Pitch Aircraft Propeller <a href="#">Erdoğan Kaygan, Dogukan Dogan, Ozan Mahir Alpagut</a>	101	110
4	Analyzing the New Global Reporting Format from the Pilot Perspective <a href="#">Arif Tuncal, Ufuk Erol</a>	111	121
5	Wildlife Hazard Management – An Intuitive Web-Based Risk Matrix for Airport Stakeholders <a href="#">Haoruo Fu, Chien-tsung Lu, Ming Cheng, Mengyi Wei</a>	122	141



# Utilizing Mel-Frequency Cepstral Coefficients for Acoustic Diagnostics of Damaged UAV Propellers

Bahadır Cinoglu<sup>1\*</sup>, Umut Durak<sup>2</sup>, T. Hikmet Karakoc<sup>3</sup>

<sup>1</sup> Eskisehir Technical University, Faculty of Aeronautics and Astronautics, Eskisehir, Türkiye  
Cappadocia University, Department of Unmanned Aerial Vehicle Technologies and Operations, Nevsehir, Türkiye  
[cinoglubahadir@gmail.com](mailto:cinoglubahadir@gmail.com) - 0000-0003-4518-0300

<sup>2</sup> German Aerospace Center, Institute of Flight Systems, Braunschweig, Germany  
[umut.durak@dlr.de](mailto:umut.durak@dlr.de) - 0000-0002-2928-1710

<sup>3</sup> Eskisehir Technical University, Faculty of Aeronautics and Astronautics, Eskisehir, Türkiye  
Istanbul Ticaret University, Information Technology Research and Application Center, Istanbul, Türkiye  
[hkarakoc@eskisehir.edu.tr](mailto:hkarakoc@eskisehir.edu.tr) - 0000-0001-8182-8667



## Abstract

In this study, the diagnostic potential of the acoustic signatures of Unmanned Aerial Vehicle (UAVs) propellers which is one of the critical components of these vehicles were examined under different damage conditions. For this purpose, a test bench was set up and acoustic data of five different damaged propellers and one undamaged propeller were collected. The methodology emphasized contains using an omnidirectional microphone to collect data under three different thrust levels which correspond to 25%, 50% and 75%. Propeller acoustics sound characteristics extracted using the Mel Frequency Cepstrum Coefficient (MFCC) technique that incorporates Fast Fourier Transform (FFT) in order to obtain feature extracted data, and the visual differences of sound patterns were discussed to underline its importance in terms of diagnostics. The results indicated that there is a potential for classifying slightly and symmetrically damaged and undamaged propellers successfully in an Artificial Intelligence-based diagnostic application using MFCC. This study aimed to demonstrate a way to effectively use MFCC detecting damaged and undamaged propellers through their sound profiles and highlighted its usage potential for future integration into Artificial Intelligence (AI) methods in terms of UAV diagnostics. The findings provided a foundation for creating an advanced diagnostic method for increasing UAV safety and operational efficiency.

## Keywords

Mel-Frequency Cepstral Coefficients  
UAV  
MFCC  
Diagnostics  
Acoustics  
Propellers

## Time Scale of Article

Received 8 June 2024  
Revised until 13 July 2024  
Accepted 5 September 2024  
Online date 2 November 2024

## 1. Introduction

UAVs generally acquire the power they need from batteries or fuel cells and are vehicles that can be remotely controlled by an operator or perform defined tasks using their autonomous capabilities, without the need for a human being inside. The use of UAVs has been increasing, especially in recent years, as they have

become more affordable to society and the technological equipment used in them can better meet people's needs (Mohsan et. al., 2022; Adamo et. al., 2017). At the same time, due to its features, it can also be deployed in areas where it is risky for people to be present, such as disaster areas and are currently preferred in many sectors including search and rescue, agricultural spraying, forest fire fighting, delivery service, environmental monitoring,

\*: Corresponding Author Bahadır Cinoglu, [cinoglubahadir@gmail.com](mailto:cinoglubahadir@gmail.com)  
DOI: 10.23890/IJAST.vm05is02.0201

advertising or film shooting (Lyu et. al., 2023; Fan et. al., 2020; Adao et. al., 2017; Baiocchi et. al, 2013). These deployments also benefit from the use of AI technology in these days which is a rapidly developing field that affect general system performance and safety (Alharasees et., al. 2023). Given their increasingly varied usage across both urban and rural applications with using new techniques, providing a high level of safety and considering the reliability of its systems are vital. These safety considerations may be summarized as human factors, organizational factors and technical factors briefly in aviation (FAA, 2013).

Human factors focus on the effects of psychological, physiological or environmental factors on human operators. This involves the investigation of issues such as decision-making (Alharasees et. al., 2022), human-machine interface, and effects of cognitive load by using hearth rate measurements from the operators (Alharasees et. al., 2023). Organizational factors are situations that may have an effect on overall safety in terms of organizational budgets or maintenance issues. These issues contain the impact of warehouse improvements or investments (Gago et. al., 2021) and maintenance planning (Chen et. al., 2020) by taking into consideration of efficient management of spare parts (Tong et. al., 2022). On the other hand, technical factors involve consideration of safety improvements which can be related to predictive maintenance or real-time monitoring (Shen et. al., 2024, Kucukkor et. al., 2023), wearable systems (Wang et. al., 2021), flight control (Zhang et. al., 2020) or other features or systems that linked to UAVs.

Although some features vary depending on under what circumstances they are used, UAV systems generally consist of avionics such as telemetry or sensors, power module, control surfaces, payload, an operator or ground station, and propulsion modules such as propellers and motors. The propellers among them play a crucial role because a malfunction in critical systems such as propulsion components directly affects flight stability and efficiency and may cause the UAV to fail to fulfill its operational duty, the flight may result in an accident, resulting in financial loss or injury to other people (Zhang et. al., 2022).

In this respect, UAVs are evolving not only in terms of aerodynamics, materials or flight stabilization, but also in terms of Information Technologies (IT), AI, embedded software or cloud-based systems. Monitoring critical systems, especially with AI, and being able to identify signals of an error or fault with the aircraft can play an important role in preventing accidents or incidents related to UAVs (Pourpanah et. al, 2018). However, the development of the capabilities of sensors and the fact that AI models generally require excessive amounts of data may result in critical systems not being monitored

properly or programs running on the UAV not working efficiently (Abdul and Al-Talabani, 2012). For this reason, as the system complexity increases, the issues of reducing the size of the data with dimensional reduction techniques, selecting and using the most useful parts from the data set have emerged which used feature extraction and feature selection techniques (Van Der Maaten et. al., 2009). The advantage of using feature extraction techniques is not only reducing the size of the data, but also enabling AI algorithms, which have become very popular today, to perform faster calculations. Therefore, nowadays, there are many feature extraction techniques used to extract the features of different types of data obtained in different application areas.

In many studies, finding the time domain, harmonics or frequency domains of the data plays a critical role, especially in revealing the relationship between collected data. While Cepstrum-based solutions such as Gamma Tone Cepstrum Coefficient (GTCC) or MFCC can focus on the spectrum properties of the data, the correlation between the harmonics or power spectrum of the data can be determined by Fourier Transform based techniques such as FFT (Abdul and Al-Talabani, 2012; Liang et. al., 2013). It is also seen in the literature section that feature extraction techniques, especially MFCC, are used in many acoustics studies either UAV-related or non-UAV-related.

This study emphasizes the importance of diagnosing UAV propeller damages by obtaining and feature-extracting acoustic signatures which may offer an effective way on monitoring malfunctions on propellers especially with the assist of AI techniques. In the study, feature extraction of acoustic data obtained from damaged and undamaged propellers using MFCC is explained. To achieve this goal, the necessary testbench was established to perform damage diagnosis from the propeller acoustic characteristics of a fixed-wing UAV. Afterward, acoustics data related to damaged and undamaged propellers were collected. Finally, feature extraction was performed on these data using the MFCC technique to obtain distinctive features for use in future studies and pave the way for using these MFCC data with AI to contribute the AI on UAV operations which is considered as a market opportunity in the literature (Ekici et. al., 2023).

## 2. Literature Review

Jiao et. al. (2023) combined MFCC and Short Term Fourier Transform (STFT) features of the acoustic signature of UAVs and used them for classification to analyze the flight attitude of the vehicle. In their model, they created a lightweight structure with separable residual connections. Thus, a reduction in parameters and an increase in network depth have been achieved.

Their method achieved a high accuracy of 98.81% in determining the flight attitude of the UAV, and a good efficiency rate compared to the VGG16 model.

Frid et. al. (2024) proposed a study and tried to detect UAVs using Radio Frequency (RF), acoustic signatures and Deep Neural Networks (DNN). For the study, they obtained the UAV's acoustics characteristics as a first step. Afterward, time-frequency properties were extracted from these data using MFCC and GTCC. These features were classified using Recurrent Neural Networks (RNN) and Support Vector Machine (SVM). As a result of the study, it was stated that UAVs were detected at a higher rate compared to classical methods by using RF and acoustic data together, including low Signal-to-Noise Ratio (SNR) cases.

Yaman et.al. (2022) developed a method based on SVM which is built for diagnosing UAV motor damage. In their method, in order to identify UAV propeller, bearing or balance faults, they used the MFCC technique to gather features from acoustic signals. Afterward, they classified these features using SVM. They achieved an accuracy of 100% for helicopters and duocopters, 99.06% for tricopters and 90.53% for quadcopters. In their study, it has been emphasized that the method can be used in real-time by implementing it in an embedded system.

Berghout ve Benbouzid (2024) suggested an acoustics-based method to detect UAV faults detection using Heterogeneous Multiverse Recurrent Expansion with Multiple Repeats (HMV-REMR). In the study, the features extracted from UAV acoustics using MFCC and used for classification. To achieve this, they used RNN variations such as Long Short-Term Memory (LSTM), Bidirectional Long Short-Term Memory (BiLSTM) and Gated Recurrent Unit (GRU). HMV-REMR algorithm has achieved a good performance in detecting UAV faults and provided a solid foundation for real-time fault detection studies.

Kołodziejczak et. al. (2023) studied on UAV rotor's acoustic data to detect faults by using MFCC and LSTM. To reduce the computational load of the model, a decision fusion strategy was applied by combining Principal Component Analysis (PCA) and weak classifiers. They conducted a research on real flight conditions and achieved more than a 33% reduction in processing time compared to regular methods. Their study stands out with its ability to perform fast and effective fault detection in processing units with limited computational power.

Katta et. al. (2022) developed an audio dataset based on real-world data to detect propeller failures of UAVs which they used to develop various deep-learning models. In their study, they obtained a record of more than 5 hours in length using a microphone array that has been placed on a UAV. In the next step, they used MFCC

for feature extraction and used these features to train DNN, Convolutional Neural Network (CNN), LSTM and Transformer Encoder (TrEnc) models. The highest performance was achieved by using the TrEnc model with 98.30% accuracy. The results of the study supported that propeller faults can be effectively detected using acoustic data.

Dumitrescu et. al. (2020) developed a method for detecting UAVs using acoustic measurements and Concurrent Neural Networks (CoNN). To achieve this goal, they made use of acoustic measurements of UAVs, extracted the time-frequency features of the data using MFCC, and then trained the CoNN model using the extracted features. With the tests performed after the developed method, good results were obtained even in low SNR conditions. The relevant model provided an increase in detection performance. Additionally, it can be said that feature extraction techniques such as MFCC are effective in detecting UAVs through acoustics.

Suman et. al. (2022) studied creating a method using the acoustic signal processing-based method to identify early mechanical faults. To achieve this, they pre-processed the acoustic signals with KLT filtering and Hamming window. Afterward, features were extracted from acoustic signals by using MFCC and Kalman Filters. Their proposed model was able to detect mechanical faults by processing signals obtained from microphone and vibration sensors.

Jiqing et al. (2021) proposed an acoustic detection method in UAVs using the Mel spectrum and CNN. In their study, Mel spectrum was used for feature extraction of UAV acoustics data and these acoustic data were converted into time-frequency domain. They used the features they obtained for training CNN. The sounds of different UAVs and other environmental sounds were also used to diversify the data set during training. They achieved an accuracy of over 99% in the tests performed after model training and demonstrated the success of feature extraction and deep learning in the field of acoustic research.

Jamil et. al. (2020) proposed a method that used both acoustics features and image features in a hybrid way for detecting UAVs. They chose MFCC to perform feature extraction from the collected UAV acoustics. In order to filter the acoustics data, FFT and Mel-filter banks were used. Then, Discrete Cosine Transform (DCT) was applied to these data to obtain MFCCs. AlexNet deep neural network was used to extract meaningful features from the images of UAVs. Afterward, SVM was used to complete the hybrid model they proposed. As a result of the tests, it was seen that the relevant method reached an accuracy value of over 95% and the model performance was high even when the data set was

reduced. The study revealed that MFCC and deep learning methods were an effective way to detect UAVs.

Utebayeva et. al. (2020) developed a classification method using Stacked BiLSTM to classify acoustic signatures emitted by UAVs. In this method, they performed feature extraction via using MFCC and filter bank. FT and DCT were used within MFCC during the feature extraction process, and LSTM hidden layers were used in the BiLSTM model. The approach they proposed had an accuracy rate of over 94%. The study is a good example of the widespread use and high success rate of MFCC in acoustic research.

Salman et. al. (2021) developed a method for detecting UAVs using Machine Learning (ML) and feature extraction. In the proposed method, some feature extraction techniques such as MFCC, GTCC, Linear Prediction Coefficients (LPC), Spectral Roll-Off (SRO) and Zero-Crossing Rate (ZCR) were used to determine the distinctive features of the data. Afterward, different SVMs were trained using these features extracted data. According to the test results obtained after the development of the method, GTCC achieved the highest success, while MFCC and LPC also achieved high success. This research showed that MFCC and other feature extraction methods were important in achieving high accuracy for UAV acoustics-related detections.

### 3. Method

Feature extraction techniques, especially MFCC, are used quite frequently in acoustic measurements as stated in the literature review. In this perspective, MFCC is a useful technique when it comes to extracting the features of acoustic data and revealing the relationship between them.

In the study, firstly, the testbench is established. For the testbench, a 1200 KV motor is used in a stationary position and six 13x6.5 propellers are preferred. Damages are slightly inflicted keeping symmetry in consideration particularly thus it is aimed that there would not be significant acoustic differences between the propeller's fingerprints. All damaged propellers used in the study were damaged intentionally symmetrically and lightly and thus, it was aimed to be able to detect the damage of minor damaged propellers in a future diagnostic application after obtaining MFCC features. It can be seen that the propellers used in studies on damage detection in the literature are asymmetrical and heavily damaged.

One of the propellers is cut 1 centimeter from both ends, named as "Damage-Type-1" (Fig. 1).

Another propeller is cut off 2.5 centimeters from the ends, similar to the first propeller, named as "Damage-Type-2" (Fig. 2).

The next two propellers suffered notch damage. The notch on both propellers is on the leading edge of the propellers. One of the propellers is notched on each side, 6 centimeters from its midpoint, named as "Damage-Type-3" (Fig. 3).

The other propeller with notch damage is notched on each side, 12 centimeters from its midpoint, named as "Damage Type-4" (Fig. 4).

A 1 cm deep horizontal partial cut is made at both ends of the last propeller, named as "Damage Type-5" (Fig. 5).



**Fig. 1.** Propeller Damage Type 1



**Fig. 2.** Propeller Damage Type 2



**Fig. 3.** Propeller Damage Type 3



**Fig. 4.** Propeller Damage Type 4



**Fig. 5.** Propeller Damage Type 5

**Table 1.** Duration of sound recordings for propellers

Damage Type	Record Duration (Sec)		
	25% Thrust	50% Thrust	75% Thrust
Type 1	200	200	200
Type 2	200	200	200
Type 3	200	200	200
Type 4	200	200	200
Type 5	200	200	200
Undamaged	1000	1000	1000

During the acoustics recording of damaged and undamaged propellers, an omnidirectional microphone is placed at the rear of the engine and approximately 15 centimeters away from the propeller, so as not to be exposed to the airflow created by the propeller.

While performing acoustic measurements with a microphone, one of the conditions that may affect the acoustic characteristics of damaged and undamaged propellers was ambient noise. The characteristics of the acoustic recording of propellers exposed to different sounds might be different. However, no special effort to prevent this disparity during the study is made. Ambient noise measurements are made in the workshop where the propellers were operated. Accordingly, it is determined that the average ambient noise was approximately 40 decibels and the maximum was around 70 decibels.

Another situation that would distort the characteristics of the recorded sounds was the thrust rate of the motor. During the study, three different thrust ratios at which the propellers would be operated were determined. These thrust ratios were 25%, 50% and 75% respectively. The reason why thrust ratios are chosen in this particular way is that the thrust ratio generally does not exceed 75% except for take-off and does not fall below 25% during level flight. A thrust ratio of around 50% has been determined as the speed at which the aircraft can produce lift and perform the necessary maneuvers during level flight.

In the next step, acoustic readings were recorded. For this purpose, a total of six propellers, five damaged and one undamaged, were operated with equal durations for each thrust amount. As a result of this operation, 6000 seconds of sound recordings were obtained, each sample being 10 seconds long (Table 1.). As a result, 3000 seconds of acoustic recordings of damaged propellers and 3000 seconds of undamaged propellers were obtained in Waveform Audio File Format (WAV).

In the MFCC features extraction process of ten-second recordings obtained from damaged and undamaged propellers, firstly, signals are split into overlapping frames. This process was of critical importance in determining the time-dependent changes of the

acoustic signal. Thus, small sections of the audio signal at a time could be examined. One of the important parameters when creating these frames was hop length that represents the distance between two adjacent signals. In the study, the number of overlapping frames was 2048 samples and the hop length was 512.

Subsequently, a window function was needed to effectively apply FFT to the signal. For this Hann window, one of the most preferred window functions which helps to reduce spectral distortion was used (Eq 1).

$$w[n] = 0.5(1 - \cos(\frac{2\pi}{N-1})) \quad (1)$$

In this equation,  $w[n]$  represents the value of the Hann window function for a specific index  $n$ . Here, the index value of  $n$  ranges from 0 to  $N-1$ , where  $N$  stands for the number of samples in a frame. By applying this formula, the Hann window minimized spectral leakage that caused by discontinuities when the acoustic signal is not periodic as desired. By applying this  $w[n]$  to the acoustic signal, a windowed frame was obtained (Eq 2).

$$y_w[n] = y[n] * w[n] \quad (2)$$

In the formula,  $y_w[n]$  represented the windowed frame which is obtained by multiplying the original discrete-time acoustic signal  $y[n]$  with the Hann window function  $w[n]$  that calculated at the previous step with respect to corresponding index  $n$ . It helped to reduce spectral leakage and minimize the sudden changes that cause the loss of high frequency components during FFT. After the windowed frame is obtained, each windowed frame must be converted from time-domain to frequency-domain. To achieve this, FFT, which is also frequently used in the literature, was used (Eq 3).

$$Y[i] = \sum_{n=0}^{N-1} y_w[n] * e^{-j\frac{2\pi}{N}in} \quad (3)$$

This equation indicated that the FFT of the windowed frame  $Y[i]$  is determined which results in converting the acoustic signal from the time domain to the frequency domain. The variable  $N$  corresponded to number of frames. Index  $i$  used in the formula ranges from 0 to  $N-1$  and represents the frequency bin index. The expression of  $y_w[n]$  on the other hand, corresponded to the windowed frame that formed after the Hann window function was applied to the acoustic signal. By applying

this equation, frequency components belonging to the acoustic signal have been computed and made it possible to analyze the spectral content of the acoustic signal. Once FFT was calculated, the resulted frequency spectrum needed to be mapped to Mel scale. The Mel scale is a nonlinear scale that matches the actual frequency (Hertz) to a sensed pitch (Mels) (Eq 4). By doing this, the center frequencies of a triangular filter on a Mel scale can be determined.

$$m = 2595 * \log_{10}(1 + \frac{f}{700}) \quad (4)$$

In this equation, m represents the Mel scale value of the signal which stand for the interpreted pitch. The variable corresponded to the frequency that was measured in Hertz. The Mel scale is designed to reflect the sensitivity to various frequencies similar to the human ear. This helped to analyze the linear frequency better and by using this conversion features of the acoustic data can be revealed for further feature extraction processes like MFCC that captures sound characteristics. As soon as the Mel scale was obtained, these frequencies were set back to linear frequency to apply filters later by using an inverse formula (Eq 5).

$$f = 700 * (10^{\frac{m}{2595}} - 1) \quad (5)$$

According to this equation, f represents the frequency measured in Hertz, m stands for the value on the Mel scale. This inverse formula converts Mel values back to their corresponding linear frequencies. This step was important for a successful application of filters in Mel filter bank precisely. In this way, it was ensured that the subsequent processing matched the actual frequency components of the signal. Next, filters were applied to the FFT output of each frame and a Mel Filter bank was obtained (Eq 6)

$$M[j] = \sum_{k=0}^{N-1} |Y[i]|^2 * H_j(i) \quad (6)$$

From the equation above, M[j] represents the output of the Mel filter bank for the j-th filter. The variable Y[i] corresponded to the FFT output for each frame and provided the frequency values of the windowed frame.  $H_j[i]$  is the triangular filter that applied at index of j, and N is the number of FFT points. The energy in each Mel scaled filter bank has been calculated by multiplying the squared magnitude of the FFT output  $|Y[i]|^2$  with the  $H_j[i]$ . The resulted Mel filter bank played a vital role in transforming acoustic signal into a form which could be used for further processes for analysis. In the next step, the logarithm of the Mel scaled power spectrum was calculated (Eq 7).

$$\log M[j] = (\log M[j]) \quad (7)$$

In this equation,  $\log M[j]$  represents the logarithm of the Mel filtered energy for the given index of j. The variable M[j] denoted the energy in the j-th Mel filter that obtained before. Taking the logarithm of the Mel filtered

energy used for compressing the dynamic range of values. This step was crucial for normalization of the energy levels and used them for further DCT application in the MFCC calculation. These processes were done to obtain a spectrum representation and by applying logarithm to compress dynamic range it was converged to an appropriate noise.

Finally, DCT was applied to the logarithm of the Mel-scaled spectrum which was crucial for emphasizing the most significant coefficients (Eq 8). This meant that the first few MFCCs were a representation of the most significant features of the propeller acoustics signal. For the i-th MFCC coefficient was computed as:

$$c_i = \sum_{j=0}^{J-1} \log M[j] * \cos(\frac{\pi i(2j+1)}{2J}) \quad (8)$$

According to this equation,  $c_i$  represents the i-th coefficient of the MFCC that captured the most significant features of the acoustic signal. The variable j stand for the number of Mel filters used. The expression  $\log M[j]$  corresponded to the logarithm of the Mel filtered energy for the j-th index. When the DCT application to logarithm of the Mel-scaled spectrum was also finished, all the Mel spectrums were converted to a set of coefficients, which is best known with its abbreviation: MFCC. MFCC results obtained from the acoustics signals of damaged and undamaged propellers were saved in a Comma-Separated Value (CSV) file to be used in advance.

#### 4. Results

As a result of the study, MFCC values were successfully obtained. These MFCC values can be used to create a setup in order to diagnose damaged and undamaged propellers using ML algorithms. With the MFCC values obtained, a heatmap was created for propellers of different damage types and for the undamaged propeller operated at 75% thrust ratio. The aim of this heatmap was to visualize the differences in the data obtained (Fig. 6-11).

Each heatmap created consists of 2 axes and different color combinations. Among these axes, the x axis shows how many seconds the relevant acoustic sample lasted. The Y axis represents the MFCC coefficients. Each coefficient (or row) shows different characteristics of the acoustic signal. While lower coefficients (those closer to the bottom) express values in a wider range, higher coefficients express values in a narrower range in terms of spectral shape or envelope. It can be seen that the coefficients at the top generally showed less intensity and therefore their colors were paler. In terms of color, it represents the intensity of MFCC values and varies between -150 and +100 dB which shows how much or little energy was in the frequency bands.

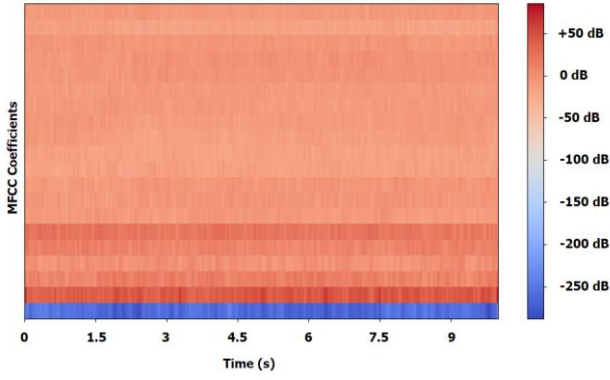


**Fig. 6.** Heatmap for Damaged Propeller Type-1 at 75% thrust ratio

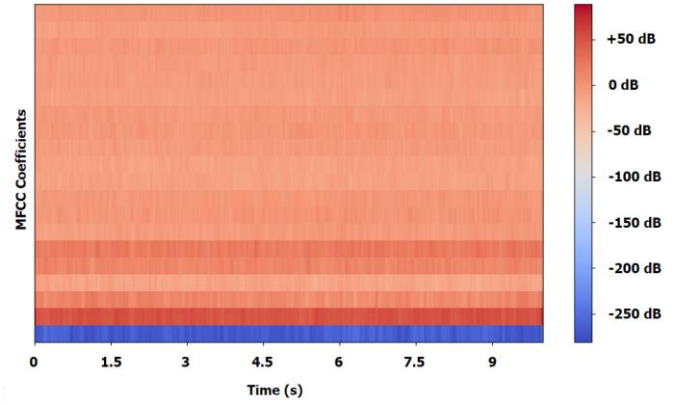


**Fig. 10.** Heatmap for Damaged Propeller Type-5 at 75% thrust ratio

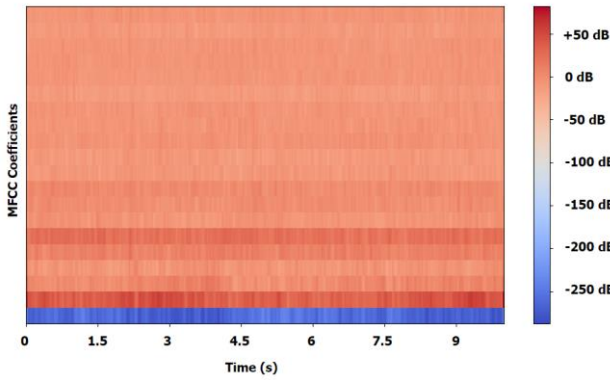


**Fig. 7.** Heatmap for Damaged Propeller Type-2 at 75% thrust ratio

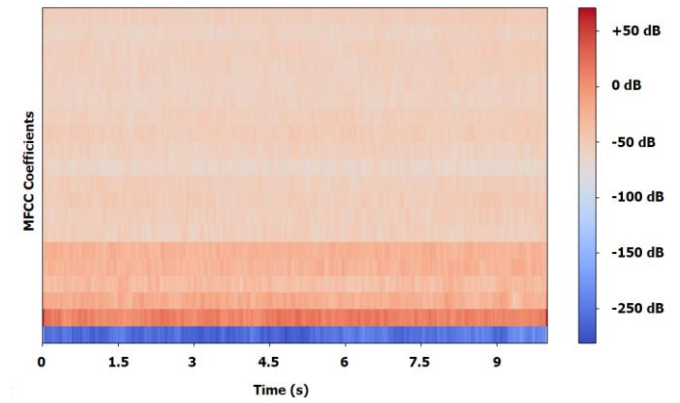


**Fig. 11.** Heatmap for Undamaged Propeller at 75% thrust ratio

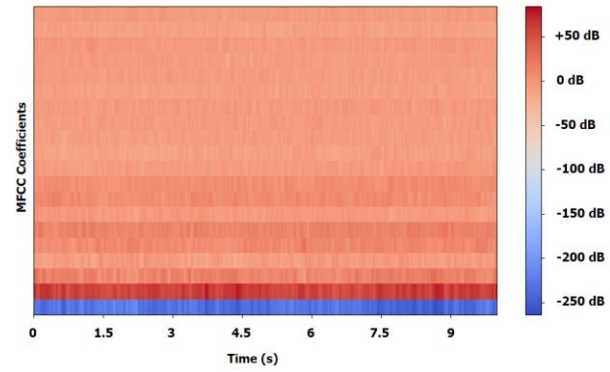


**Fig. 8.** Heatmap for Damaged Propeller Type-3 at 75% thrust ratio

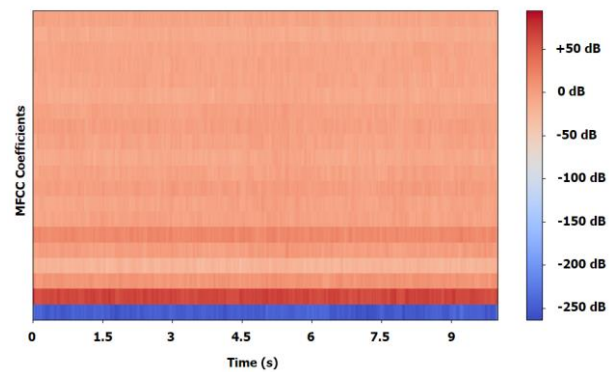


**Fig. 9.** Heatmap for Damaged Propeller Type-4 at 75% thrust ratio

## 5. Discussion

Considering the lower coefficients from the results, it was seen that the colors formed were generally slightly more intense than the higher coefficients. This meant that energy densities were more variable in parts with low coefficients. The coefficients showed in the figures were vital for recognizing differences in acoustic characteristics. Each coefficient represented a different aspect of the spectral envelope of the audio signal. The lower coefficients captured the broad spectral shape, while the higher coefficients captured finer details.

Although the coefficients in this part showed that the energy densities were lower, the coefficients in the upper part provided distinctive information in terms of the timbre and texture properties of the acoustic signature. When the acoustic properties of damaged and undamaged propellers on the Y axis were compared, it was seen that the damaged propellers had more dense colors than the undamaged propeller, even at high levels, and therefore it indicated that these parts contained higher energy for undamaged propellers which was a distinguishing feature.

On the other hand, the changes in colors on the x-axis showed how the spectral character of the acoustic data

changed over a period of ten seconds. Especially patterns that did not change much over time and whose colors were close to each other revealed a consistent propeller acoustic profile. When damaged and undamaged propellers were compared over time (along the y-axis), it was seen that the acoustic data characteristics of undamaged propellers mostly remained constant, therefore the sound profile was consistent. In the case of damaged propellers, the acoustic signal characteristics varied more than the undamaged propeller. This meant that the sound characteristics of damaged propellers differed significantly even within a period of ten seconds.

The use of MFCC has a widespread use in feature extraction of acoustic signals. While some researches focused on fault detection of UAV components, others were focused on the identification of UAVs. Suman et. al. (2022) studied early detection of mechanical faults using acoustics with MFCC and used a pre-processed database for signals. They used a signal enhancement filter before applying MFCC method which is not involved in this study for the ultimate purpose of making it as light as possible with the use of AI technologies. Similarly, Yaman et. al. (2022) has focused on developing a fault detection method and used MFCC extracted features on SVM classifier for UAV motors. They used a microphone that is connected to a mobile phone which might had an effect on overall weight. Also, the propeller in their study was asymmetrically and heavily damaged which simplified the classification on SVM and achieved an accuracy over 99%. On the other hand, Katta et. al. (2024) conducted a research to detect and identify UAVs presence using acoustics and deep learning. Their study also involved using an audio filtering technique besides MFCC. With feature extraction technique they were able to achieved accuracies over the 98% for different AI algorithms including DNN, CNN, LSTM and TrEnc.

## 6. Conclusions

This study demonstrated applying feature extraction successfully to the acoustic signatures of differently and slightly damaged and undamaged propellers using the MFCC technique, which is one of the feature extraction methods and is highly preferred in studies in the literature. The results indicated important differences in the acoustics characteristics of the propellers that were visualized using heatmaps. By addressing the differences between different thrust ratios and damage types, this study provides a solid background for the further development of diagnostic applications that use ML algorithms with a potential of high accuracy rates.

The findings of this study have importance in the context of suggesting that even slightly and symmetrically damaged propellers can be classified using MFCC and AI.

Thus, increased safety and reliability in UAV operations can be achieved across many operational fields from agricultural monitoring to search and rescue missions. The ability to detect propeller damage early also contributes to preventing propulsion-based failures and accidents with an increase of the overall performance.

Possible applications of this study include the integration of AI based diagnostic systems into UAVs for real time monitoring and fault detection. This way, potential issues can be addressed and early precautions can be taken for both maintenance and repair tasks. Additionally, the approach could be used for other components of the UAVs such as sensors or motors.

In future studies, the success of the model can be evaluated by using the data obtained with the MFCC feature extraction technique in various ML algorithms such as SVM, Random Forest, and LSTM. Differences that can be seen even visually in MFCC heatmaps can be associated much more easily by an ML algorithm, and damaged and undamaged propellers can be diagnosed using the classification method. In addition, a high-accuracy diagnostic application for UAV propellers can be made by using a feature extraction technique with measurements other than acoustics or using various parts of the UAV and combining them with the results in this study. Based on this result, it can be concluded that the study is a potential solution for diagnostics in UAVs and can be tested with ML algorithms in future studies.

## 7. Limitations

Even though this study emphasizes the efficacy of using the MFCC extraction technique in diagnosing UAV propeller damages, some limitations need to be taken into account. First, the process of data collection was done under conditions of a stationary test bench and in which only a few types of damages were made to the propellers. Real-world factors like variations in airflow that affect microphone response as well as having diverse kinds of propellers may compromise the accuracy and reliability.

Another limitation can be expressed as focusing on only slightly and symmetrically damaged propellers. While this study aimed to detect damages under these conditions, more severe or asymmetrical damages were not taken into account in the study. Future studies may include these adverse conditions and the comparison of MFCC performance with different damages. Additionally, exploring other techniques for feature extraction can provide aspects for determining the best solution for diagnosis problems. Also, the study relied on only the use of acoustic signatures of the propellers. This can be combined with other sensor data such as vibration or thermal measurements in order to improve the method's reliability and diagnostic accuracy.

## Acknowledgements

This article is formed with the studies based on Bahadır Cinoğlu's doctoral thesis titled "Smart Sensing for Electric Aircraft Propulsion".

## CRedit Author Statement

**Bahadır Cinoğlu:** Methodology, Software, Formal analysis, Investigation, Writing – Original Draft. **Umut Durak:** Writing – Review & Editing, Supervision. **T. Hikmet Karakoc:** Writing – Review & Editing, Supervision.

## Nomenclature

UAV	: Unmanned Aerial Vehicle
IT	: Information Technologies
AI	: Artificial Intelligence
GTCC	: Gamma Tone Cepstrum Coefficient
MFCC	: Mel Frequency Cepstrum Coefficient
FT	: Fourier Transform
FFT	: Fast Fourier Transform
TVAR	: Time-Varying Autoregressive
SCD	: Singular Value Decomposition
RBF	: Radial Basis Function
ANN	: Artificial Neural Network
DTW	: Dynamic Time Warping
LFT	: Logarithmic Fourier Transformation
PCA	: Principal Component Analysis
MLC	: Maximum Likelihood Classification
SVM	: Support Vector Machines
RF	: Radio Frequency
RNN	: Recurrent Neural Networks
SNR	: Signal-to-Noise Ratio
CoNN	: Concurrent Neural Networks
STFT	: Short Term Fourier Transform
CNN	: Convolutional Neural Network
DCT	: Discrete Cosine Transform
BiLSTM	: Bidirectional Long Short-Term Memory
WAV	: Waveform Audio File Format
Sec	: Seconds

CSV	: Comma-Separated Value
dB	: Decibel
LSTM	: Long Short-Term Memory
GRU	: Gated Recurrent Unit
HMV-REMR	: Multiverse Recurrent Expansion with Multiple Repeats
DNN	: Deep Neural Network
TrEnc	: Transformer Encoder
ML	: Machine Learning

## References

- Abdul, Z.K. and Al-Talabani, A.K., 2022. Mel frequency cepstral coefficient and its applications: A review. *IEEE Access*, 10, pp.122136-122158.
- Adamo, F., Andria, G., Di Nisio, A., Carducci, C.G.C., Lanzolla, A.M. and Mattencini, G., 2017, June. Development and characterization of a measurement instrumentation system for UAV components testing. In *2017 IEEE International Workshop on Metrology for AeroSpace (MetroAeroSpace)* (pp. 355-359). IEEE.
- Adão, T., Hruška, J., Pádua, L., Bessa, J., Peres, E., Morais, R. and Sousa, J.J., 2017. Hyperspectral imaging: A review on UAV-based sensors, data processing and applications for agriculture and forestry. *Remote sensing*, 9(11), p.1110.
- Alharasees, O., Adali, O.H. and Kale, U., 2023, June. Human Factors in the Age of Autonomous UAVs: Impact of Artificial Intelligence on Operator Performance and Safety. In *2023 International Conference on Unmanned Aircraft Systems (ICUAS)* (pp. 798-805). IEEE.
- Alharasees, O., Adali, O.H. and Kale, U., 2023, November. UAV Operators' Cognition and Automation: Comprehensive Measurements. In *2023 New Trends in Aviation Development (NTAD)* (pp. 15-20). IEEE.
- Alharasees, O., Abdalla, M.S. and Kale, U., 2022, November. Analysis of human factors analysis and classification system (HFACS) of UAV operators. In *2022 New Trends in Aviation Development (NTAD)* (pp. 10-14). IEEE.
- Baiocchi, V., Dominici, D. and Mormile, M., 2013. UAV application in post-seismic environment. *The International Archives of the Photogrammetry, Remote Sensing and Spatial Information Sciences*, 40, pp.21-25.
- Berghout, T. and Benbouzid, M., 2024, May. Acoustic

- Emission-based Fault Diagnosis for Drones with Heterogeneous Multiverse Recurrent Expansion: Avoiding Representation Glitch. In 2024 International Conference on Control, Automation and Diagnosis (ICCAD) (pp. 1-6). IEEE.
- Chen, S., Meng, W., Xu, W., Liu, Z., Liu, J. and Wu, F., 2020, November. A warehouse management system with uav based on digital twin and 5g technologies. In 2020 7th International Conference on information, cybernetics, and computational social systems (ICCSS) (pp. 864-869). IEEE.
- Dumitrescu, C., Minea, M., Costea, I.M., Cosmin Chiva, I. and Semenescu, A., 2020. Development of an acoustic system for UAV detection. *Sensors*, 20(17), p.4870.
- Ekici, S., Dalkiran, A., Karakoc, T.H. (2023). A Short Review on New Development Achievements and Market Opportunities in Unmanned Systems. In: Karakoc, T.H., Yilmaz, N., Dalkiran, A., Ercan, A.H. (eds) *New Achievements in Unmanned Systems*. ISUDEF 2021. Sustainable Aviation. Springer, Cham. [https://doi.org/10.1007/978-3-031-29933-9\\_1](https://doi.org/10.1007/978-3-031-29933-9_1)
- FAA (2013), "Operational Use of Flight Path Management Systems", Available at: [https://www.faa.gov/sites/faa.gov/files/aircraft/air\\_cert/design\\_approvals/human\\_factors/OU\\_FPMR\\_Report.pdf](https://www.faa.gov/sites/faa.gov/files/aircraft/air_cert/design_approvals/human_factors/OU_FPMR_Report.pdf)
- Fan, B., Li, Y., Zhang, R. and Fu, Q., 2020. Review on the technological development and application of UAV systems. *Chinese Journal of Electronics*, 29(2), pp.199-207.
- Frid, A., Ben-Shimol, Y., Manor, E. and Greenberg, S., 2024. Drones Detection Using a Fusion of RF and Acoustic Features and Deep Neural Networks. *Sensors*, 24(8), p.2427.
- Gago, R.M., Pereira, M.Y. and Pereira, G.A., 2021. An aerial robotic system for inventory of stockpile warehouses. *Engineering Reports*, 3(9), p.e12396.
- Jamil, S., Fawad, Rahman, M., Ullah, A., Badnava, S., Forsat, M. and Mirjavadi, S.S., 2020. Malicious UAV detection using integrated audio and visual features for public safety applications. *Sensors*, 20(14), p.3923.
- Jiao, Q., Wang, X., Wang, L. and Bai, H., 2023. Audio features based ADS-CNN method for flight attitude recognition of quadrotor UAV. *Applied Acoustics*, 211, p.109540.
- Jiqing, L., Husheng, F., Qin, Y. and Chunhua, Z., 2021, June. Quad-rotor UAV Audio Recognition Based on Mel Spectrum with Binaural Representation and CNN. In 2021 International Conference on Computer Engineering and Application (ICCEA) (pp. 285-290). IEEE.
- Katta, S.S., Vuojärvi, K., Nandyala, S., Kovalainen, U.M. and Baddeley, L., 2022, May. Real-world on-board uav audio data set for propeller anomalies. In ICASSP 2022-2022 IEEE International Conference on Acoustics, Speech and Signal Processing (ICASSP) (pp. 146-150). IEEE.
- Kołodziejczak, M., Puchalski, R., Bondyra, A., Sladic, S. and Giernacki, W., 2023, June. Toward lightweight acoustic fault detection and identification of UAV rotors. In 2023 International Conference on Unmanned Aircraft Systems (ICUAS) (pp. 990-997). IEEE.
- Kucukkor, O., Aras, O., Ozbek, E., Ekici, S. and Karakoc, T.H., 2023. Design and analysis of an IoT enabled unmanned aerial vehicle to monitor carbon monoxide: methodology and application. *International Journal of Global Warming*, 29(1-2), pp.66-77.
- Liang, B., Iwnicki, S.D. and Zhao, Y., 2013. Application of power spectrum, cepstrum, higher order spectrum and neural network analyses for induction motor fault diagnosis. *Mechanical Systems and Signal Processing*, 39(1-2), pp.342-360.
- Lyu, M., Zhao, Y., Huang, C. and Huang, H., 2023. Unmanned aerial vehicles for search and rescue: A survey. *Remote Sensing*, 15(13), p.3266.
- Mohsan, S.A.H., Khan, M.A., Noor, F., Ullah, I. and Alsharif, M.H., 2022. Towards the unmanned aerial vehicles (UAVs): A comprehensive review. *Drones*, 6(6), p.147.
- Pourpanah, F., Zhang, B., Ma, R. and Hao, Q., 2018, October. Anomaly detection and condition monitoring of UAV motors and propellers. In 2018 IEEE SENSORS (pp. 1-4). IEEE.
- Salman, S., Mir, J., Farooq, M.T., Malik, A.N. and Haleemdeen, R., 2021, January. Machine learning inspired efficient audio drone detection using acoustic features. In 2021 International Bhurban Conference on Applied Sciences and Technologies (IBCAST) (pp. 335-339). IEEE.
- Shen, F.Y., Li, W., Jiang, D.N. and Mao, H.J., 2024. Autonomous predictive maintenance of quadrotor UAV with multi-actuator degradation. *The Aeronautical Journal*, pp.1-25.
- Suman, A., Kumar, C. and Suman, P., 2022. Early detection of mechanical malfunctions in vehicles using sound signal processing. *Applied Acoustics*, 188, p.108578.
- Tong, B., Wang, J., Wang, X., Zhou, F., Mao, X. and Zheng, W., 2022. Optimal route planning for truck-drone delivery using variable neighborhood tabu search

- algorithm. Applied sciences, 12(1), p.529.
- Wang, X., Yadav, V. and Balakrishnan, S.N., 2007. Cooperative UAV formation flying with obstacle/collision avoidance. IEEE Transactions on control systems technology, 15(4), pp.672-679.
- Utebayeva, D., Almagambetov, A., Alduraibi, M., Temirgaliyev, Y., Ilipbayeva, L. and Marxuly, S., 2020, November. Multi-label UAV sound classification using Stacked Bidirectional LSTM. In 2020 Fourth IEEE International Conference on Robotic Computing (IRC) (pp. 453-458). IEEE.
- Van Der Maaten, L., Postma, E.O. and van den Herik, H.J., 2009. Dimensionality reduction: A comparative review. Journal of Machine Learning Research, 10(66-71), p.13.
- Yaman, O., Yol, F. and Altinors, A., 2022. A fault detection method based on embedded feature extraction and SVM classification for UAV motors. Microprocessors and Microsystems, 94, p.104683.
- Zhang, B., Song, Z., Zhao, F. and Liu, C., 2022. Overview of propulsion systems for unmanned aerial vehicles. Energies, 15(2), p.455.
- Zhang, X. and Zhao, X., 2020. Architecture design of distributed redundant flight control computer based on time-triggered buses for UAVs. IEEE Sensors Journal, 21(3), pp.3944-3954.



# An Empirical Analysis on The Use of Sustainable Fuels in the Aviation Industry

Yaşar Köse<sup>1\*</sup>, Emre Oğuzhan Polat<sup>2</sup>,

<sup>1</sup> University of Turkish Aeronautical Association, Faculty of Business Administration, Ankara, Türkiye  
[ykose@thk.edu.tr](mailto:ykose@thk.edu.tr) - 0000-0003-0073-2095

<sup>2</sup> University of Turkish Aeronautical Association, Ankara, Türkiye  
[oguzhan.polat@hotmail.com](mailto:oguzhan.polat@hotmail.com) - 0009-0008-9352-1839



## Abstract

This study aims to analyze and evaluate different types of alternative fuels for aviation from a life cycle and cost perspective. It aims to analyze different alternative fuels and their use in aircraft for this purpose in the aviation sector in relation to their potential to be a suitable transition solution towards sustainable transformation. Using the GREET (Greenhouse gases, Regulated Emissions, and Energy use in Technologies) aviation module developed by the US National Research Laboratory (Argonne), the life cycles of petroleum and six different sustainable aviation fuel production methods were calculated, and the environmental impact of kerosene and sustainable aviation fuels in terms of cost and carbon dioxide emissions on long, medium and short-haul flights were analyzed. The life cycle values of carbon dioxide formed as a result of the production of corn, soybean and canola products, which are the most preferred to produce biofuel in the aviation industry, with hydro-processed esters and fatty acids (HEFA), alcohol-to-jet (ATJ), ethanol-to-jet (ETJ) methods, were calculated. As a result of the study, it was determined that the cost of the sustainable aviation fuels examined was higher than fossil fuel. The key to greater acceptance and deployment of sustainable aviation fuel is cost reduction. In the long term, this will require investment in advanced technologies to process feedstocks more efficiently on a larger scale and in the development of sustainable and scalable feedstock options. However, in the short term, temporary support from governments and other stakeholders through policy incentives is needed.

## Keywords

Sustainable aviation fuels  
 Life cycle assessment  
 Life cycle cost  
 Carbon emissions  
 Environmental impact

## Time Scale of Article

Received 25 March 2024  
 Revised to 4 September 2024  
 Accepted 6 September 2024  
 Online date 27 November 2024

## 1. Introduction

Demand for passenger and cargo flights has increased significantly over the past few years. Global air travel is expected to increase further, due to continued globalization and almost unlimited travel possibilities. According to studies by leading aircraft manufacturers Airbus and Boeing before COVID-19, it is estimated that flight demand will increase by up to 4.5% per year, resulting in air traffic doubling every 16 years. Although the COVID-19 pandemic has led to a 75% decrease in air

travel according to 2020 data and slowed down this growth in the short term, the demand for flights is entering a recovery process and a strong positive trend is expected in the long term. However, while this development is seen as a positive development in economic terms, it is predicted that the effects of increasing global warming on the climate, especially the emission of greenhouse gases and carbon dioxide (CO<sub>2</sub>), will cause an increase in factors that negatively affect the environment. According to the 2019 EASA report, the aviation sector's global carbon dioxide emissions are 2.6%. It has been seen as responsible for the greenhouse

\*: Corresponding Author Yaşar Köse, [ykose@thk.edu.tr](mailto:ykose@thk.edu.tr)  
 DOI: [10.23890/IJAST.vm05is02.0202](https://doi.org/10.23890/IJAST.vm05is02.0202)

gas emissions and 5.9% of the global greenhouse gas. Although approximately 25% fuel efficiency has been achieved thanks to new generation aircraft, the rate of emissions at high altitudes is expected to be 3 times more effective than those at ground level by 2050, due to the anticipated growth in flights.

This study aims to analyze and evaluate different alternative fuel types for aviation in terms of life cycle and cost. Life cycle and price analyzes of kerosene and six bio-fuels were made; The environmental effects in terms of cost and carbon dioxide emissions in long, medium and short-haul flights were examined. Since sustainable aviation fuel data produced by the different production techniques used in the research can only be provided by the US Federal Aviation Administration, calculations regarding sustainable aviation fuels were made based on these data. It is evaluated that the study can be a practice guide for the managers of our country and global airline companies, those working in the sector and the relevant academic environment.

In the next or second part of the study, regulations to reduce the greenhouse gas effect, and in the third part promising aviation fuels are defined, fossil fuels and sustainable aviation fuels are compared and the environmental and cost analysis results are presented. The conclusion section provides a summary of the benefits of the study and the prospects for future research.

The transition from fossil fuels to sustainable aviation fuels has become the focus of aircraft manufacturers, energy companies, researchers and governments in combating climate change. It is evaluated that the study will contribute to policy makers, airline companies and researchers by making carbon dioxide emissions and cost comparisons of fossil fuels and sustainable fuels. Introduction section should consist of information that presents the purpose of the research and the studies on the subject, prepares the article for reading and facilitates the understanding of the general article. In this section, citations to the current and important literature related to the subject covered are made. Literature review should be included in this section. You may use a second level heading for literature review or any focused section.

## 2. Literature Review

Climate change is generally defined as statistical changes in the average state or variability of the climate that last for many years (Türkeş, 2008). Changes in climate are seen as changes in temperatures and changes in precipitation in some parts of the world. Over the years, changes have occurred in the climate system on Earth. Changes in sea level and glacier movements

have caused major changes in the ecological system (Türkeş, 2000).

Climate change causes many negative consequences. When we look at the variability in climate, it is revealed by the standard deviations of the climate average and the changes in other statistics. Climatic variability can occur due to natural processes or external effects caused by forcing. Climate change can occur through natural processes or external factors, as well as human-induced factors in land use. For example; agricultural activities, use of fossil fuels that cause greenhouse gases, increase in waste, industrialization, etc. factors can be counted. Human-induced factors pose a great threat to the world. Climate and weather are different matters. Weather is a short-term factor, for a day or two or a week. Climate, on the other hand, is a cumulative situation. It covers all very long-term meteorological conditions of a region (Gerste, 2017).

When we look at the causes of climate change, it is seen that natural factors emerge and cause this change. The main reason for climate change is the change in the radiation balance in the world. Detection of this change is understood with long-term data. Under normal conditions, solar energy and radiation entering the atmospheric system must be balanced. Some gases found in the atmospheric system are known as "greenhouse gases". These gases are; They are "CO<sub>2</sub>, CH<sub>4</sub>, N<sub>2</sub>O and O<sub>3</sub>" gases. The short wave coming from the sun is permeable, while the long wave is less permeable. For this reason, greenhouse gases trap the heat energy reflected from the sun, causing the world to warm up more. This situation is explained as the "greenhouse effect" (Gündoğan et al., 2015).

When we look at the causes of climate change, it is seen that natural factors emerge and cause this change. The main reason for climate change is the change in the radiation balance in the world. Detection of this change is understood with long-term data. Under normal conditions, solar energy and radiation entering the atmospheric system must be balanced. Some gases found in the atmospheric system are known as "greenhouse gases". These gases are; They are "CO<sub>2</sub>, CH<sub>4</sub>, N<sub>2</sub>O and O<sub>3</sub>" gases. The short wave coming from the sun is permeable, while the long wave is less permeable. For this reason, greenhouse gases trap the heat energy reflected from the sun, causing the world to warm up more. This situation is explained as the "greenhouse effect" (Gündoğan et al., 2015).

In the IPCC sixth assessment report (AR 6) published in August 2021, it was emphasized that the climate is changing as a result of human activities and that these activities have increased global warming to a level not seen in at least the last two thousand years. Due to climate change that has occurred since 1880, global

temperature has increased by 1°C. The amount of snow and ice has decreased and sea levels have risen. 19 of the 20 hottest years on record have occurred since 2001. The level of CO<sub>2</sub> in the air has reached its highest level in 650 thousand years. The cost of 2020, which was a year of disasters, reached billions of dollars. For example; The cost of the locust invasion in East Africa was 8.5 billion dollars, the cost of the hurricane in the USA was 41 billion dollars, and the cost of the forest fire in Australia was 5 billion dollars. In Turkey, 1.1 billion lira damage was detected in agriculture due to extreme weather events such as storms, floods and tornadoes.

According to OurWorld 2021a, the transportation industry generated almost 21% of all greenhouse gas emissions in 2018, while the aviation industry contributed 11.6% (OurWorld 2021a). Similar to the United States, regional aviation was the second largest source of transportation-related greenhouse gas emissions in 2017 in the European Union, accounting for 13.9% of emissions from the transportation sector (EC, 2021). Regulations for the transportation industry were created in Europe (under the Emissions Trading System, or ETS) to reduce emissions, and the aviation industry has been using them since 2012. Regarding CO<sub>2</sub> emissions from airlines, there are international rules in addition to these European ones. One of them is the International Civil Aviation Organization's (ICAO) Carbon Offsetting and Reduction Plan for International Aviation (CORSIA). In order to attain emissions above 2020 levels for international flights beginning in 2016, 191 nations were required by the ICAO to create plans in October 2016 (Gill, 2017). Although the CORSIA program is voluntary for least developed nations, small island developing countries, and landlocked developing countries, it is not required for them. The CORSIA program will be implemented in four phases: the basic phase, which runs from 2019 to 2020; the pilot phase, which is voluntary; phase 1, which is voluntary; and phase two, which runs from 2027 to 2035. The International Air Transport Association (IATA) wants to cut carbon emissions by 50% by 2050 compared to current levels (IATA 2017).

Studies on the effectiveness of aircraft carbon emission reduction have started to appear in the literature as a result of these rules (Wang et al., 2020; Liu et al., 2017).

There are three distinct types of travel distances in the aviation industry: medium, long, and short. As the aviation sector grows, so does the amount of energy used and the negative effects it has on the environment. In order to stop rising energy consumption, the issue of airplane energy efficiency is becoming increasingly important for all modes of transportation. Albeit extremely long travel is more costly and utilizes more fuel, it is in any case liked over different types of movement. Because of the significant expense of fuel,

mileage basically eco-friendliness implies in the flying industry. About 3% of all fossil fuel consumption worldwide is for aviation fuel. Consequently, aviation accounts for 3% of all CO<sub>2</sub> emissions (Khandelwal et al., 2013).

Based on a policy assessment, he created the Aviation Integrated Model, which provides a comprehensive analysis of the local and global interactions between aviation and the environment (Jimenez et al., 2012).

The Warning Board for Flying Exploration in Europe (ACARE) was laid out to foster an essential examination program to accomplish the objectives of Vision 2020. The Gathering makes sense of its goals for 2020 as later:

The aviation activities are contributing significantly to the environmental pollution and the current situation of increasing climate change concerns has abundant support to the growing need for sustainable practices (Singh et al., 2023). The major environmental effects comes through the noise and carbon emissions and pollution through air logistics (Karaman et al., 2018). This discussion has highlighted the responsibility of industries to address carbon emissions and noise pollution. Organizations are facing the challenge of aligning their operations with environmental considerations, incorporating eco-friendly practices, and investing in alternative fuels and propulsion systems to enhance sustainability (Undavalli et al., 2023).

Besides the technological and environmental factors, the aviation industry is also vulnerable to unforeseen challenges and external disruptions. The ability, flexibility, or the capacity of the organizations operations to respond the disasters or any unforeseen events or challenges is termed the "agility" and is crucial for the organizations resilience (Ding et al., 2024). Research by Pettit and Beresford (2019) underscored the importance of agility in navigating uncertainties, such as economic fluctuations, geopolitical events, and global health crises (Lim et al., 2019). The recent pandemic of COVID-19 has urged the significance of organizational agility in adapting to rapidly changing circumstances (Wils et al., 2006).

One key aspect of sustainable performance in aviation is the industry's environmental impact, particularly its contribution to carbon emissions and climate change. Researchers have emphasized the need for the aviation sector to address its carbon footprint and adopt measures to mitigate environmental harm (Ding et al., 2024; Gudmundsson et al., 2021). This sustainability means the vibrant investments in fuel-efficient aircraft, introducing the alternative efficient fuel fuels, and to extend the efforts to increase operational efficiency and to reduce emissions (Undavalli et al., 2023).

Hollingsworth and others (2008), as well as Schäfer Furthermore, Tetzloff and Crossley (2014) created

improvement programming that decides the ideal designation of current and future airplane numbers in a course organization.

Technology has continuously impacted the aviation business and is known one of the main pillars supporting the aviation industry's expansion. This journey took start from the Wright brothers' groundbreaking flight to the current era of sophisticated aircraft design and state-of-the-art avionics (Ding et al., 2024). It is essential that to for the improvement in the operational efficiency and safety the aviation industry shall have a strong technological adoption strategy (Williams, 2019). In this regard the adaptability, or capacity of aviation industry's to adhere and quickly accept and incorporate new technology has become a key concern for the aviation operations businesses and it is considered a crucial to stay ahead of the competition (Ding et al., 2024).

The term Triple-A consist of the Adoptability, Alignment and Agility, and is known as the Triple-A Framework. In the sustainability perspective the role of the triple-A is vital in terms of sustainability and it stands at the forefront of strategic considerations. This framework provides a guides for aviation organizations and it interlinks the paradigms of environmental and social responsibility with a harmonious balance. The adoptability in aviation industry is now beyond the concept of traditional aircraft design which shall include the fuel efficiency, now the pace of adoptability is extended to electric propulsion and autonomous aircrafts. This advancement has bring the concept of the autonomous aircrafts, advance materials, learning of the organization culture and to bring a continuous improvement into the overall system (Ding et al., 2024; Nazeer et al., 2020).

The alignment perspective in the aviation industry means the synchronization of various aviation operational strategies in its pursuit of sustainable practices e.g. environmental and social sustainable perspectives. In the current scenario the environmental considerations are at the top of the aviation industry alignment efforts and the significant efforts has been noticed to shift the aviation operations towards eco-friendly and less corban emission technology. Various studies has been carried on to scores the importance of the alignment of aviation operational with environmental regulations and fuel efficient operations (Seo et al., 2018).

The term Agility is coined as an ability of an aviation organization to respond the fluctuation and immediate challenges in the prompt and more effective way. The agility is crucial and plays a vital role in the aviation industry resilience and the organization capability to handle and implement the sustainability practices in efficient and effective way (Yılmaz, 2023). The sudden

disruption due to the geopolitical issue, global health crises and weather factors are the common aspects of aviation industry. In such scenarios, organizational agility becomes imperative for the industry's survival and continued sustainable performance.

Owen and others (2010), as well as Terekhov et al. (2018) centers around the investigation of new flight innovations. Consider applying these examinations to cutting edge airplane, uncovering future carbon dioxide emanations. The primary finding of these studies is that new application technologies are only slowly making their way into the market. Other areas need to be cut back, like the use of environmentally friendly alternative fuels and operational measures. As per IATA's methodology, the improvement of avionics biofuels has the best potential to lessen flying CO<sub>2</sub> outflows (Hassan et al., 2017). As a result, the number of publications on biofuels has increased and biofuels have become a top priority for aircraft manufacturers, biofuel companies, researchers, and governments. in recent years significantly increased (Wang et al., 2019). The majority of these studies concentrate on various processing technologies, various raw materials, and production technology.

Thanks to the GREET application module, the environmental impact of raw materials required for sustainable aviation fuel production can be calculated. There is no open source module that can perform calculations in this way.

The output of Lissys' commercial Piano-X model has been used to calculate flight-specific emissions (ICAO, 2017) and global carbon accounting (Graver et al., 2019, Winther and Rypdal, 2019). Dray (2018) used Piano-X to explore interactions between passengers, airlines, airports, and other system actors in an integrated evaluation model.

The Atmosfair Airline Index has been calculated since 2011 by the independent German organization Atmosfair to measure carbon emissions (Atmosfair, 2021). In the calculation, each airline earns efficiency points between 0 and 100 in the index depending on flight duration. Piano-X and Atmosfair modules are developed only for corporate companies.

### 3. Method

Two different techniques were used to collect data in the research. In order to search the literature, the method of using secondary sources was preferred, current publications, academic studies and articles were examined. The Excel program-based GREET aviation (Greenhouse gases, Regulated Emissions, and Energy use in Technologies) life cycle analysis (LCA) module developed by the US National Research Laboratory

(Argonne) was applied. LCA, generally allows a holistic comparison of environmental measurements of various systems and is used to evaluate the environmental impacts of various technologies. In the conclusion and evaluation section, life cycles of oil and six different sustainable aviation fuel production methods are calculated with the GREET aviation module. Price analysis evaluation was made using secondary sources.

Since sustainable aviation fuel data produced by the different production techniques used in the research can only be provided by the US Federal Aviation Administration, calculations regarding sustainable aviation fuels were made based on these data. Due to time constraints, the life cycle and price analysis of oil and six biofuels was conducted; The effects of kerosene and sustainable aviation fuels on the environment in terms of cost and carbon dioxide emissions in long, medium and short-haul flights were investigated. In order for the study to be generalized to all aviation fuel products, a larger population needs to be studied. While sustainable aviation fuel raw material products were preferred, products with available price data were preferred.

The life cycle values of carbon dioxide formed as a result of the production of the most preferred corn, soybean and canola products for the production of biofuels in aviation using hydroprocessed esters and fatty acids (HEFA), alcohol-to-jet (ATJ), ethanol-to-jet (ETJ) methods has been calculated. Examining the life cycle of oil and six biofuels constitutes the limitation of the study.

### 3.1. Greet aviation module

Developed by the United States Argonne National Laboratory, the GREET (Greenhouse gases, Regulated Emissions and Energy Utilization in Technologies) aviation LCA module aims to assess the environmental impact of various aviation fuel production routes, including both fossil and bioderived aviation fuels. Life cycle analysis is often performed to assess the environmental impacts of technologies, providing a holistic comparison of systems' environmental measures.

The GREET model is developed and updated annually with support from various programs at the U.S. Department of Energy. It is structured to systematically examine the energy and environmental impacts of a wide range of products, including petroleum-based and sustainable aviation fuels (SAF). By using the GREET module, life cycle analysis results can be created at the process level and the emissions of technologies throughout the supply chain can be determined.

In the GREET aviation module, users can change key parameters for LCA simulation. In the aviation module,

users can add production routes of new sustainable aviation fuels and then generate the results. In addition to the US Department of Energy, the US Federal Aviation Administration (FAA) supported the development and implementation of the GREET aviation module.

Argonne National Laboratory has developed the "GREET for ICAO CORSIA" (ICAO, GREET) version that is built into GREET 2019 and includes parameters for ICAO-approved pathways used for CORSIA. It has joined the International Civil Aviation Organization's (ICAO's) Fuels Task Group (FTG) to contribute to the calculation of the life cycle and greenhouse gas emissions (carbon intensities) of sustainable aviation fuels production routes for carbon offsetting and reduction and is used by other participating bodies (ICAO 2019b).

Historically, a GREET aviation module within the GREET model and ICAO-GREET have been used to assess the environmental impacts of aviation fuels and aircraft. With all the current life cycle inventory (LCI) offered by GREET and ICAO, the interest in a standalone and user-friendly version of the aviation module enables users to easily generate results for aviation fuels and aircraft operations. To this end, Argonne National Laboratory has developed an interactive, standalone aeronautical module to have an aeronautical LCA platform consistent with the most current datasets. For ease of use, the module uses Microsoft Excel to enable an interactive user interface. Comparable LCA results based on reliable and consistent datasets are produced using a user-friendly interface. Above all, it enables transparent comparison of inputs and outputs of various processes/pathways.

An attempt has been made to create a data structure that can be used for all routes. Data sets can be easily imported from other sources, and data/results can be exported for other purposes. Additionally, the module has a dashboard where users can change parameters and interactively check relevant results (Wang et al., 2021).

## 4. Results and Discussion

The findings obtained when comparing aviation fuels in terms of carbon emissions and cost are given on the next page.

When Figure 1 is examined, it is observed that oil has a much higher value than corn obtained by using the ethanol-to-jet (ETJ) method, which has 81,67085 grams of carbon dioxide emissions per megajoule and the closest carbon dioxide emission value of 53,32535 g/MJ. It has been observed that corn obtained by using the hydroprocessed esters and fatty acids (HEFA) method has the most beneficial environmental impact in terms of carbon dioxide emissions with a value of 14,73431 g/MJ.

**Table 1.** Life/Energy Cycle and Cost Chart

Product Name	CO <sub>2</sub> Life Cycle (g/MJ)	Total Energy Life Cycle (MJ)	Current Price (kg/US Dolar)
Jet_A1	81,67085	1,08513	1,09
HEFA_Corn	14,73431	2,16851	27,3
HEFA_Soybean	25,79986	1,33447	55,91
HEFA_Canola	29,39803	1,40311	71,53
ATJ_Corn	42,24828	1,64473	27,3
ATJ_Soybean	25,79986	1,33447	55,91
ETJ_Corn	53,32535	1,84929	27,3

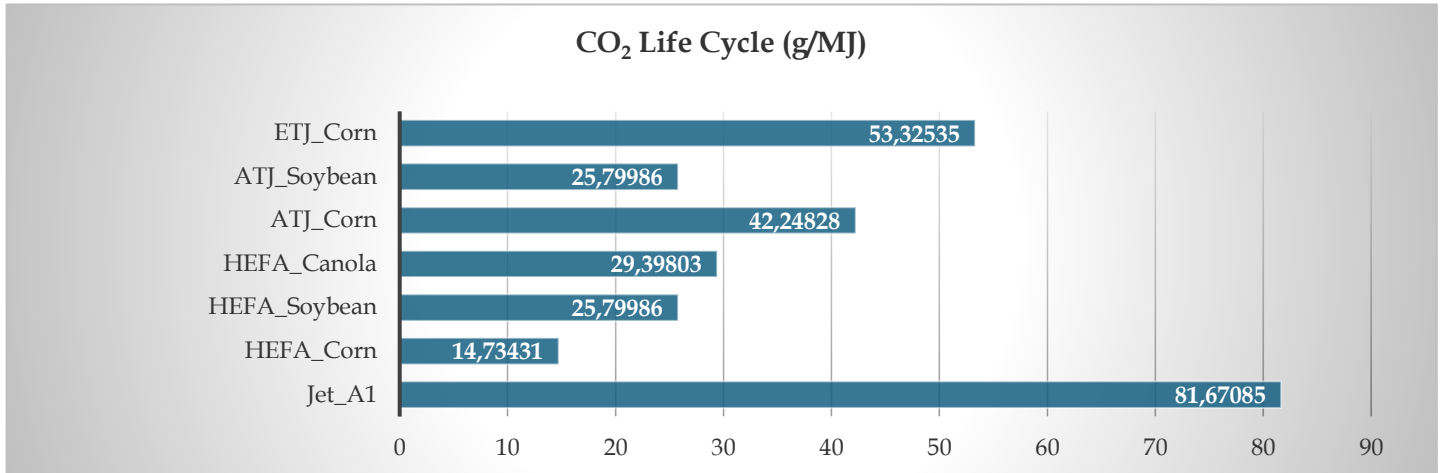


**Fig. 1.** Carbon Dioxide Life Cycle Graph.

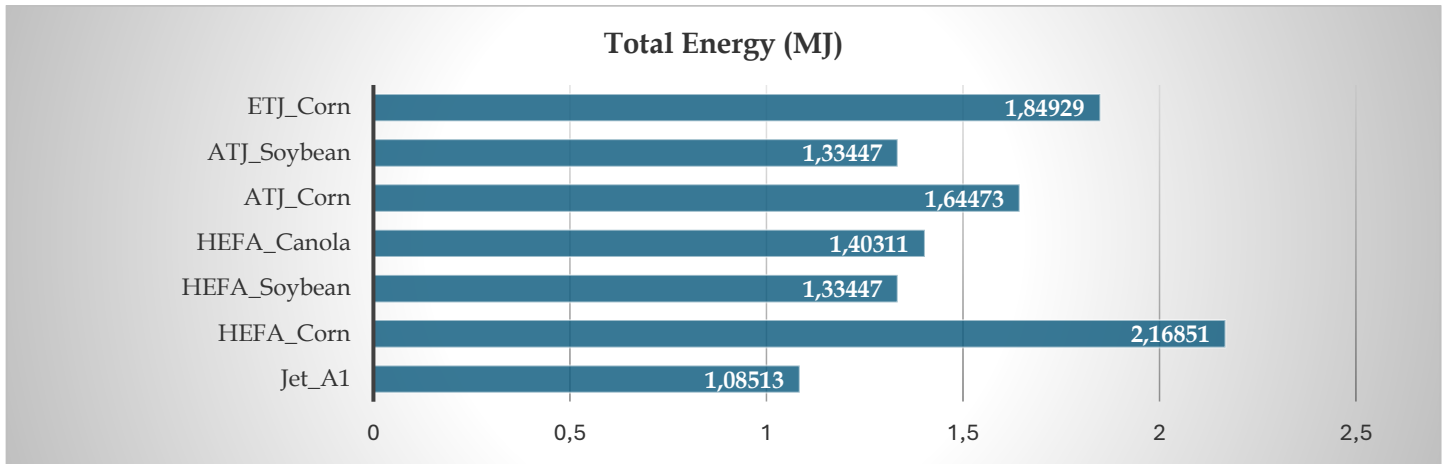


**Fig. 2.** Total Energy Graph.

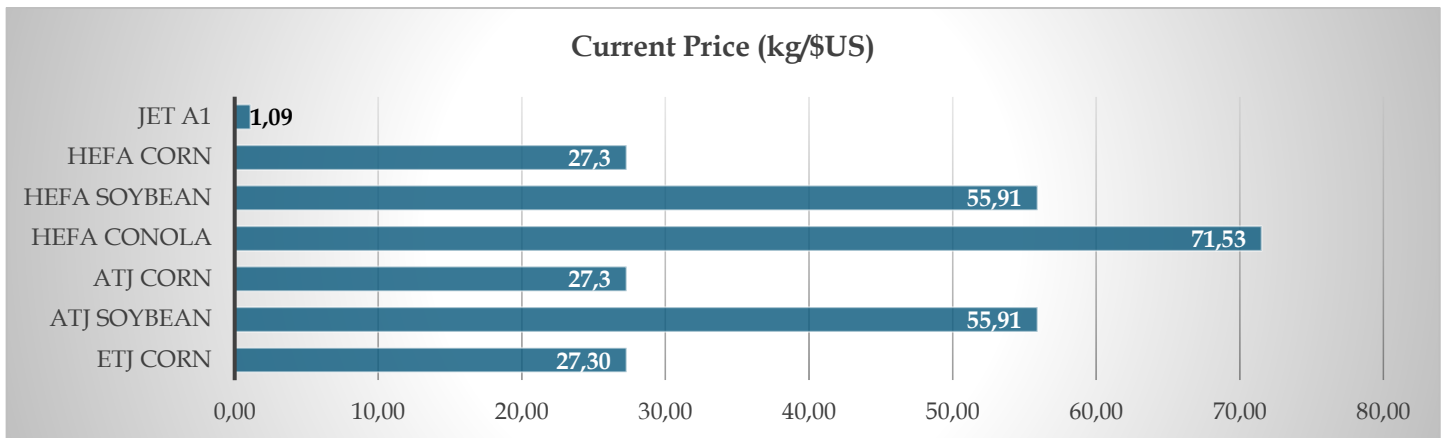


**Fig 3.** Cost Graph.

When Figure 2 is examined, it can be seen that the corn obtained using the Hydroprocessed esters and fatty acids (HEFA) method has the highest value with 2.16851 megajoules, while the total energy life cycle values of soybeans obtained using the alcohol to jet (ATJ) method are calculated as 1.33447 MJ. It was observed that it had the same results as the soybean value obtained using the hydroprocessed esters and fatty acids (HEFA) method, while the total energy life cycle of oil had the smallest value with a value of 1.08513.

When Figure 3 is examined, it is observed that the cost of oil, which is 1.09 US dollars, is 25 times lower than the cost of corn, which is 27.3 dollars, obtained using other methods, which is the closest cost to it. It was observed that the highest cost belonged to canola obtained by the Hydroprocessed esters and fatty acids (HEFA) method, which is 65.6 times more costly than oil, with 71.53 US dollars.

Published as part of the European Commission's climate package, the ReFuelEU proposal obliges fuel suppliers to include sustainable aviation fuel (SAF) in aviation fuel supplied at European Union airports (Weforum, 2023).

The obligation is projected to start with 2-5% sustainable aviation fuel from 2025 and gradually increase to 63% by 2050. In our study, 5% sustainable aviation fuel was added to jet fuel and jet fuel. Hydroprocessed esters and fatty acids (HEFA), which are one of the lowest priced products and specified as the usage method in the 2021 sustainability report by Turkish Airlines, the flag carrier airline of our country. The price of corn obtained using the method is taken as basis (turkishairlines, 2021).

In the study, flights up to 800 km were considered short distance, flights between 800 and 3000 km were considered medium distance, and flights over 3000 km were considered long distance flights (lufthansagroup, 2021).

Table 2 presents the data calculated for the distance of approximately 500 kilometers from Istanbul Airport (LTFM) to Ankara Esenboğa Airport (LTAC). Flight duration was calculated as 50 minutes and fuel consumed was 1350 liters. According to Lufthansa Airlines 2021 data, the approximate fuel consumption value for such a short-haul flight is 6.67 liters per 100 passenger kilometers, and carbon dioxide emissions are 16.78 kg. While there was a price increase of 1782 dollars between jet fuel and fuel with 5% biofuel added, it was observed that there was a decrease of 4.19 kg in carbon dioxide emissions.

Table 3 presents the calculated data for the distance of approximately 2000 kilometers from Germany Munich Airport (EDDM) to Ankara Esenboğa Airport (LTAC). The flight time was calculated as 180 minutes and the fuel consumed as 3500 liters.

**Table 2.** İstanbul- Ankara Flight

	İstanbul- Ankara		Difference
	Jet A1 Oil	5% Bio Oil Contribution	
Price (USD)	1471	3253	1782
CO <sub>2</sub> Emission (Kg)	83,9	79,7	4,19

**Table 3.** Munich-Ankara Flight

	Munich- Ankara		Difference
	Jet A1 Oil	5% Bio Oil Contribution	
Price (USD)	3815	8400	4585
CO <sub>2</sub> Emission (Kg)	191,4	181,3	10,1

**Table 4.** New York- Ankara Flight

	New York- Ankara		Difference
	Jet A1 Oil	5% Bio Oil Contribution	
Price (USD)	16132	35527	19395
CO <sub>2</sub> Emission (Kg)	1392,6	1323	69,5

**Table 5.** Cost-CO<sub>2</sub> Emission Comparing

	Costs (\$)	CO <sub>2</sub> Emission (kg)
Jet A1 Fuel	100	100
Bio Oil	12000	94,74
Percentage(%)	120,00	-5,26

According to Lufthansa Airlines 2021 data, the approximate fuel consumption value for such a medium-distance flight is 3.80 liters per 100 passenger kilometers, and carbon dioxide emissions are 9.57 kg. While there was a price increase of 4585 dollars between jet fuel and fuel with 5% biofuel added, it was observed that there was a 10.1 kg decrease in carbon dioxide emissions.

Table 4 presents the calculated data for the distance of approximately 9100 kilometers from the United States New York Airport (KJFK) to Ankara Esenboğa Airport (LTAC). Flight duration was calculated as 600 minutes and fuel consumed was 14800 liters. According to Lufthansa Airlines 2021 data, the approximate fuel consumption value for such a long-distance flight is 3.75 liters per 100 passenger kilometers, and carbon dioxide emissions are 9.41 kg. While there was a price increase of 19395 dollars between jet fuel and fuel with 5% biofuel added, it was observed that there was a decrease of 69.5 kg in carbon dioxide emissions (lufthansagroup, 2021).

When the values for three different distances are examined, it is seen that as the distance increases, the fuel consumed by the aircraft is more; It is observed that while the price increase increases, the amount of carbon dioxide emissions decreases. Prices increased at the

same percentage rate, and carbon emissions decreased at the same percentage rate. As shown in Table 5, it is seen that the use of aviation fuel with the addition of sustainable 5% biofuel reduces carbon dioxide emissions by 5.26%, but the cost increases by 120%.

The findings obtained in the study are reported in the literature by Undavalli et al., 2023 Gudmundsson et al., 2021; Ding et al., 2024; Owen et al., 2010; Therekhov et al., 2018; Wang et al., 2019; It partially overlaps with the studies carried out by. Because all of these studies focus on reducing carbon emissions caused by the airline industry. This study also emphasizes reducing carbon emissions but focuses on its costs and the feasibility of sustainable eco-friendly fuels in the future as well.

## 5. Conclusions

In aviation, carbon dioxide emissions are priced through the European Emissions Trading Scheme (EU-ETS). To reduce the price gap, one option could be to increase carbon dioxide emissions costs from the use of conventional fuels, while exempting users from any taxes, duties or emissions allowances on the portion of fuel consumption from sustainable aviation fuels.

As stated in the literature review, sustainability in the aviation sector in general has been examined and evaluated in terms of adaptation, agility and technology adoption criteria. When examined the mentioned articles in terms of our study, sustainable fuel use is related to all three determined factors. In this sense, sustainable fuel use in the aviation sector will be an important component of sustainability practices and policy in the aviation sector as a whole.

Another effective policy measure is the introduction of green certificates. Certificates are a means of proving that biofuels are used somewhere in the aviation system. The green certification system can be considered a hybrid solution between blending quota and surcharge. As an element of the mixing quota, the total amount of certificates determines the average share of biofuels in the system. As one element of the surcharge, money collected through green certificates can be redistributed to producers or users of biofuels. Also, regarding the number of regulated entities, an upstream approach would be preferred as there are only a very small number of fuel suppliers and a much larger number of aircraft operators. This can ultimately lead to a reduction in transaction costs. For example, the redistribution of money to biofuel users/producers appears preferential for a number of issues, such as overcoming the logistical problems of a uniform blending quota and the possibility given for a phased implementation.

The key to greater acceptance and deployment of sustainable aviation fuel is cost reduction. In the long

term, this will require investment in advanced technologies to process raw materials more efficiently on a larger scale and in the development of sustainable and scalable raw material options. However, in the short term, temporary support from governments and other stakeholders through policy incentives is needed.

Broader strategic concepts are extremely important for developing the independence of the aviation sector and sustainable aviation. Although aviation technologies are assumed to be constantly improved, increasing existing technologies will not be sufficient to reduce harmful environmental impacts. For this purpose, it is considered that the aviation industry's focus on developing the use of alternative power transmission technologies such as fuel cell-based and battery-based concepts in aircraft fleets can be much more effective in protecting the environment.

The necessity of reducing costs in the intensely competitive environment in the aviation industry and the obligation to comply with global environmental regulations will enable airline companies to develop and implement the most appropriate strategies based on cost and regulation, minimizing carbon emissions that are both low-cost and environmentally friendly. In this sense, it is evaluated that this study can be a practice guide for the managers of our country and global airline companies, those working in the sector and the relevant academic environment.

In this sense, it is evaluated that this study can be a practice guide for the managers of our country and global airline companies, those working in the sector and the relevant academic environment.

Since sustainable aviation fuel data produced by the different production techniques used in the research can be provided by the US Federal Aviation Administration, calculations regarding sustainable aviation fuels were made based on these data.

Due to time constraints, the life cycle and price analysis of petroleum and six biofuels was conducted; The environmental impact of kerosene and sustainable aviation fuels in terms of cost and carbon dioxide emissions in long, medium and short-haul flights was examined. In order for the study to be generalizable to all aviation fuel products, it is necessary to study a wider scope.

In the future, it is recommended that researchers analyze other sustainable fuel use and their costs in the airline industry and present their findings and inferences to industry managers.

## Acknowledgement

The authors of the paper submitted declare/declares that nothing which is necessary for achieving the paper

requires ethical committee and/or legal-special permissions.

The authors declare that they have no known competing financial interests or personal relationships that could have appeared to influence the work reported in this paper.

The authors of the paper declare that not use of generative AI and AI assisted technologies in the writing process.

Data will be made available on request.

### CRedit Author Statement

**Emre Oğuzhan Polat:** Conceptualization, Methodology, Software, Visualization, Investigation, Validation, Writing- Reviewing and Editing. **Yaşar Köse:** Conceptualization, Data curation, Writing- Original draft preparation, Supervision, Software, Validation, Writing- Reviewing and Editing

### Nomenclature

ATJ	: Alcohol-to-jet
CORSIA	: Carbon Offsetting and Reduction Scheme for International Aviation
EASA	: European Aviation Safety Agency
ETJ	: Ethanol-to-jet
EU-ETS	: European Emissions Trading Scheme
FAA	: US Federal Aviation Administration
REET	: Greenhouse gases, Regulated Emissions, and Energy use in Technologies)
HEFA	: Hydro-processed esters and fatty acids
IATA	: The International Air Transport Association
IPCC	: Intergovernmental Panel on Climate Change
LCA	: Life cycle analysis
SAF	: Sustainable aviation fuels

### References

Abdelhafez, A.A. ve Forsyth, A.J., 2009. A review of more-electric aircraft. 13th international conference on aerospace sciences & aviation technology.

Contreras, A.S., Özay, Y.K. ve Veziro T.N.,1997. Hydrogen as aviation fuel: a comparison with hydrocarbon fuels. *Int J Hydrogen Energy*. 22, 1053-1060.

Ding, Y., Zheng, P., Yang, L., Wang, Q., & Han, Q. (2024). The present and future of sustainable aviation fuels

in China. *Annual Report on China's Petroleum, Gas and New Energy Industry (2022-2023)*, 333-356.

Dray L, Andreas W. Schäfer, Kinan A., 2018. The Global Potential for CO2 Emissions Reduction from Jet Engine Passenger Aircraft, *Transportation Research Record: Journal of the Transportation Research Board*, <https://doi.org/10.1177/0361198118787361>

EASA, 2019. European Aviation Environmental Report. European Union Aviation Safety Agency, Brussels, Belgium.

European Commission Aviation, 2021. Havacılıktan kaynaklanan emisyonların azaltılması, [https://ec.europa.eu/clima/policies/transport/aviation\\_en](https://ec.europa.eu/clima/policies/transport/aviation_en), Accessed 29.01. 2021.

European Commission, 2017. White Paper on the Future of Europe, Reflections and scenarios for the EU27 by 2025.

Gerste, R. D., 2017. Hava Nasıl Tarih Yazar- Antikçağdan Günümüze İklim Değişiklikleri ve Felaketler, (Çev. M. Karaismailoğlu), Kolektif Kitap.

Gill, M., 2021. Preparing for CORSIA take-Off. IETA insights. [https://www.ietat.org/resources/Resources/GHG\\_Report/2017/Preparing%20for%20CORSIA%20Take-off-%20Gill.pdf](https://www.ietat.org/resources/Resources/GHG_Report/2017/Preparing%20for%20CORSIA%20Take-off-%20Gill.pdf), Accessed 09.01.2021.

Godula-Jopek, A. ve Westenberger, A., 2016. Hydrogen-fuelled aeroplanes. *Compend Hydrogen Energy*. 67-85.

Graver B, Zhang K, Rutherford D., 2018. CO2 Emissions From Commercial Aviation, *International Council on Clean Transportation*,1-13

Gudmundsson, S. V., Cattaneo, M., & Redondi, R. (2021). Forecasting temporal world recovery in air transport markets in the presence of large economic shocks: The case of COVID-19. *Journal of Air Transport Management*, 91, 102007.

Gündoğan, A., Baş, D., Sayman, R., Arıkan, Y. ve Özsoy, G., 2015. A'dan Z'ye İklim Değişikliği Başucu Rehberi, Bölgesel Çevre Merkezi REC, Türkiye.

Hassan, M., Pfaender, H. ve Mavris, D.N., 2017. Feasibility Analysis of Aviation CO2 Emission Goals Under Uncertainty. In: 17th AIAA Aviation Technology, Integration, and Operations Conference.

Hollingsworth, P., Pfaender, H. ve Jimenez, H., 2008. A Method for Assessing the Environmental Benefit of Future Aviation Technologies. In: ICAS Secretariat - 26th Congress of International Council of the Aeronautical Sciences. ICAS, 1, 3708-3719.

- IATA, 2017. World air traffic statistics. Report of IATA. Canada.
- IATA, 2002. CORSIA Bilgi Sayfası” 2019<https://www.iata.org/en/iata-repository/pressroom/fact-sheets/fact-sheet---corsia/>, Accessed 14.10.2022.
- ICAO, 2019a. CORSIA Default Life Cycle Emissions Values for CORSIA Eligible Fuels. <https://www.icao.int/environmentalprotection/CORSIA/Documents/ICAO%20document%2006%20-%20Default%20Life%20Cycle%20Emissions.pdf>, Accessed 13.01.2020.
- ICAO, 2019b. CORSIA Supporting Document: CORSIA Eligible Fuels–Life Cycle Assessment Methodology. [https://www.icao.int/environmentalprotection/CORSIA/Documents/CORSIA%20Supporting%20Document\\_CORSIA%20Eligible%20Fuels\\_LCA%20Methodology.pdf](https://www.icao.int/environmentalprotection/CORSIA/Documents/CORSIA%20Supporting%20Document_CORSIA%20Eligible%20Fuels_LCA%20Methodology.pdf), Accessed 13.01.2020.
- ICAO, 2020. Operational Impact on Air Transport, <https://data.icao.int/coVID-19/operational.htm>, Accessed 12.01.2020.
- ICAO, 2023. CORSIA Default Life Cycle Emissions Values for CORSIA Eligible Fuels., Accessed 12.01.2020.
- Investing.com, 2023. ABD Mısır Endeks Verileri. <https://www.investing.com/commodities/us-corn-historical-data>, Accessed 26.02.2023.
- Investing.com, 2023. ABD Soya Fasülyesi Endeks Verileri. <https://www.investing.com/commodities/us-soybeans>, Accessed 26.02.2023.
- IPCC, 2013. IPCC Fifth Assessment Report.
- Jimenez, H., Pfaender, H. ve Mavris, D., 2012. Fuel Burn and CO<sub>2</sub> System-Wide Assessment of Environmentally Responsible Aviation Technologies. *Journal of Aircraft*, 49, 1913–1930. <https://doi.org/10.2514/1.C031755>.
- Karaman, A. S., Kilic, M., & Uyar, A. (2018). Sustainability reporting in the aviation industry: Worldwide evidence. *Sustainability Accounting, Management and Policy Journal*, 9(4), 362–391.
- Khandelwal, B., Karakurt, A., Sekaran, P.R., Sethi, V. ve Singh, R., 2013. Hydrogen powered aircraft: The future of air transport. *Progress in Aerospace Sciences*, 60, 45–59.
- Lim, S., Pettit, S., Abouarghoub, W., & Beresford, A. (2019). Port sustainability and performance: A systematic literature review. *Transportation Research Part D: Transport and Environment*, 72, 47–64.
- Liu, X., Zhou, D., Zhou, P. ve Wang, Q., 2017. Dynamic carbon emission performance of Chinese airlines: a global Malmquist index analysis. *Journal of Air Transport Management*, 65, 99–109.
- Lufthansa Airlines, 2021 Yılı Sürdürülebilirlik Raporu. <https://www.lufthansagroup.com/en/responsibility> 2021, Accessed 01.03.2023.
- Nazeer, S., Saleem, H. M. N., & Iqbal, J., 2024. Triple-A Paradigm: Examining its Role in Shaping Sustainable Performance. *Foundation University Journal of Business & Economics*, 9(1).
- Nazeer, S., Saleem, H. M. N., & Shafiq, M. (2024). Examining the Influence of Adoptability, Alignment, and Agility Approaches on the Sustainable Performance of Aviation Industry: An Empirical Investigation of Supply Chain Perspective. *International Journal of Aviation, Aeronautics, and Aerospace*, 11(1), 8.
- OurWorld, 2021. Annual total CO<sub>2</sub> emissions, by world region. <https://ourworldindata.org/grapher/annual-co-emissions-by-region?country=Asia~Africa~North+America~South+America~Oceania~Europe>, Accessed 29.01.2021.
- OurWorld, 2021a Cars, planes, trains: where do CO<sub>2</sub> emissions from. <https://ourworldindata.org/co2-emissions-sport>, Accessed 29.01.2021.
- Owen, B., Lee, D.S. ve Lim, L., 2010. Flying Into the Future: Aviation Emissions Scenarios to 2050. *Environmental Science and Technology*, 44, 2255–2260. <https://doi.org/10.1021/es902530z>.
- Schaefer, M., 2012. Development of a Forecast Model for Global Air Traffic Emissions, Yüksek Lisans Tezi.
- Seo, Y., Park, B., & Kim, J.-h. (2018). A Study on Establishing Performance Measurement and Evaluation System of ATM. *Journal of the Korean Society for Aviation and Aeronautics*, 26(1), 37–43.
- Singh, J., Rana, S., Abdul Hamid, A. B., & Gupta, P. (2023). Who should hold the baton of aviation sustainability? *Social Responsibility Journal*, 19(7), 1161–1177.
- Soykan, G. ve Baharozu, E. 2015. Power flow application on an air vehicle electrical power systems. 1th international symposium on sustainable aviation.
- Terekhov, I., Schilling, T., Niklaß, M. ve Ghosh, R., 2018. Assessing the Impact of New Technologies in Aviation Using a Global Aircraft Fleet Forecasting Model, AEGATS 1–12.
- Tetzloff, I.J. ve Crossley, W.A., 2014. Measuring Systemwide Impacts of New Aircraft on the Environment. *Journal of Aircraft*, 51, 1483–1489. <https://doi.org/10.2514/1.C032359>.

- Tradingeconomics.com, 2023. ABD Canola Endeks Verileri, <https://tradingeconomics.com/commodity/canola>, Accessed 26.02.2023.
- Türk Hava Yolları, 2021. 2021 Yılı Sürdürülebilirlik Raporu. <https://investor.turkishairlines.com/documents/sustainability/turkish-airlines-sustainability-report-2021.pdf>., Accessed 29.12.2022.
- Türkeş, M., Sümer, U.M. ve Çetiner, G., 2020. Küresel iklim değişikliği ve olası etkileri. Çevre Bakanlığı, Birleşmiş Milletler İklim Değişikliği Çerçeve Sözleşmesi Seminer Notları (İstanbul Sanayi Odası).
- Türkeş, M., 2008. Küresel iklim değişikliği nedir? Temel kavramlar, nedenleri, gözlenen ve öngörülen değişiklikler, İklim Değişikliği ve Çevre, 1, 27.
- Undavalli, V., Olatunde, O. B. G., Boylu, R., Wei, C., Haeker, J., Hamilton, J., & Khandelwal, B. (2023). Recent advancements in sustainable aviation fuels. *Progress in Aerospace Sciences*, 136, 100876.
- United States Environmental Protection Agency (US EPA), 2020. Global greenhouse gas emissions, <https://www.epa.gov/ghgemissions/global-greenhouse-gas-emissions-data>., Accessed 04.08.2021.
- UNFCCC, 2021. Kyoto Protocol -Targets for the first commitment period. <https://unfccc.int/process-and-meetings/the-kyoto-protocol/what-is-the-kyoto-protocol/kyoto-protocol-targets-for-the-first-commitment-period>., Accessed 04.08.2021.
- US Energy Information Administration, 2023. ABD Körfez Kıyısı Kerosen Tipi Jet Yakıtı Spot Fiyat Verileri, [https://www.eia.gov/dnav/pet/hist/LeafHandler.ashx?n=pet&s=eer\\_epjk\\_pf4\\_rgc\\_dpg&f=m](https://www.eia.gov/dnav/pet/hist/LeafHandler.ashx?n=pet&s=eer_epjk_pf4_rgc_dpg&f=m)., Accessed 26.02.2023.
- Wang, M., Dewil, R., Maniatis, K., Wheeldon, J., Tan, T., Baeyens, J. ve Fang, Y., 2019. Biomass-Derived Aviation Fuels: Challenges and Perspective, *Progress in Energy and Combustion Science*, 74, 31-49.
- Wang, M., Amgad, E., Lee, U., Bafana, A., Banerjee, S., Thathiana, P., Bobba, P., 2021. Burnham, A., Cai, H. ve Gracida-Alvarez, U.R. Summary of Expansions and [1] Updates in GREET®, Argonne National Lab.(ANL), Argonne, IL (United States).
- Wang, Z., Xu, X., Zhu, Y. ve Gan, T., 2020. Evaluation of carbon emission efficiency in China's airlines, *Journal of Cleaner Product*, 243, 118500.
- Wheeler P., 2016. Technology for the more and all electric aircraft of the future. IEEE international conference on automatica (ICA-ACCA).
- Wils, A., Van Baelen, S., Holvoet, T., & De Vlaminc, K. (2006). *Agility in the avionics software world*. Paper presented at the Extreme Programming and Agile Processes in Software Engineering: 7th International Conference, XP 2006, Oulu, Finland, June 17-22, 2006. Proceedings 7.
- Winther M, Rypdal K., 2019. EMEP/EEA Air Pollutant Emission Inventory Guidebook.
- Yılmaz, R. (2023). Examining The Effects of Employees' visionary Leadership Perceptions on Organizational Agility With Structural Equation Model: A Research In Aviation Sector. *Yönetim Bilimleri Dergisi*, 21(50), 1077-1098.



## Aerodynamic Investigation of Fixed - Pitch Aircraft Propeller

Erdogan Kaygan<sup>1\*</sup>, Dogukan Dogan<sup>2</sup>, Ozan Mahir Alpagut<sup>3</sup>

<sup>1</sup> Lentatek Space Aviation and Technology Inc., Ankara, Türkiye

[erdogan.kaygan@lentatek.com](mailto:erdogan.kaygan@lentatek.com) - 0000-0003-3319-3657

<sup>2</sup> Lentatek Space Aviation and Technology Inc., Ankara, Türkiye

[dogukan.dogan@lentatek.com](mailto:dogukan.dogan@lentatek.com) - 0009-0009-6993-0242

<sup>3</sup> Lentatek Space Aviation and Technology Inc., Ankara, Türkiye

[mahir.alpagut@lentatek.com](mailto:mahir.alpagut@lentatek.com) - 0009-0008-7913-0276



### Abstract

An investigation of fixed - pitch propeller aerodynamics is described in this paper. The impetus for the work was to identify the proposed propeller's efficiency, thrust coefficient, power coefficient, and pressure contours. All computational analyses were performed using Computational Fluid Dynamics (CFD) software called Cradle scFLOW. During the simulation process, velocity was set to 60 knots (30.87 m/s) and the initial RPM (Revolution per Minute) was kept constant at 3100 to specify efficiency. Subsequently, the RPM value was varied to achieve thrust force. According to results, a thrust value of 1700N was achieved and propeller efficiency was found 0.79. Thrust value was then compared with the data obtained from experimental studies and the notable match was achieved. An increase in advance ratio was found to raise propeller efficiency at some point, and then reduction was observed in terms of efficiency due to thrust reduction. After these investigations, the obtained thrust force was compared with experimental data. The CFD results indicated a good agreement with the experimental results.

### Keywords

Aerodynamics  
CFD simulation  
Propeller  
Performance analysis  
Propulsive efficiency

### Time Scale of Article

Received 26 July 2024  
Revised until 16 October 2024  
Accepted 21 October 2024  
Online date 27 November 2024

### 1. Introduction

A propeller is a device consisting of two or more blades that produces a flow of air towards the rear, which in turn provides the thrust to push an airplane forward. Thrust from a propeller is exerted along and parallel to the longitudinal axis of the device, and this axis coincides with the airplane's direction of motion. Propellers can be classified into two general types: fixed-pitch propellers and variable-pitch propellers. Most of the analysis necessary for understanding and designing both types is the same. Fixed-pitch propellers impart a fixed amount of thrust for a given power setting; that is, the total force exerted on the airplane is always the same for a given

position of the throttle. The advantage of this configuration is its simple structure and cheap cost. However, the efficiency of FPP is slightly lower than that of a variable pitch propeller (VPP) due to the inconvenience of the appropriate pitch angle which is suitable for the aircraft state or flight condition. In contrast, a propeller pitch angle will be changed automatically in a variable-pitch propeller to accomplish any specific power. Most recent engine airplanes such as corporate and air transport aircraft use some type of variable-pitch propeller. However, in most modern general aviation airplanes (such as light training aircraft), fixed-pitch propellers are more affordable and less complex, and this is reason enough to consider their aerodynamic characteristics.

\*: Corresponding Author Erdogan Kaygan, [erdogan.kaygan@lentatek.com](mailto:erdogan.kaygan@lentatek.com)  
DOI: [10.23890/IJAST.vm05is02.0203](https://doi.org/10.23890/IJAST.vm05is02.0203)

Over the century, propellers have been an essential part of air transportation; unfortunately, these devices are far from remaining static technology. Though propellers have an extensive history, the recent era is marked by progressions in materials, computational capabilities, and aerodynamic perceptions. Combining all of these advancements is leading a revolution in propeller technology, enabling them to develop and meet the growing demands of industries endeavoring for enhanced performance, reduced environmental effect, and greater safety. The literature on propeller aerodynamics is scattered and, in some respects, inconsistent and incomplete. In this regard, summaries the theory of aircraft propellers by highlighting a systematic design procedures and deeper understanding of associated methods for computational performance models (Wald, 2006).

The propeller's design can alter any existing feature that the propeller's performance or adding a new feature on the propeller to improve its performance. For instance, increasing the number of blades positively impacts the blade's performance since the distribution of thrust and power is even in the propeller's wake. Therefore, the efficiency is slightly improved but not very significant. investigated the effects of blade numbers on aerodynamic performance of propellers (Bertetta *et al.*, 2012). Likewise, several researchers mentioned recent studies on different propeller design and analysis methods by using various experimental and computational methodologies (Ol *et al.*, 2008; Singh *et al.*, 2011; Asl *et al.*, 2017; Zao *et al.*, 2019). According to the results, it was observed that the rotation speed decreased as the number of blades increased. It has also been found to cause a decrease in propeller efficiency. However, increasing the number of blades will demand more power from the engine to produce thrust. For a given power and thrust, the propeller blades will be narrow as the number of blades increase. Having a large diameter propeller can significantly influence the performance, especially the propeller's efficiency. This is due to the ability to produce a greater fluid volume and better distribution of thrust and power compared to smaller diameter propeller. However, more power will be needed to rotate the propeller, can cause high fuel consumption and if it is an electric aircraft, the motor will potentially burn out.

Moreover, slotted propeller design concepts were also investigated by (Kutty *et al.*, 2017; Seeni *et al.*, 2019; Song *et al.*, 2019). (Ramzi *et al.*, 2011) investigated the performance variations of passive slotted blade in highly loaded compressor cascade. Slotted design on high cambered blade with

NACA 65-(18)10 airfoil sections were studied using CFD. The effect of slot location, slot width and slot slope on cascade performance was investigated. A reduction in

pressure loss coefficient of up to 28.3% was observed among the various designs analyzed. Similarly, a numerical investigation of passive slotted wind turbine designed and investigated with S809 airfoil for  $Re$  of  $2 \times 10^6$  (Kang and Park, 2013). Five different angles of attack cases were used. It was found that at 0.6 chord slot location and  $14.24^\circ$  angle of attack, the maximum lift coefficient ( $C_L$ ) was observed. Furthermore, at 0.024chord and angles of attack of  $14.24^\circ$  and  $20.15^\circ$ , stall delay was observed. performed a slotted blade design study with slot opening extending from pressure side to suction side with slot width of 3 mm through both numerical and experimental methods (Xie *et al.*, 2013). The angles of attack are varied for identical flow conditions. It was found that at lower angle of attack from  $0^\circ$  to  $10^\circ$  the flow remained unchanged. At angle of attack of  $20^\circ$ , a 4.9% increase in  $C_L$  was observed. At  $15^\circ$  angle of attack, only a 1.6% increase in  $C_L$  value was found. Overall, taking CFD results into consideration, high rate of performance enhancement was achieved using slotted geometry. Additionally, better acoustic performance benefits were seen with higher number of blades (Lieser *et al.*, 1997).

Current conventional methodologies for predicting propeller performance are through momentum theory (McCormick, 1994) and blade element theory (Houghton and Carpenter, 2005). However, momentum theory is completely idealistic and completely independent of the airfoil to find performance parameters. Blade element theory, on the other hand, predicts performance relatively realistically by considering the airfoil as discrete wing elements. Nevertheless, both theories cannot reach the practical situation where the flow is truly complex due to the presence of 3D vortices created in the shear flow of the propeller. Using CFD enables to study viscous flow and to investigate the flow pattern across a propeller blade, which is not so applicable for other numerical methodologies (Kaidi, 2012). Comparing CFD simulation with experimental methods, CFD simulations was found to be less time required to obtain results. The numerical method in CFD is therefore chosen over other methods for the current study.

Ongoing research continues to uncover innovative design approaches, optimize performance through computational and experimental methods, and address the modern challenges of efficiency and environmental impact. In this paper, aerodynamic properties of proposed propeller model investigated by using CFD methods (application: Cradle scFLOW) and thrust data then validated through experimental data.

## 2. Method

Momentum and Blade element theory are the most common methods used to define aerodynamic

properties as aforementioned above in the introduction section. Due to complex flow regimes around the propeller geometry, both methods seem insufficient with an actual scenario. Hence, CFD has been used to identify the performance parameters a propeller blade.

### 2.1. CFD Governing Equations

In general, continuity and Reynolds-averaged momentum equations are the two main parts of the points while governing CFD equations (Versteeg et al., 1997). The continuity equation for an incompressible flow is given as follows:

$$\text{div } \mathbf{u} = 0 \quad (1)$$

Applying the Reynolds averaging approach (Osborne, 1845) to turbulence modeling produces time-averaged governing equations, also known as Reynolds Averaged Navier Stokes Equations (RANS) equations, which can be written in Cartesian tensor form as:

$$\frac{\partial \rho}{\partial t} + \frac{\partial}{\partial x_j} (\rho u_j) = 0 \quad (2)$$

$$\frac{\partial (\rho \bar{u}_i)}{\partial t} + \frac{\partial (\rho \bar{u}_i \bar{u}_j)}{\partial x_j} = -\frac{\partial \bar{p}}{\partial x_i} + \frac{\partial}{\partial x_j} \left[ \mu \left( \frac{\partial \bar{u}_i}{\partial x_j} + \frac{\partial \bar{u}_j}{\partial x_i} - \frac{2}{3} \delta_{ij} \frac{\partial \bar{u}_m}{\partial x_m} \right) \right] + \frac{\partial}{\partial x_j} (-\rho \bar{u}'_i \bar{u}'_j) \quad (3)$$

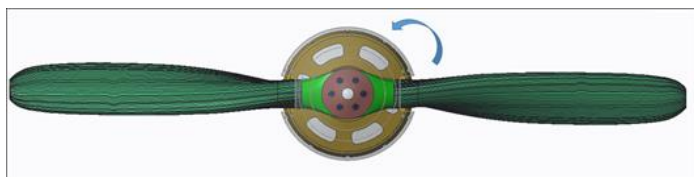
where  $x_i$  are Cartesian coordinates ( $i = 1, 2, 3$ );  $\rho$  is the density;  $t$  is the time;  $u_i$  are Cartesian velocity components ( $i = 1, 2, 3$ );  $\bar{p}$  and  $\mu$  indicate the pressure and dynamic viscosity, respectively,  $\delta_{ij}$  represent the Kronecker delta,  $-\rho \bar{u}'_i \bar{u}'_j$  is the Reynolds stresses. Reynolds stresses can be related to mean deformation rates as indicated by the Boussinesq hypothesis (François, 2007) and can be written as:

$$-\rho \bar{u}'_i \bar{u}'_j = \mu_t \left( \frac{\partial \bar{u}_i}{\partial x_j} + \frac{\partial \bar{u}_j}{\partial x_i} \right) - \frac{2}{3} \left( \rho k + \mu_t \frac{\partial \bar{u}_i}{\partial x_i} \right) \delta_{ij} \quad (4)$$

where  $\mu_t$  represents the turbulent viscosity. Then,  $\mu_t$  will be estimated by the turbulence model equalities.

### 2.2 Propeller Model

The selected basic propeller was utilized with a diameter (D) of 1.45 m and a fixed pitch ( $\beta$ ) of  $11.5^\circ$  (Fig. 1). The propeller is designed with estimated ARA-D 10% airfoil sections near the hub and Clark-Y airfoil sections near the tip. This propeller-like feature is commonly used in applications operating at low Reynolds number such as UAVs.



(a)



(b)

**Fig. 1.** Propeller model (a) Computer Aided Design model and (b) Structural model.

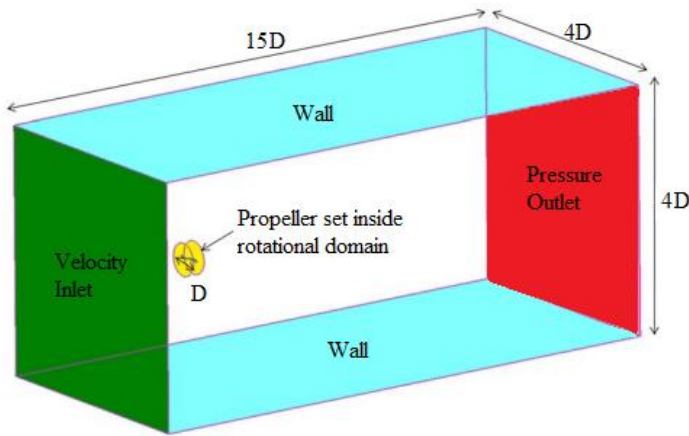
### 2.3 CFD Steady State-Rans Solver

In this study, the CFD finite volume-based solver Cradle scFLOW is chosen to solve the RANS equations for an incompressible flow. The flow around the propeller is always unstable, and the presence of turbulence patterns makes the flow unstable. However, the RANS turbulence model provides closure to the Reynolds Stress tensor, which signifies the influence of turbulent fluctuations in the mean flow. This allows steady-state simulations to be performed in Cradle scFLOW. The boundary conditions applied for this study are shown in Fig. 2.

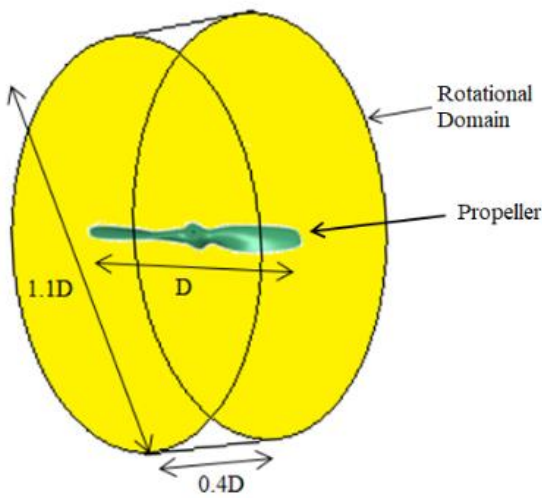
### 2.4 Grid Generation and Flow Field Solution

3D numerical grid was applied in which the velocity components  $u$ ,  $v$  and  $w$  and the pressure component  $p$  at the center of the control volumes are computed. The propeller was designed using Computer Aided Design software MSC Apex and then imported into Cradle SCFlow for domain creation. The simulation's flow domain is modeled based on the Multiple Reference Frame and consists of two regions: fixed and rotational (Fig. 2). A rotating reference frame that rotates at a constant angular speed of 3100 rpm surrounds the propeller. Subsequently, this value varied in order to measure how much thrust propeller can provide with diverse RPM settings.

The boundary conditions and computational domain are set according to (Seeni et al., (2020) and (Sanjeevi et al., 2009). The rotating reference frame is designed to have a cylinder-shaped geometry with a diameter of  $1.1D$ . The fixed reference frame is assigned with a rectangular geometry with sides of dimensions  $15D \times 4D \times 4D$ , as shown in Fig. 2. The adjusted dimensions were found to be sufficient for the simulation to reach steady state and for the trace of the flow to disappear below the impeller. An offset condition is set on rectangular walls while inlet and outlet labels are assigned to the front and back of the geometry. The carousel is maintained at a length of approximately  $2D$  from the front of the geometry to  $12D$  from the rear side of the geometry. The rotating frame is rotated at a small angle with the propeller set inside. The axis of rotation is adjusted to be aligned with the hub axis of the propeller.



(a)



(b)

**Fig. 2.** Boundary conditions for (a) Stationary Computational Domain (b) Rotational-Computational Domain.

The area is connected using polyhedral elements in the two regions (Fig. 3). The mesh in the rotating frame close to the propeller is knitted with finer elements than the outer frame. Mesh generation is performed via simultaneous discretization in both regions using unstructured mesh. An unstructured mesh was chosen over structured network as both network schemes produced almost similar results. The curvature of the propeller geometry affected the mesh skew, which increased the complexity of the field geometry to be meshed. For an unstructured network, the number of Y+ walls to be protected in the fan wall must be less than 300 according to (Tian et al., 2015) and (Alakashi et al., 2014). The mesh independence study finds the right mesh resolution to get accurate results by reducing the simulation's errors. The accuracy of the result can be determined by comparing the results with existing experimental results.

The front and back parts of the fixed area are assigned as velocity input and pressure output, respectively. A no-

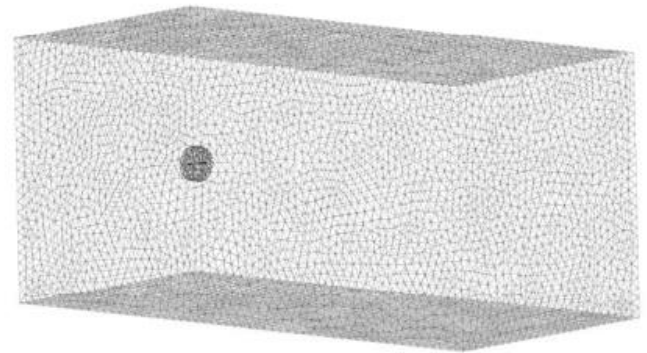


**Fig. 3.** Mesh-network structure created for propeller simulation.

slip condition is assigned to the wall of the rotating area. The turbulence intensity was set to 0.1% based on experimental assumptions (Brandt et al., 2011). The output is specified with a static pressure of 0 Pa. The semi-indirect method for pressure linked equations is assumed as a pressure-velocity coupling diagram. It is assumed that the fluid is air at 20°C, with a density of 1.225 kg/m<sup>3</sup> and a dynamic viscosity of 1.83x 10<sup>-4</sup> kgm<sup>-1</sup>s<sup>-1</sup>. Flow speed was set as 60 knots (30.87m/s).

### 2.5 Aerodynamic Coefficient and Propeller Efficiency

A relatively common and easiest method of computing the performance of a propeller is the use of Blade Element Theory. Using this method, the propeller split into many independent segments along its length. A balance of forces is applied to each section, including the thrust and torque generated by the segment and the lift and drag of the 2D section. At the same time, axial and angular momentum balance is applied. This yields a set of non-linear equations that can be solved iteratively for each blade section. The resulting cross-sectional thrust and torque values can be aggregated to estimate the overall performance of the propeller.

There are some performance parameters that need to be identified to shape out propeller characteristics aerodynamically. These parameters are:

- Thrust Coefficient ( $C_T$ ): A dimensionless number that represents thrust performance relative to the air density, the propeller diameter, and the rotational speed.
- Power Coefficient ( $C_p$ ): This dimensionless coefficient represents the power required to turn the propeller relative to the air density, diameter, and rotational speed.
- Efficiency ( $\eta$ ): The ratio of the useful power (thrust power) generated by the propeller to the actual power input, expressed as a percentage.

The thrust coefficient is defined by the following expression:

$$C_T = \frac{T}{\rho n^2 D^4} \quad (5)$$

where T is the thrust force,  $\rho$  is the air density, n is the revolutions per second and D is the propeller's diameter. The advance ratio is defined by the following correlation:

$$J = \frac{V}{nD} \quad (6)$$

where V is the free stream velocity.

The power coefficient is defined as follows:

$$C_P = \frac{P}{\rho n^3 D^5} \quad (7)$$

The efficiency of the propeller is defined by the following correlation:

$$\eta = J \frac{C_T}{C_P} \quad (8)$$

Furthermore, propeller performance can be predicted by using the equation below;

$$\eta = \eta(C_P, J) \quad (9)$$

(Gur, 2013) proposed an example of such procedures. It should be noted that propeller power depends on torque and angular speed. Torque can be viewed as the resistive force due to rotation. Torque causes a twist from the hub towards the tip axis and is therefore undesirable.

## 2.6 Experimental Setup

The experimental studies were carried out by examining the propeller thrust generated on ground. The orientation and location of the accelerometer used during these tests are given in Fig. 4. The data were read from the Burster 8524-6020 type load cell placed on the engine test stand (relative linearity deviation:  $\pm 0.25\%$ ). The obtained data were later compared with the current numerical values.

## 3. Results and Discussion

### 3.1 Comparison between Numerical and Experimental Results of Thrust

Fig. 5 shows the comparison between CFD and experimental results. A maximum of 1700N were achieved with a maximum engine speed., Increasing propeller revolutions up to 3100 RPM tends to raise the thrust value further. This would be expected due to increased air component across the blades creating higher-pressure difference in order to accelerate aircraft, hence thrust increased. As can be seen from the graph (Fig. 5), experimental data are in close proximity with data obtained from Cradle scFLOW. There is a slight difference between the experimental and simulation results. This difference is observed because wind, speed and/or similar factors are not included in the simulation environment.

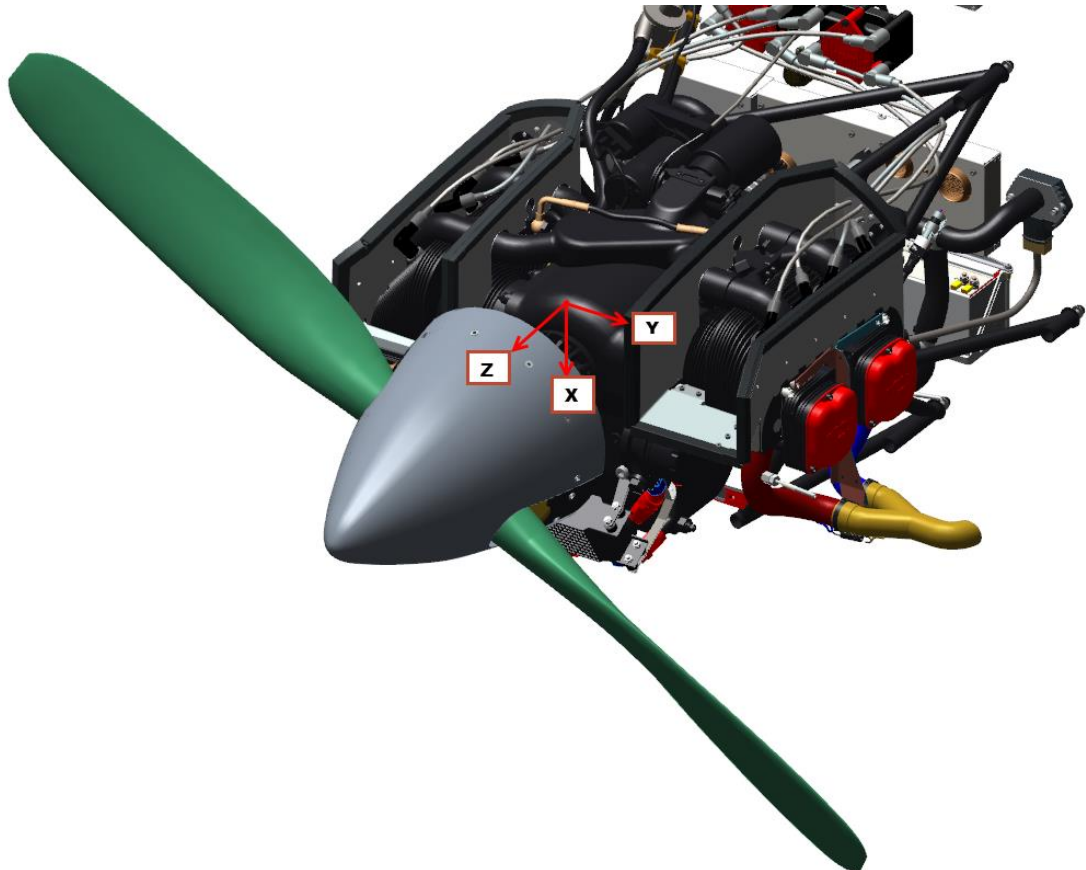


**Fig. 4.** Accelerometer attachment point and orientation of the coordinate system.

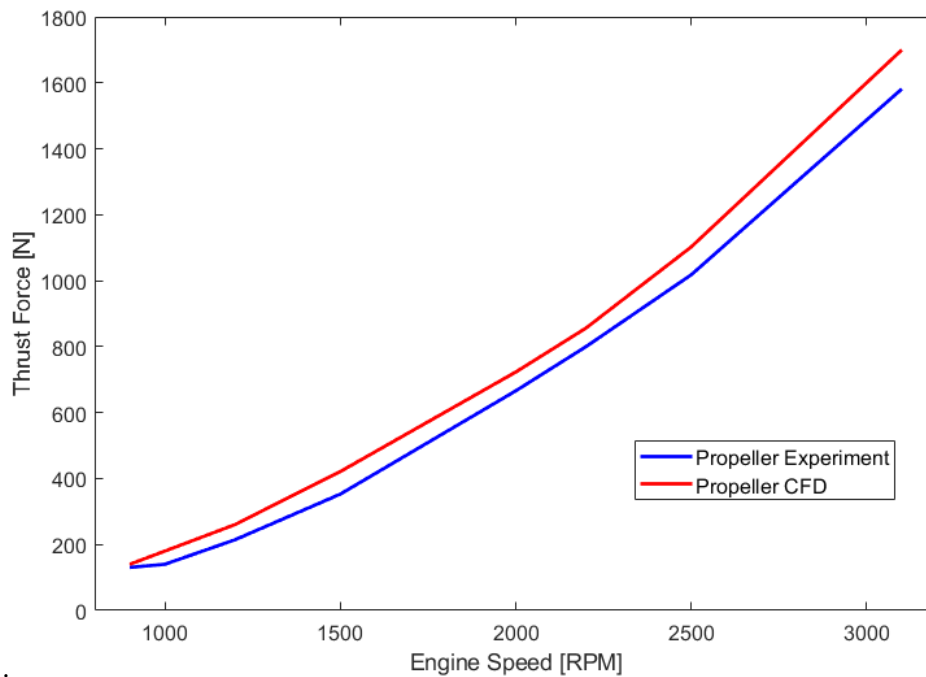


Fig. 5. Comparison between numerical and experimental results for thrust.

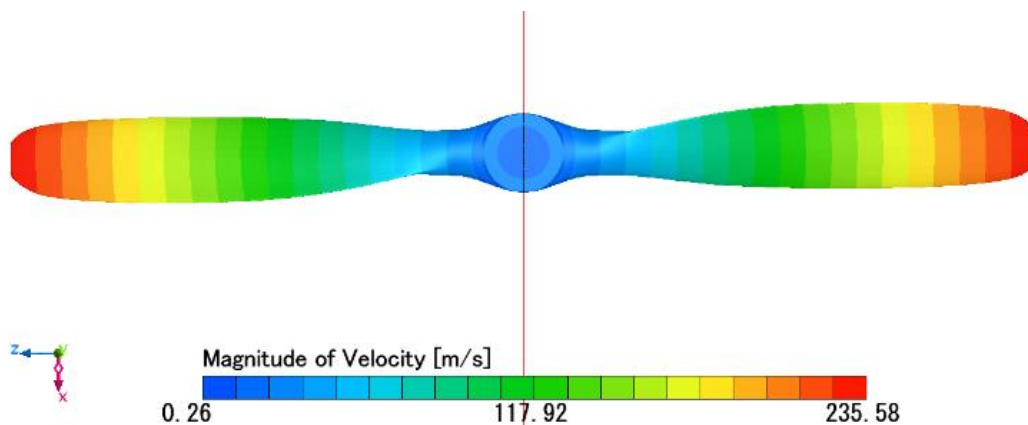


Fig. 6. Velocity distribution along the propeller.

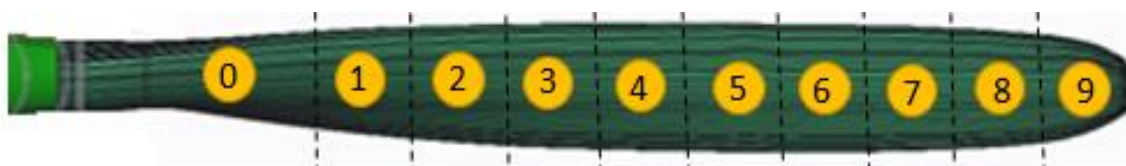


Fig. 7. Propeller sections.

### 3.2 Aerodynamic performance characterization of a propeller

It is a well-known concept that velocity distribution on the propeller varies according to the pressure distribution. It increases proportionally from the hub to the tip. Fig. 6 clearly shows the speed differences that gradually occur on the propeller. This distribution in speed values is evidence that the drag effect created by the propeller increases from the hub to the tip, as in theory (Marcus *et al.*, 2018). This would be expected, because when the rotating object is away from the center of rotation, the faster it moves.

In addition to the fixed pitch of the propeller, the amount

of twisting also plays a role in shaping the fluidity and subsequently changing the values of the acting forces. The twist angle generally changes the angle of attack of the profile on the propeller, causing a decrease from the bottom of the blade to the tip, and then a non-linear lifting and drag force occurs (a decrease in force is expected at the tip point) as agreement with (Marcus *et al.*, 2018). The propeller sections are showing in Fig. 7. Fig. 8 (a) and (b) illustrate lift and drag forces obtained over the propeller surface. It can be seen that both drag and lift forces are increased up to some point around section 6 and then reduced as expected due to variation occurs at an angle of blades.

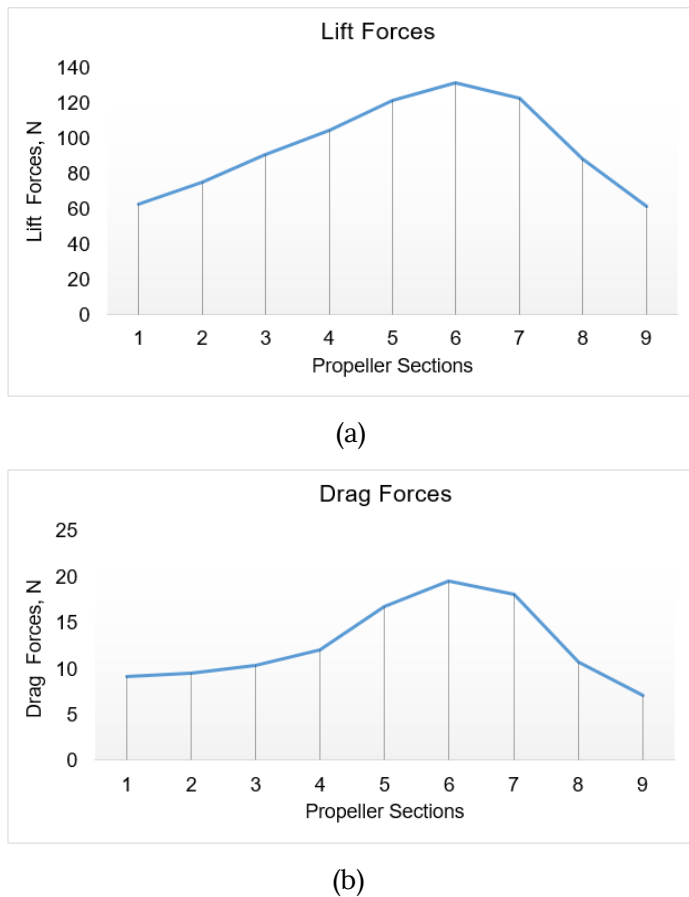


**Fig. 8.** Aerodynamic Forces produced by the propeller model (a) Lift and (b) Drag forces

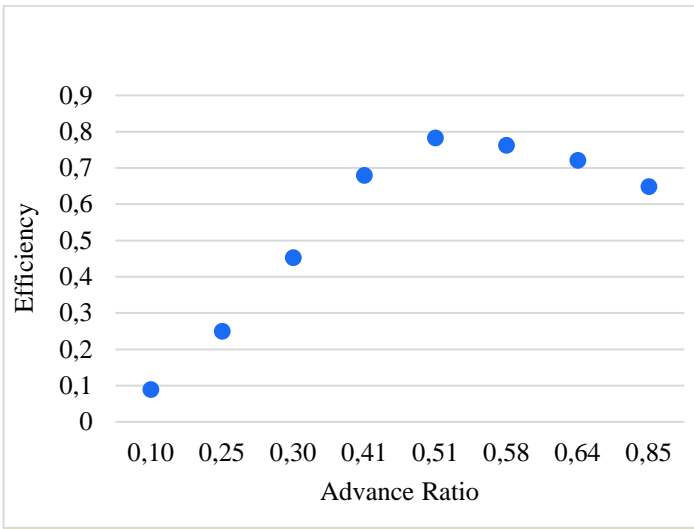
Having the right distribution of lift and drag along the propeller blade often points out airfoils' composition in the blade. When the blade rotates, the propeller blade tip rotates faster than the blade section closer to the hub. Hence, the selection of airfoil along the blade is crucial due to this very reason.

Drag depends on several geometry properties including the airfoil shape, camber, thickness, etc., and on the operating conditions, Reynolds number, Mach number, and angle of attack. As aforementioned, the propeller model includes a twist section, which generates higher load (both lift and drag) values. Regarding drag force (Fig. 8(b)), the maximum drag occurs at approximately 60% of the propeller length. This corresponds to the region where both the twist and angle of attack of the propeller are at their highest. Beyond this point, the forces acting on the propeller surface decrease. A similar trend is observed for the lift force as well (see Fig. 8(a)).

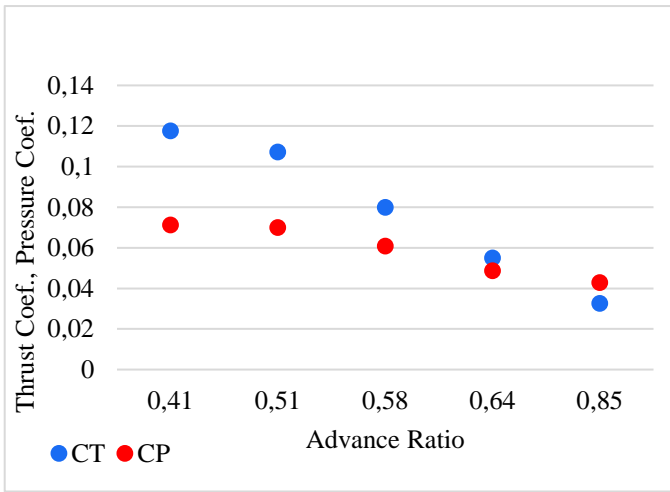
In the conceptual design phase or sometimes before that, the efficiency of the propeller is needed for designers to calculate the maximum thrust value of an aircraft. This thrust value will be used to define endurance of an aircraft. In this regard, analytical methods suggested to identify the propeller efficiency (Glauert, 1935). Fig. 9 (a) indicates proposed propeller efficiency by changing advance ratio ( $J$ ). It is worth

mentioning that advance ratio depends on velocity, RPM and propeller's diameter. It can be seen that maximum propeller efficiency ( $\eta=0.79$ ) achieved at  $J=0.51$ . Since efficiency is inversely proportional to the power coefficient, the propellers with higher power coefficient have lower efficiency. The data points show that as the Advance Ratio ( $J$ ) increases, the efficiency of the propeller initially increases, reaches a peak, and then begins to decrease. At very low Advance Ratios ( $J = 0.10$ ), the efficiency is very low. This is typical for situations where the propeller is spinning rapidly, but the forward speed is very low, such as during takeoff or when the air vehicle is stationary. As  $J$  increases ( $J = 0.51$  to  $J = 0.64$ ), the efficiency of the propeller peaks ( $J = 0.51$ ). This range represents the optimal operating condition for the propeller, where it is most effective at converting engine power into thrust. At higher Advance Ratios ( $J > 0.64$ ), the efficiency starts to decrease. This indicates that at higher speeds (relative to the propeller's rotational speed), the propeller becomes less efficient, likely due to aerodynamic losses and the reduced ability to generate thrust. For maximum fuel efficiency and performance, the aircraft should aim to operate at or near the Advance Ratio that corresponds to the peak efficiency. Consequently, the maximum efficiency occurs at a moderate Advance Ratio, suggesting that there is an optimal range of operating conditions where the propeller performs best. Low efficiency at very low and very high Advance Ratios indicates that the propeller is not well-suited for those conditions. At low  $J$ , the propeller is not effective because the forward speed is too low, and at high  $J$ , the propeller is less efficient because it cannot generate sufficient thrust relative to the power input. For maximum fuel efficiency and performance, the aircraft should aim to operate at or near the Advance Ratio that corresponds to the peak efficiency.

Moreover, Fig. 9 (b) illustrates the propeller thrust and power coefficient values versus advance ratio which play an important role in determining the power required to rotate the propeller. Taking as reference value of advance ratio ( $J=0.51$ ) at which the propeller efficiency is highest,  $C_T$  and  $C_P$  values are found as 0.1 and 0.07, respectively. Looking details in graph, the x-axis represents the Advance Ratio ( $J$ ), which is the ratio of the forward speed of the aircraft to the product of the propeller's rotational speed and diameter. The y-axis represents the values of the Thrust Coefficient ( $C_T$ ) and the Power Coefficient ( $C_P$ ). According to general trends, as the Advance Ratio ( $J$ ) increases from 0.41 to 0.85, both  $C_T$  and  $C_P$  decrease. Thrust Coefficient ( $C_T$ ) starts higher at lower advance ratios and decreases as the advance ratio increases. This indicates that the propeller is more effective at generating thrust at lower advance ratios (higher relative rotational speeds).



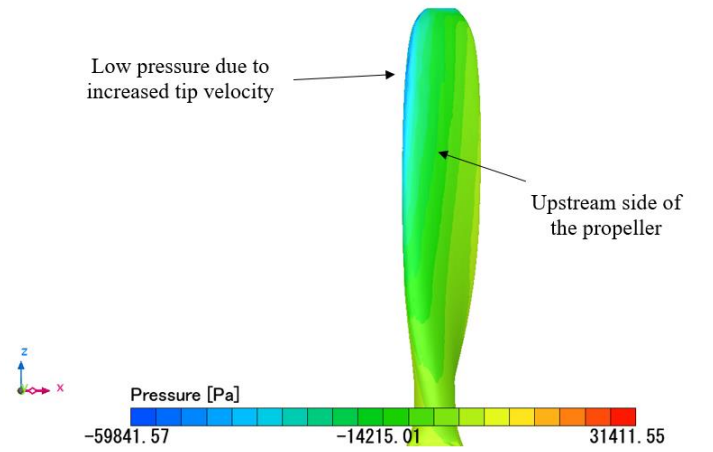
(a)



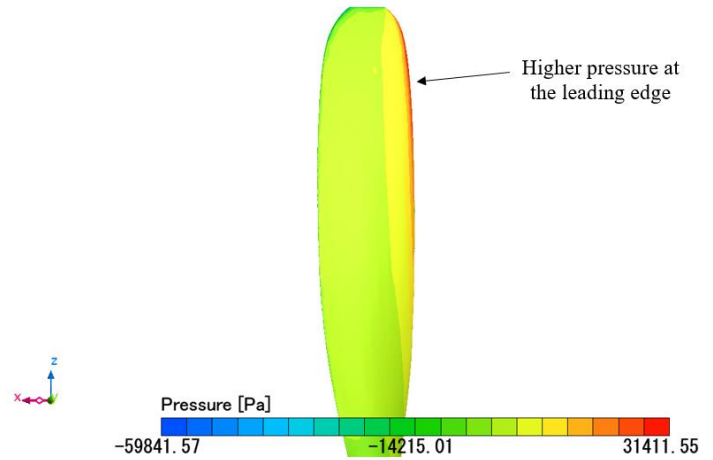
(b)

**Fig. 9.** Propeller performance values: (a) Propeller Efficiency and (b) Propeller Thrust Coefficient and Pressure Coefficient

Power Coefficient ( $C_p$ ) also decreases with increasing advance ratio, but it does so more gradually compared to  $C_T$ . At lower Advance Ratios (e.g.,  $J = 0.41$ ): The propeller produces more thrust relative to power absorbed, indicated by higher  $C_T$  values. This is typical for takeoff or low-speed operations. At higher Advance Ratios (e.g.,  $J = 0.85$ ): Both  $C_T$  and  $C_p$  are lower, meaning that the propeller is operating in a more efficient regime, where less thrust and power are needed as the vehicle is moving faster. This is more representative of cruise conditions. The decreasing trend of both  $C_T$  and  $C_p$  with increasing  $J$  suggests that as the forward speed increases (relative to propeller speed), the propeller becomes less effective at generating thrust, and the power required to maintain that thrust also decreases. This graph is useful for understanding the performance of a propeller across different operating conditions, particularly how effective it is at converting rotational power into thrust at various speeds.



(a)



(b)

**Fig. 10.** Pressure distribution over the propeller: (a) pressure contours on the upstream side of the propeller (3100RPM) and (b) pressure contours on the downstream side of the propeller (3100RPM)

Fig. 10 (a) and (b) show the pressure contours on the propeller structure. With constant RPM (3100), the speed on the propeller sections increased proportionally from hub to tip. This causes a gradual decrease in pressure due to the increase in velocity from the hub to the tip as agreement with (Krishnan et al., 2009). Furthermore, the higher pressure is seen as expected at the front point where the propeller meets the fluid towards the direction of rotation. The downstream side of the propeller shows evenly distributed higher pressure; this flow creates a pressure difference with the unevenly distributed low pressure on the upstream and downstream sides, thus producing thrust.

#### 4. Conclusions

Characterizing the aerodynamic performance of a propeller is essential for applications ranging from aviation to marine propulsion. It delivers insights that aid in the design process, ensuring that propellers perform

optimally under targeted operating conditions. In general, the fixed pitch produced propeller model has been analyzed aerodynamically in this research. As a result of this analysis, considering maximum 3100 RPM value;

- Propeller provided a thrust value of 1700N. This value was compared with the data obtained from experimental studies and the notable match was achieved.
- Aerodynamic performance data are considered; proposed propeller model was found to have 0.79 efficiency value at  $J=0.51$ .
- Thrust coefficient and pressure coefficient values are found as 0.1 and 0.07, respectively.
- When looking at the fluidity of the model, similar observation was achieved with theory.

As future work, the full range of efficiency of the propeller can be achieved by taking measurements at different RPM values, and the optimum angle of the propeller can be found by measurements made with different pitch angles.

### Acknowledgment

This research is supported by Lentatek Aerospace, Aviation and Technology Inc. - R&D center, under 'Indigenous Propeller Project', No: AGTMPR90482.

### CRediT Author Statement

**Erdogan Kaygan:** Conceptualization, Methodology, Software, Visualization, Investigation, Data curation, Writing- Original draft preparation. **Doğukan Doğan:** Methodology, Software, Data curation, Writing- Original draft preparation. **Ozan Mahir Alpogut:** Investigation, Supervision, Validation, Writing- Reviewing and Editing.

### Nomenclature

$C_L$	: Lift coefficient
$C_D$	: Drag coefficient
$C_T$	: Thrust coefficient
$C_P$	: Power coefficient
$\eta$	: Propeller efficiency
$T$	: Thrust, N
$\rho$	: Density, kg/m <sup>3</sup>
$n$	: Rotational speed, rev/s
$D$	: Diameter, m
$J$	: Advance ratio

$V$	: Freestream velocity, m/s
$c$	: Chord length, m
$r$	: Radial distance from hub centre, m
$R$	: Propeller radius, m
$\mu_t$	: Turbulent viscosity
$\beta$	: Pitch angle

### References

- Alakashi, A. M. and Basuno, I. B. (2014). Comparison between Structured and Unstructured Grid Generation on Two Dimensional Flows Based on Finite Volume Method (FVM), *Int. J. Mining, Metall. Mech. Eng.*
- Asl, H. H., Monfared, A. R. K. and Manouchehr, R. (2017). Experimental investigation of blade number and design effects for a ducted wind turbine., *Renewable Energy* 105.
- Bertetta, D., Brizzolara, S., Gaggero, S., Viviani, M., & Savio, L. (2012). CPP propeller cavitation and noise optimization at different pitches with panel code and validation by cavitation tunnel measurements. *Ocean Engineering*, 53, 177-195.
- Brandt, J. and Selig, M. (2011). Small-Scale Propeller Performance at Low Speeds – Online Database, 49th AIAA Aerospace Sciences Meeting, Orlando, FL.
- François G. Schmitt. (2007). About Boussinesq's turbulent viscosity hypothesis: historical remarks and a direct evaluation of its validity. *Comptes Rendus Mécanique*, 335 (9-10), pp.617-627. [ff10.1016/j.crme.2007.08.004](https://doi.org/10.1016/j.crme.2007.08.004). [ffhal-00264386](https://doi.org/10.1016/j.crme.2007.08.004)
- Glauert, H. (1935). "Airplane Propellers," *Aerodynamic Theory: A General Review of Progress*, edited by Durand, F. W., Vol. 4, Springer, Berlin.
- Gur, O. (2013). Practical Propeller Efficiency Model, *Proceedings of the 53rd Israel Annual Conference on Aerospace Sciences*, Technion-Israel Institute of Technology Haifa, Israel.
- Houghton and Carpenter., 2005. *Aerodynamics for Engineering students*, fourth edition.
- Kaidi, S., Smaoui, H. and Sergent, P. (2012). CFD Investigation of Mutual Interaction between Hull, Propellers, and Rudders for an Inland Container Ship in Deep, Very Deep, Shallow, and Very Shallow Waters, *J. Waterw. Port, Coastal, Ocean Eng.*, vol. 144, no. 6.
- Kang, T., and Park., W.G. (2013). "Numerical investigation of active control for an S809 wind turbine airfoil," *Int. J. Precis. Eng. Manuf.*, vol. 14, no. 6, pp. 1037-104.

- Krishnan, P.S., Sathian, S. P. (2009). Numerical Investigation of VE-7 Airplane Propeller through CFD, Proceedings of ICEAE 2009.
- Kutty, H. A., Parvathy, R. and Akshay, M. (2017). Performance analysis of small scale UAV propeller with slotted design. 2nd International Conference for Convergence in Technology (I2CT), pp. 695-700. IEEE. <https://doi.org/10.1109/i2ct.2017.8226219>
- Lieser, J. A., Lohmann, D. and Rohardt, C. H. (1997). "Aeroacoustic design of a 6-bladed propeller." *Aerospace science and technology*, no. 6: 381-389. [https://doi.org/10.1016/s1270-9638\(97\)90012-2](https://doi.org/10.1016/s1270-9638(97)90012-2)
- Marcus, E. A. P., Vries, R. de, Kulkarni, A. Raju and Veldhuis, L. L. M. (2018). Aerodynamic Investigation of an Over-the-Wing Propeller for Distributed Propulsion, AIAA, Doi: 10.2514/6.2018-2053
- McCormick, B. W. (1994). *Aerodynamics, Aeronautics and Flight Mechanics*, John Wiley & sons Inc., second edition.
- Ol, M., Zeune, C., and Logan, M. (2008). Analytical/Experimental Comparison for Small Electric Unmanned Air Vehicle Propellers, AIAA Paper 2008-7345,
- Osborne, Reynolds (1895). On the Dynamical Theory of Incompressible Viscous Fluids and the Determination of the Criterion. *Philosophical Transactions of the Royal Society of London A*. 186: 123164. doi:10.1098/rsta.1895.0004. JSTOR 90643
- Ramzi, M., Bois, G., Abderrahmane, G. and De Constantine, R. (2011). "Numerical Study of Passive Control with Slotted Blading in Highly Loaded Compressor Cascade at Low Mach Number," *Int. J. Fluid Mach. Syst.*, vol. 4, no. 1, pp. 97-103.
- Rezaeiha, A., Hamid M. and Bert B. (2019). On the accuracy of turbulence models for CFD simulations of vertical axis wind turbines. *Energy*180: 838-857. <https://doi.org/10.1016/j.energy.2019.05.053>
- Sanjeevi, K., Sathish, P. & Sathian, Sarith. (2009). Numerical Investigation of VE-7 Airplane Propeller through CFD. IISc Centenary International Conference and Exhibition on Aerospace Engineering (ICEAE 2009), Bangalore, India
- Seeni, A. (2019). Aerodynamic Performance Characterization of Slotted Propeller: Part B Effect of Angle. *INCAS Bulletin*11, no. 4: 155-170. <https://doi.org/10.13111/2066-8201.2019.11.4.14>
- Seeni, A. and Rajendran, P. (2020). CFD Analysis of a Novel Propeller Design Operating at Low Reynolds Number. In: Rajendran, P., Mazlan, N., Rahman, A., Suhadis, N., Razak, N., Abidin, M. (eds) *Proceedings of International Conference of Aerospace and Mechanical Engineering 2019*, Springer, Singapore. [https://doi.org/10.1007/978-981-15-4756-0\\_13](https://doi.org/10.1007/978-981-15-4756-0_13)
- Seeni, A., Ismail, F., and Rajendran, P. (2020). The Aerodynamic Performance Characteristics of a Grooved Propeller Using a RANS solver: Effect of Groove Geometry and Positioning of Multiple Grooves. *Proceedings of the International Conference on Innovations in Thermo-Fluid Engineering and Sciences [ICITFES - 2020]* NIT Rourkela, India.
- Singh, P. and Nestmann, F. (2011). "Experimental investigation of the influence of blade height and blade number on the performance of low head axial flow turbines." *Renewable Energy*36, no. 1: 272-281. <https://doi.org/10.1016/j.renene.2010.06.033>
- Song X, Qi Y, Zhang M, Zhang G, Zhan W (2019) Application and optimization of drag reduction characteristics on the flow around a partial grooved cylinder by using the response surface method. *Eng Appl Comput Fluid Mech* 13(1):158-176
- Tian, W., Song, B., Van Zwieten, J. H. and Pyakurel, P. (2015). Computational fluid dynamics prediction of a modified savonius wind turbine with novel blade shapes, *Energies*, vol. 8, no. 8, pp. 7915-7929.
- Versteeg, H. and Malalasekera, W. (1995). *An introduction to Computational Fluid Dynamics*. Pearson Prentice Hall.
- Wald, Q. R. (2006). *The aerodynamics of propellers*, Progress in Aerospace Sciences, Volume 42, Issue 2, 2006, Pages 85-128
- Xie, Y., Chen, J., Qu, H., Xie, G., Zhang, D., and Moshfeghi, M. (2013). Numerical and Experimental Investigation on the Flow Separation Control of S809 Airfoil with Slot, *Math. Probl. Eng.*, vol. 2013.
- Zao, N., Dhanak, M., and Su, T. (2019). "Improved performance of a slotted blade using a novel slot design." *Journal of Wind Engineering and Industrial Aerodynamics*189: 34-44. <https://doi.org/10.1016/j.proeng.2015.11.309>



## Analyzing the New Global Reporting Format from the Pilot Perspective

Arif Tuncal<sup>1\*</sup>, Ufuk Erol<sup>2</sup>,

<sup>1</sup> International Science and Technology University, Department of Aviation Systems and Technologies, Warsaw, Poland

[arif.tuncal@istu.edu.pl](mailto:arif.tuncal@istu.edu.pl) - 0000-0003-4343-6261

<sup>2</sup> Istanbul Esenyurt University, Istanbul, Türkiye

[ufukerol@esenyurt.edu.tr](mailto:ufukerol@esenyurt.edu.tr) - 0000-0001-5711-2423



### Abstract

Global Reporting Format (GRF) for runway surface conditions is an important step in improving aviation safety by providing standardized and consistent information. The aim of the study was to evaluate the effectiveness and implementation of the GRF among pilots. Qualitative and quantitative methods were used to comprehensively address all aspects of the study. The sample consisted of 266 pilots. Findings showed that the majority of pilots are aware of the GRF and value its benefits, such as consistency, reliability, and standardized terminology, despite it being a new method. Pilots highlighted the role of the GRF in improving communication and decision-making for take-off and landing. However, the study also identified challenges, including occasional inaccuracies in reporting, the need for real-time updates, the length of ATIS reports, and inconsistencies in application across airports in different regions. These issues highlight the human factor and the need to develop the GRF. The study makes a unique contribution by highlighting both the practical benefits and the challenges of the GRF from the perspective of the pilots. It is recommended that future research include a more diverse sample of pilots from all regions and that technical studies be undertaken to compare runway surface conditions with aircraft performance under the GRF. This will provide a more complete understanding of the effectiveness of the GRF and identify areas for further improvement.

### Keywords

Aviation Safety  
Global Reporting Format  
Pilot  
Runway Excursions  
Runway Safety

### Time Scale of Article

Received 12 July 2024  
Revised until 11 October 2024  
Accepted 15 October 2024  
Online date 27 November 2024

### 1. Introduction

Runway excursions stand out as the highest risk category, highlighting the critical importance of runway safety, especially in the field of aviation safety (Kornstaedt, 2019). According to global estimates, the aviation industry incurs an average of \$500 million per month in costs due to runway-related accidents and incidents (Van Eekeren et al., 2018). Between 2013 and 2022, a total of 125 runway excursion accidents were

recorded. Notably, there were no runway excursion accidents in the year 2021, in contrast to the seven runway excursion accidents that occurred in the year 2022. It is important to note that the runway excursion accident rate in 2022, at 0.22, was lower than the 5-year average (2018-2022) runway excursion accident rate, which was calculated at 0.27 per million sectors. Of the 125 runway excursion accidents, 98 were related to passenger flights, and the remaining 27 were related to cargo flights (International Air Transport Association [IATA], 2023). In the initial reports for the year 2023,

\*: Corresponding Author Arif Tuncal, [arif.tuncal@istu.edu.pl](mailto:arif.tuncal@istu.edu.pl)

DOI: [10.23890/IJAST.vm05is02.0204](https://doi.org/10.23890/IJAST.vm05is02.0204)

runway excursion incidents accounted for the highest number of accidents and serious incidents (European Union Aviation Safety Agency [EASA], 2024). Furthermore, according to the 2023 edition of the Statistical Analysis of Commercial Aircraft Accidents 1958-2023 by Airbus (2024), a significant portion, nearly 60%, of fatal accidents and hull losses occurred during the landing phase. In addition, runway excursion incidents ranked as the third most important factor in fatal accidents (18%) and the most critical factor in hull losses (36%) between 2003 and 2023 (Airbus, 2024). Therefore, it is essential to carefully monitor and assess runway conditions to mitigate the associated risks.

Based on runway excursion accident/incident reports, it is generally recognized that several factors are involved. Some studies identified factors such as runway and touchdown zone characteristics, flight control during approach, aircraft malfunction, weather factors, and runway surface and braking conditions (Garcia et al., 2023). Weather factors were identified as a contributing factor to runway excursions (Distefano and Leonardi, 2019; Maeng et al., 2012). Specifically, weather conditions such as wet or flooded runways, rain, and thunderstorms were found to increase the risk of runway excursions (Chang et al., 2016; Karyawan, 2021).

The risk of runway excursions can be increased during wet weather conditions, mainly due to the accumulation of water on the runway surface (Pasindu et al., 2016). It was emphasized that the effect of accumulated water on runway friction and aircraft braking ability, which can contribute to excursions, can potentially lead to loss of control during landing or take-off (Brassard et al., 2019; Klein-Paste, 2018; Kornstaedt and Lignee, 2010; Niu et al., 2021; Procházka and Kameník, 2013). In addition, pilots identified wet or containment runways and weather issues as important risk factors for runway excursions (Brassard et al., 2022; Chang et al., 2016; Distefano and Leonardi, 2019).

The reporting, assessment, and accuracy of runway surface conditions for contaminated runways can pose risks to braking performance and overall runway safety (Brassard et al., 2022; Sama et al., 2022). Poor runway braking performance is a significant factor in runway excursions (Hu et al., 2022).

International Civil Aviation Organization (ICAO) introduced a new Global Reporting Format (GRF) for runway surface conditions based on human observers on 4 November 2021. The purpose of the GRF is to improve runway safety and minimize the risks associated with poor braking performance, as well as to provide a standardized method for reporting and assessing runway surface conditions worldwide. By providing a consistent and accurate description of runway surface conditions, the GRF helps flight crews make informed

decisions during take-off and landing, especially in adverse weather conditions (Brassard et al., 2022; Chen et al., 2022; ICAO, 2021; Tuncal et al., 2021).

The previous method of reporting runway surface conditions showed significant variation between regions and airports, potentially causing confusion and inconsistencies for pilots. The lack of a standardized method for reporting runway surface conditions made it difficult for pilots to make informed decisions during take-off and landing, particularly in adverse weather conditions. In addition, many safety incidents were attributed to runway surface conditions, and investigations revealed deficiencies in the accuracy and timeliness of assessment and reporting methods outlined in ICAO regulations and guidance material (Kornstaedt, 2019).

The GRF is based on objective criteria to reduce subjectivity and promote consistency in the assessment of runway surface conditions. The integration of standardized terminology and runway condition codes serves to increase the accuracy and consistency of reported data. The Runway Condition Assessment Matrix (RCAM), as shown in Table 1, plays a key role in providing a consistent method for assessing runway conditions, taking into account factors such as surface type, contaminants, depth, and coverage. The RCAM, as defined by ICAO, categorizes runway conditions on a scale from 6 (dry) to 0 (the worst conditions, including wet ice and snow on ice). This classification enables pilots to assess the expected braking performance in different weather and runway conditions, providing vital information for safe landing and take-off. This standardized approach not only improves safety but also facilitates more efficient and effective airport operations by providing pilots with accurate information (Bylica and Pashkevich, 2022; Vorobyeva et al., 2020).

Based on observations linked to RCAM, a Runway Condition Report (RCR) is generated. RCR includes mandatory aircraft performance assessments and an optional situational awareness section, integrating operational details for taxiways and aprons, as shown in Figure 1. RCR is disseminated via ATIS (Automatic Terminal Information Service) and/or SNOWTAM.

The GRF outlines information on runway surface conditions to be provided to the pilot, in particular with regard to aircraft performance, and requires manufacturers to provide performance data for the evaluation of the pilot, particularly on winter-contaminated runways (ICAO, 2020). The relationship between the landing distance factors (LDFs) and runway condition code (RWYCC) based on the landing performance data and related procedures determined for the existing conditions during landing for turbojets and turboprops is presented in Table 2.

GG EADBZQZX EADNZQZX EADSZQZX  
 170229 EADDYNYX  
 SWEA0151 EADD 02170225  
 (SNOWTAM 0151  
 EADD  
 02170055 09L 5/5/5 100/100/100 NR/NR/03 WET/WET/WET SNOW  
 02170135 09R 5/2/2 100/50/75 NR/06/06 WET/SLUSH/SLUSH  
 02170225 09C 2/3/3 75/100/100 06/12/12 SLUSH/WET SNOW/WET SNOW  
 RWY 09L SNOW BANK R20 FM CL. RWY 09R ADJ SNOW BANKS. TWY B POOR. APRON NORTH POOR)

**Fig. 1.** RCR example (ICAO, 2018, p. APP 4-11)

**Table 1.** The Runway Condition Assessment Matrix (RCAM) (ICAO, 2019)

Runway Condition Code	Runway Condition Description	Pilot- Reported Braking Action
6	Dry	No action required
5	Frost Wet (The runway surface is covered by any visible dampness or water up to and including 3 mm depth) Slush (Up to and including 3 mm depth) Dry Snow (Up to and including 3 mm depth) Wet Snow (Up to and including 3 mm depth)	Good
4	Compacted Snow (15°C and lower outside air temperature)	Good to Medium
3	Wet (“Slippery Wet” Runway) Dry Snow or Wet Snow (any depth) on top of Compacted Snow Dry Snow (More than 3 mm depth) Wet Snow (More than 3 mm depth) Compacted Snow (Higher than -15°C outside air temperature)	Medium
2	Standing Water (More than 3 mm depth of water or slush) Slush (More than 3 mm depth of water or slush)	Medium to Poor
1	Ice	Poor
0	Wet Ice Water on top of Compacted Snow Dry Snow or Wet Snow on top of Ice	Less than poor

**Table 2.** Landing distance factors (ICAO, 2020)

RWYCC	6	5	4	3	2	1
Turbojet, no reverse	1.67	2.6	2.8	3.2	4.0	5.1
Turbojet, with reverse	1.67	2.2	2.3	2.5	2.9	3.4
Turboprop	1.67	2.0	2.2	2.4	2.7	2.9

Pilots are integral to the success of the GRF for runway surface conditions in several critical ways. They play a key role in receiving and understanding GRF reports and use standardized data to inform their take-off and landing decisions, communicating this information to Air Traffic Control (ATC) units such as Tower and Approach Control to ensure coordinated operations via reports, particularly in adverse weather conditions. Pilots also contribute to the accuracy of the reports by providing first-hand feedback on runway conditions, thus ensuring the accuracy of the information presented in the GRF. The observed braking capability and lateral control are dependent on a number of factors, including the aircraft type, weight, and the specific runway segment utilized for braking. Pilots are required to classify these conditions using a set of standardized terms, which are as follows: GOOD, GOOD TO MEDIUM, MEDIUM,

MEDIUM TO POOR, POOR, and LESS THAN POOR (ICAO, 2019). This data is essential for flight planning, as pilots rely on standardized terminology and runway condition codes to make informed decisions about aircraft performance, braking, and landing distances, especially in challenging weather conditions. In addition, pilots provide essential feedback on the effectiveness of the GRF in improving the accuracy and consistency of runway surface condition reporting, contributing to continuous improvement and ensuring aviation safety.

Therefore, evaluations based on the pilots' experience with the GRF are crucial. This valuable feedback allows the new method to be continually improved, potential problems to be identified, and improvements to be made in problem areas. The information shared by pilots helps the aviation industry provide more accurate and consistent reports, ultimately improving aviation safety.

This pilot input will improve the effectiveness of the GRF. It will ensure safer aviation operations in the future.

The aim of the study is to examine pilot feedback on the GRF and to highlight its crucial role in the continuous improvement of this new approach. By examining how pilot experience helps to identify potential problems and implement necessary improvements, the research aims to highlight its essential role in advancing aviation safety. Ultimately, the aim is to clarify how pilot input enhances the effectiveness of the GRF, ensuring that future aviation operations are conducted with even greater safety and precision.

## 2. Method

The survey-based research approach was used as the most suitable method for the study. Survey-based data collection is an efficient method for gathering insights from large and diverse samples in academic research (Blondel et al., 2006; Kelley et al., 2003; Schoenherr et al., 2015).

### 2.1 Data collection process and instrument

A survey was conducted online between March and June 2024, with 266 pilots participating. The survey was divided into three sections: demographic information, questions about the reporting of runway surface conditions, and evaluations of the GRF. The third section of the survey used a 5-point Likert scale ranging from "(1) Strongly Disagree" to "(5) Strongly Agree".

Participants were informed of the aims of the research and their consent was obtained on a voluntary basis. The survey was designed to ensure the protection of participants' personal information and confidentiality throughout the process. Ethical approval for the study was obtained from İstanbul Esenyurt University Ethics Committee with decision number 2024-02 on 05.03.2024.

### 2.2 Statistical analysis

Descriptive statistics, including frequency (n), percentage (%), mean, and standard deviation, were initially used in the study. Factor analysis was used to assess the validity of the survey and Cronbach's alpha test was used to assess its reliability. After confirming the normality assumption as specified by Tabachnick and Fidell (2019), independent samples t-test and one-way ANOVA (Analysis of Variance) were performed for group comparisons. These statistical analyses were carried out using IBM SPSS (Statistical Package for the Social Sciences) v27.

In addition, a qualitative methodology was used. Responses to the open-ended question about concerns related to the GRF were subjected to qualitative content analysis to identify underlying themes. Data from 26

pilots who responded to the open-ended question were analyzed. Each response was coded, with initial coding carried out independently by two researchers to ensure reliability. Any discrepancies were resolved through discussion. To enhance the validity of the findings, the final codes and themes identified were reviewed by an expert in aviation safety and reporting, and their feedback was incorporated into the analysis. The findings are presented in thematic sections, each supported by direct quotes from participants. Quotes are identified by a "p" followed by a number, with codes in brackets at the end of each statement. This comprehensive qualitative methodology provides a clear understanding of pilots' concerns with the GRF and offers valuable insights for improving its design and implementation.

## 3. Results

### 3.1 Demographic information

The demographic information of the pilots is presented in Table 3. The data provides insight into the age, gender, title, experience, type of operation, flight frequency, and region of the 266 pilots who participated in the study.

The majority of pilots were in the 35-44 age group, representing 38.3% (n=102) of the sample. The 25-34 age group represented 27.8% (n=74) of the sample, while the 45-54 age group represented 19.2% (n=51). The group aged 55 and over represented 8.3% (n=22) of the sample. The smallest group was that of pilots aged 18-24, with 6.4% (n=17) of the total sample. The sample was evenly split between captains and co-pilots, with each group comprising 50.0% (n=133) of the total number.

The distribution of experience among pilots was fairly balanced, with each category (less than 5 years, 5-10 years, and 11-20 years) representing 26.7% (n=71) of the sample. Pilots with more than 20 years of experience represented 19.9% (n=53) of the sample. The majority of pilots worked in the airline sector, representing 87.6% (n=233) of the sample. Other types of operations (including private, charter, military, training, etc.) accounted for 12.4% (n=33). The largest group of pilots, representing 39.8% (n=106) of the sample, were those who flew more than 20 flights per month. The next largest group, representing 30.1% (n=80) of the sample, were those who flew between 10 and 20 flights per month, with less than 10 flights per month. The majority of pilots, representing 73.7% (n=196) of the sample, flew primarily in Europe. The remaining 26.3% (n=70) of the sample consisted of pilots flying in other regions.

### 3.2 Runway surface conditions

The survey included a question asking if pilots had ever been involved in an incident or accident caused by runway surface conditions. The majority of pilots, 94.4%,

indicated that they had not experienced such an incident. However, 5.6% of pilots stated that they had been involved in an incident or accident due to runway surface conditions.

Of those pilots who responded in the affirmative to the question of whether they had experienced an incident or accident, several factors were identified as contributing to these events, as shown in Table 4. The most frequently cited factor was “incorrect or incomplete runway surface information”, cited by 30.95%. This highlights the critical need for accurate and comprehensive runway surface condition reports to ensure flight safety. Inadequate procedures were cited by 16.67% of pilots, indicating that procedural errors or omissions also play a significant role in such incidents. A further 14.29% of pilots cited “inconsistent runway surface condition reports with aircraft performance” as a factor, indicating the importance of matching runway condition reports with actual aircraft performance data. In addition, 14.29% of pilots cited unexpected or sudden changes in weather conditions, highlighting the unpredictable nature of weather and its impact on runway safety. A further 11.90% of pilots stated that aircraft malfunctions

or technical problems were a contributing factor. This suggests that mechanical problems can compound the challenges posed by adverse runway conditions. Non-standard terminology was cited by 9.52% of pilots, indicating that unclear or inconsistent language in reports can lead to misunderstandings and safety risks. Finally, fatigue was cited by 2.38% of pilots, highlighting the role of human factors in aviation safety.

The survey included questions on the frequency with which pilots encounter runway surface conditions that require reporting and the frequency with which they encounter conditions that are not accurately reported. The responses are summarized in Table 5 and Table 6.

Regarding the frequency with which they encounter reportable runway surface conditions, 54.9% of pilots indicated that this occurs rarely (less than 10% of the time). A further 34.6% of pilots reported that they sometimes encountered such conditions (between 10% and 50% of the time). A smaller percentage, 3.0%, reported that they often (more than 50% of the time) encounter conditions that require reporting. Only 7.5% reported that they had never encountered runway surface conditions requiring a report.

**Table 3.** Demographic info

		n	%
Age	18-24 years old	17	6.4
	25-34 years old	74	27.8
	35-44 years old	102	38.3
	45-54 years old	51	19.2
	55 years old or older	22	8.3
Title	Captain	133	50.0
	Co-pilot	133	50.0
Experience	< 5 years	71	26.7
	5-10 years	71	26.7
	11-20 years	71	26.7
	> 20 years	53	19.9
Operation type	Airline	233	87.6
	Other (Private. Charter. Military. Training etc.)	33	12.4
Flight frequency	Less than 10 flights	80	30.1
	10-20 flights	80	30.1
	More than 20 flights	106	39.8
Flight region	Europe	196	73.7
	Other	70	26.3
Total		266	100.0

**Table 4.** Factors involved in the accident or incident caused by runway surface conditions

Incorrect or incomplete runway surface information	%30.95
Inappropriate procedures	%16.67
Inconsistent runway surface conditions report with aircraft performance	%14.29
Unexpected or sudden changes in weather condition	%14.29
Aircraft malfunction or technical issue	%11.90
Non-standard terminology	%9.52
Fatigue	%2.38

**Table 5.** Encounter runway surface conditions that require reporting

	%
Never	7.5
Rarely (less than 10% of the time)	54.9
Sometimes (between 10% and 50% of the time)	34.6
Often (more than 50% of the time)	3.0

**Table 6.** Frequency of encountering inaccurately reported runway surface conditions

	%
Never	10.9
Seldom (less than 10% of the time)	71.1
Occasionally (between 10% and 50% of the time)	15.0
Frequently (more than 50% of the time)	3.0

Regarding the frequency of encountering inaccurate runway surface conditions, the majority of pilots, 71.1%, reported that this occurred rarely, less than 10% of the time. In addition, 15.0% of pilots reported that they sometimes encountered inaccurate reports, ranging from 10% to 50% of the time. Similar to the previous question, 3.0% of pilots indicated that they often (more than 50% of the time) encounter inaccurate reported conditions. A small proportion, 10.9%, stated that they had never encountered inaccurately reported runway surface conditions

### 3.3 Global reporting format (GRF) perspective

#### *Awareness*

The survey included a question asking whether pilots had heard of the new GRF for assessing runway surface conditions. The majority of pilots, 79.7%, said they had heard of the new GRF. However, 20.3% of pilots said they had not heard of it.

Of those who responded in the affirmative to the question of whether they had heard of the new GRF, several sources were cited as the means by which they became aware of the format, as shown in Table 7. The most commonly cited source was “company training/notification”, cited by 54.85% of pilots. This underlines the crucial role of organizational training and communication in disseminating important updates such as the GRF.

Online resources or publications were cited by 17.09% of pilots, indicating that digital materials also play an important role in raising awareness. Discussions with colleagues or aviation professionals were cited by 11.73% of pilots, highlighting the importance of peer communication in spreading knowledge about the GRF.

A notice or circular issued by the Civil Aviation Authority (CAA) or Air Navigation Service Provider (ANSP) was mentioned by 8.93% of pilots, indicating the role of official communication in informing pilots. Finally, 7.40% of pilots indicated that research or personal interest was

a source of awareness, suggesting that individual initiatives also contribute to understanding new reporting formats.

Factor analysis of the survey items developed to assess pilot GRF revealed a KMO (Kaiser–Meyer–Olkin) of 0.886 ( $>0.50$ ), Bartlett's sphericity test with a p-value of 0.000 ( $\chi^2=959.775$ ;  $df:15$ ;  $p<0.001$ ), and a single-factor explained variance of 68.503% ( $>60\%$ ). The inter-item correlation values ranged from 0.514 to 0.707 ( $>0.30$ ), the factor loadings were between 0.624 and 0.719 ( $>0.32$ ), and the Cronbach's alpha value was 0.907 ( $>0.50$ ), all of which are considered acceptable levels (Büyüköztürk, 2020; George and Mallery, 2003; Hair et al., 2019; Tabachnick and Fidell, 2019).

The evaluation of the GRF revealed some key aspects regarding its effectiveness and reception among pilots, as shown in Table 8. The mean scores and standard deviations provide a comprehensive understanding of pilots' perceptions. Firstly, pilots found the GRF to provide a consistent and reliable assessment of runway surface conditions, with a mean score of 4.06 and a standard deviation of 0.740, indicating relatively low variability in responses and broad agreement among pilots. Secondly, the GRF was appreciated for its standardized terminology across airports and regions, as evidenced by the highest mean score of 4.23 and a standard deviation of 0.789. This high score demonstrates the importance of consistent language in ensuring clear communication, with responses showing a strong consensus among pilots. In terms of providing detailed and accurate information for take-off and landing decision-making, the GRF achieved a mean score of 4.09 and a standard deviation of 0.752. This indicates moderate variability in the responses, with a strong consensus on the effectiveness of the GRF in this regard. The ease of use and understanding of the GRF in all conditions received a mean score of 4.12 and a standard deviation of 0.897, indicating considerable agreement among pilots on this attribute. In terms of facilitating better communication between pilots, air traffic control,

and airport operators, the GRF achieved a mean score of 4.16 and a standard deviation of 0.841. This reflects moderate variability and strong agreement on the role of the GRF in improving communication. Finally, the role of the GRF in reducing the risk of runway accidents and incidents caused by poor runway surface conditions was recognized with a mean score of 3.98 and a standard deviation of 0.805. Although slightly lower than the other scores, this still reflects a positive reception and indicates the contribution of the GRF to safety.

Table 9 shows the rating of the GRF based on the current job title, with a t-test used to assess the statistical significance of the results. The mean scores for captains and co-pilots were found to be almost identical, with captains scoring a mean of 4.1128 and co-pilots scoring a

mean of 4.1003. The results of the t-test indicated that there was no significant difference between the two groups ( $t = .153$ ,  $df = 264$ ,  $p = .878$ ).

Table 10 shows the GRF scores based on years of experience using one-way ANOVA. The groups had mean scores ranging from 4.0751 to 4.1289. The results of the ANOVA indicated that there were no significant differences between the different experience groups ( $F = .078$ ,  $p = .972$ ).

Table 11 shows the GRF scores based on the number of flights performed per month using one-way ANOVA. The mean scores for the groups ranged from 4.0042 to 4.1085. The ANOVA results indicated that there were no significant differences based on flight frequency ( $F = 1.856$ ,  $p = .158$ ).

**Table 7.** Source of GRF information

	%
Training/Notification provided by the company	54.85
Online resources or publications	17.09
Discussions with colleagues or aviation professionals	11.73
A notice or circular issued by the CAA or ANSP	8.93
Research or personal interest	7.40

**Table 8.** The mean score, standard deviation, skewness, and kurtosis of GRF survey

	Mean	Sd.	Skewness	Kurtosis
GRF provides consistent and reliable assessment of runway surface conditions.	4.06	.740	-.659	.880
GRF provides standardized terminology across all airports and regions.	4.23	.789	-.942	.887
GRF provides detailed and accurate information to take decisions about take-off and landing.	4.09	.752	-.579	.154
GRF is user-friendly and easy to understand in all conditions.	4.12	.897	-.895	.554
GRF enables better communication between pilots, air traffic control, and airport operators.	4.16	.841	-.958	.922
GRF reduces the risk of runway accidents and incidents caused by poor runway surface conditions.	3.98	.805	-.627	.364

**Table 9.** Evaluation of the GRF according to the current job title (t-test)

Groups	n	Mean	Sd.	t	Df.	p
Captain	133	4.1128	.64437	.153	264	.878
Co-pilot	133	4.1003	.68870			

**Table 10.** Evaluation of the GRF according to the experience (ANOVA)

Groups	n	Mean	Sd.	F	p	Dif.
< 5 years	71	4.0751	.60866	.078	.972	-
5-10 years	71	4.1150	.74140			
11-20 years	71	4.1127	.69281			
> 20 years	53	4.1289	.60944			

**Table 11.** Evaluation of the GRF according to the flight frequency per month (ANOVA)

Groups	n	Mean	Sd.	F	p	Dif.
Less than 10 flights	80	4.0042	.79731	1.856	.158	-
10-20 flights	80	4.2063	.55388			
More than 20 flights	106	4.1085	.62743			

*Challenges and considerations in implementing the GRF*

The following four themes emerged from the qualitative content analysis: (1) lack of clarity and training, (2) frequency and timeliness of updates, (3) specific operational concerns, and (4) international implementation issues.

*Theme 1: Lack of clarity and training*

Many pilots mentioned that the lack of standardization and clarity in the new GRF is a significant issue. Pilots noted that there are some problems and confusion in reporting via SNOWTAM and ATIS, particularly in relation to the measurement of pollution and braking efficiency (p90). It was highlighted that there is inconsistency between airports in how the format is applied, leading to misunderstandings and difficulties in interpretation (p62, p71). Pilots stated that this is particularly challenging when GRF parameters are not clearly described for take-off or landing performance tools (p61) and noted that the new format made the process more complex, with extended coding making it difficult to understand (p118, p115, p116). There is a call for regular and comprehensive training for all parties to adapt effectively to the new system (p153, p181, p126, p103).

*Theme 2: Frequency and timeliness of updates*

Several pilots emphasized the need for more frequent and timely updates, noting that updates should be more frequent to accurately reflect real-time runway conditions. Pilots mentioned that receiving old runway assessment reports can lead to discrepancies in actual conditions (p52, p149, p25) and said that airport operators sometimes use outdated observation parameters, which negatively affect performance calculations (p246).

*Theme 3: Specific operational concerns*

Pilots raised specific operational concerns related to the GRF, mentioning that the GRF format sometimes makes ATIS reports too long, especially for airports with multiple runways, and suggested simplified reporting methods such as terms like “valid for both runways” (p268, p223). It was noted that there is a need for greater confidence in the assessment methods used by airport operators, as there is a perceived lack of reliability in the current system (p113), and that some pilots prefer to use letters (e.g., good, medium) rather than numbers to describe runway conditions, as this is easier to understand (p18).

*Theme 4: International implementation and adaptation*

It was noted that global implementation of the GRF requires a universal approach, with pilots emphasizing that the format should be made universal across different regions, including North America and Asia

(p88). Pilots said that some countries have not fully adhered to the new format (p90). It was suggested that the adaptation of company performance calculation tools to the GRF format should be enforced by airport operators to ensure consistency and reliability (p61).

**4. Discussion**

The findings of the study provide important insights into the perception and implementation challenges of the GRF among pilots. The majority of pilots who participated in the study are well aware of the GRF, indicating successful dissemination of information by aviation authorities and operators. Most pilots found the GRF useful, citing its consistency, reliability, and standardized terminology as key benefits. However, the study also identified several challenges that need to be addressed to improve the effectiveness of the GRF.

The majority of pilots encounter situations that require reporting, underlining the need for reliable reporting and assessment systems for runway surface conditions. The presence of occasional inaccuracies in these reports poses a serious risk to flight safety. The GRF was developed to address these challenges by standardizing the terminology and procedures for reporting runway conditions, thereby reducing the risks associated with inconsistent or inaccurate reporting. In addition, GRF values are directly related to aircraft braking performance, making accurate reporting essential for safe take-off and landing operations. This underlines the critical role of the GRF in improving aviation communications and safety.

The GRF was highly regarded for its role in providing consistent and reliable assessments of runway surface conditions. Pilots appreciated the standardized terminology used across airports and regions, which simplifies communication and reduces the risk of misunderstandings. The ability of the format to provide detailed and accurate information for take-off and landing decisions was another significant benefit. The GRF was also praised for its user-friendliness and its contribution to better communication between pilots, air traffic control, and airport operators. Overall, the role of the GRF in improving aviation safety by reducing the risk of runway accidents and incidents caused by poor runway surface conditions was well received.

However, it is important to note that the average score for the role of the GRF in reducing the risk of runway accidents and incidents was slightly lower than for the other aspects. This may be influenced by various factors identified in runway incidents and accidents, such as inappropriate procedures, unexpected weather changes, aircraft malfunctions, and fatigue, as highlighted by study participants. Additionally, issues like incorrect or incomplete runway surface information

and non-standard terminology were also noted as contributing factors. The GRF aims to mitigate these risks by providing accurate and standardized information, which is critical to improving runway safety.

Despite the positive reception, the study highlighted several challenges to the implementation of the GRF. A key issue is the lack of standardization and clarity, particularly in the reporting of pollution and braking efficiency through SNOWTAM and ATIS. Inconsistencies in the application of the GRF at different airports lead to misunderstandings and difficulties in interpretation. To ensure effective adaptation to the new system, there is a clear need for comprehensive and regular training for all stakeholders.

The frequency and timeliness of updates was also a concern. Pilots emphasized the need for real-time updates to accurately reflect runway conditions, as out-of-date reports can lead to discrepancies and affect performance calculations. The importance of the lack of up-to-date runway conditions is further confirmed by Chang et al. (2016) in their research on risk factors associated with pilots in runway excursions. Specific operational concerns were also raised, such as the length of ATIS reports. The aircraft performance section of the GRF includes observation times, runway descriptions, runway codes, contamination percentage, depth, and type separately for each runway. This comprehensive reporting within the GRF contributes to the length of ATIS broadcasts, which include operational and critical meteorological information. Longer broadcasts can increase the workload in the cockpit.

Additionally, pilots expressed concerns about the perceived reliability of the assessment methods used by airport operators. Bylica and Pashkevich (2022) highlighted in their study that human factors are the main challenge in this regard. Currently, the GRF relies entirely on human observation and experience. To mitigate the risks associated with human factors in runway surface assessment, Pestana et al. (2021) presented an innovative approach using laser scanning equipment for automated runway inspection. Sama et al. (2022) developed a model that performs autonomous and automatic measurements using additional materials. Although the results obtained with this model are slightly different from those expected, the actual runway conditions are not significantly affected.

Global implementation of the GRF requires a more universal approach, in line with its original purpose. The pilots highlighted the importance of a consistent format across different regions, including North America and Asia. The lack of full compliance with the GRF in some countries is a challenge to its universal applicability. There is also a need for airport operators to align their

performance calculation tools with the GRF format to ensure consistency and reliability.

## 5. Conclusions

The aim of the study was to evaluate the new GRF for runway surface conditions, which represents a significant step forward in improving aviation safety worldwide. The GRF provides a standardized method for reporting and assessing runway surface conditions to provide more accurate and consistent information that can help reduce the risk of accidents and incidents caused by poor runway conditions. Early feedback from pilots and stakeholders has been positive, suggesting that the GRF has the potential to significantly improve aviation safety in the future.

Comprehensive evaluations were carried out using both quantitative and qualitative analysis to ensure a thorough assessment. This dual approach is particularly noteworthy as it incorporates direct feedback from pilots, the primary users of this new reporting format. By grounding the findings in practical, real-world experience, the study enhances the reliability and relevance of its findings. Such a multi-faceted evaluation underlines the importance of the new methodology and its potential impact on improving aviation safety.

The study has several limitations. The sample consisted mainly of pilots operating in Europe, which may limit the generalizability of the findings to other regions. In addition, the study focused on pilots' attitudes and perceptions without including technical assessments of runway surface conditions and aircraft performance. Future research should address these limitations by including a more diverse sample of pilots from different regions. It is also recommended that technical studies be conducted comparing runway surface conditions with aircraft performance under the GRF. Such studies would provide a more complete understanding of the effectiveness of the GRF and identify areas for improvement in its implementation.

In conclusion, while the GRF has been well received and offers several benefits, addressing the challenges identified and conducting further research will be critical to realizing its full potential in improving runway safety and operational efficiency. Aviation safety is paramount and continuous improvement of systems such as the GRF is essential to ensure the highest standards of safety and performance in the aviation industry.

## CRediT Author Statement

**Arif Tuncal:** Methodology, Investigation, Data curation, Visualization, Writing-Original Draft, Writing-Review and Editing, Formal Analysis. **Ufuk Erol:** Supervision,

Conceptualization.

Season in Poland. *Sustainability*, 15(1), 167. <https://doi.org/10.3390/su15010167>

## Nomenclature

ANOVA : Analysis of Variance

ANSP : Air Navigation Service Provider

ATIS : Automatic Terminal Information Service

CAA : Civil Aviation Authority

EASA : European Union Aviation Safety Agency

GRF : Global Reporting Format

IATA : International Air Transport Association

ICAO : International Civil Aviation Organization

RCAM : Runway Condition Assessment Matrix

RCR : Runway Condition Report

RWYCC : Runway Condition Code

Chang, Y. H., Yang, H. H., & Hsiao, Y. J., 2016. Human risk factors associated with pilots in runway excursions. *Accident Analysis & Prevention*, 94, 227-237. <https://doi.org/10.1016/J.AAP.2016.06.007>

Chen, X., Zhang, Q., Cheng, C., Zhou, X., & Yu, X., 2022. Accuracy Assessment of SRTM DEM, ASTER GDEM, AW3D30 DSM, and TanDEM-X 90 m DEM Based on Runway Elevation Data. In 2022 2nd International Conference on Big Data, Artificial Intelligence and Risk Management (ICBAR) (pp. 30-34). IEEE. <https://doi.org/10.1109/icbar58199.2022.00013>

Distefano, N., & Leonardi, S., 2019. Aircraft runway excursion features: a multiple correspondence analysis. *Aircraft Engineering and Aerospace Technology*, 91(1), 197-203. <https://doi.org/10.1108/AEAT-11-2017-0244>

European Union Aviation Safety Agency [EASA], 2024. Annual Safety Review (ASR) 2024. Available online at: <https://www.easa.europa.eu/en/document-library/general-publications/annual-safety-review-2024> (Accessed on 10 July 2024).

Garcia, J. S., Jaedicke, C., Leng Lim, G., & Truong, D., 2023. Predicting the Severity of Runway Excursions from Aviation Safety Reports. *Journal of Aerospace Information Systems*, 1-10. <https://doi.org/10.2514/1.I011145>

George, D., & Mallery, P., 2003. *SPSS for Windows step by step: A simple guide and reference*. 11.0 update (4th ed.). Boston: Allyn & Bacon.

Hair, J.F., Black, W.C., Babin, B. J., & Anderson, R.E., 2019. *Multivariate Data Analysis* (8th Edition). Hampshire: Cengage Learning.

Hu, J., Zhao, K., Zheng, P., Mi, C., Liu, W., & Gong, H., 2022. Nondestructive testing of the airfield pavement structural condition based on the GPR and HWD. In *Second International Conference on Testing Technology and Automation Engineering (TTAE 2022)* (Vol. 12457, pp. 139-145). SPIE. <https://doi.org/10.1117/12.2660552>

International Air Transport Association [IATA], 2023. Annual Safety Report. Available online at: <https://www.iata.org/en/publications/safety-report/interactive-safety-report/> (Accessed on 10 March 2024).

International Civil Aviation Organization [ICAO], 2018. Doc 10066, Procedures for Air Navigation Services - Aeronautical Information Management. ISBN 978-92-9258-597-6

International Civil Aviation Organization [ICAO], 2019.

## References

Airbus, 2024. Statistical Analysis of Commercial Aviation Accidents 1958 - 2023. Available online at: [https://accidentstats.airbus.com/wp-content/uploads/2024/02/20230873\\_A-Statistical-analysis-of-commercial-aviation-accidents-2024-version.pdf](https://accidentstats.airbus.com/wp-content/uploads/2024/02/20230873_A-Statistical-analysis-of-commercial-aviation-accidents-2024-version.pdf) (Accessed on 11 October 2024).

Blondel, B., Zein, A., Ghosn, N., Du Mazaubrun, C., & Bréart, G., 2006. Collecting population-based perinatal data efficiently: the example of the Lebanese National Perinatal Survey. *Paediatric and perinatal epidemiology*, 20(5), 416-424. <https://doi.org/10.1111/j.1365-3016.2006.00732.x>

Brassard, J. D., Beaulieu, A., Tremblay, M. M., & Momen, G., 2022. Assessment of Runway Surface Conditions by British Pendulum Testing under the Global Reporting Format Winter Conditions. *Applied Sciences*, 12(19), 9646. <https://doi.org/10.3390/app12199646>

Brassard, J. D., Laforte, C., Tremblay, M. M., & Volat, C., 2019. Runway deicing product anti/deicing performance assessment: review and future directions. *SAE Technical Paper 2019-01-1974*. <https://doi.org/10.4271/2019-01-1974>

Büyüköztürk, Ş., 2020. *Data Analysis Handbook for Social Sciences: Statistics, Research Design, SPSS Applications, and Interpretation* (27th Edition). Ankara: Pegem Academy

Bylica, A., & Pashkevich, A., 2022. Introduction of Global Reporting Format: Summary of the First Winter

- Cir 355, Assessment, Measurement and Reporting of Runway Surface Conditions, ISBN 978-92-9258-719-2
- International Civil Aviation Organization [ICAO], 2020. Doc 10064, Aeroplane Performance Manual, ISBN 978-92-9265-279-1
- International Civil Aviation Organization [ICAO], 2021. Implementation of Global Reporting Format for Runway Surface Conditions (GRF), Guidance based on management of change (MOC), Version 1.0
- Karyawan, I., 2021. Analysis of the causes and prevention of runway excursions. Analysis of the causes and prevention of runway excursions. In *Proceeding International Conference on Science (ICST) (Vol. 2, pp. 156-166)*.
- Kelley, K., Clark, B., Brown, V., & Sitzia, J., 2003. Good practice in the conduct and reporting of survey research. *International Journal for Quality in health care*, 15(3), 261-266. <https://doi.org/10.1093/intqhc/mzg031>
- Klein-Paste, A., 2018. Airplane braking friction on dry snow, wet snow or slush contaminated runways. *Cold regions science and technology*, 150, 70-74. <https://doi.org/10.1016/j.coldregions.2017.02.004>
- Kornstaedt, L., & Lignee, R., 2010. Operational Landing Distances, A new standard for in-flight landing distance assessment. *Safety*, 10, 1-5.
- Kornstaedt, L., 2019. GRF Methodology History and Development Process. GRF Workshop, Frankfurt
- Maeng, S. K., Jung, Y. S., Choi, J. K., & Kwon, B. H., 2012. Development of runway incursion risk assessment checklist. *Journal of the Korean Society for Aviation and Aeronautics*, 20(1), 46-54. <https://doi.org/10.12985/KSAA.2012.20.1.044>
- Niu, Y., Jiang, X., Meng, F., Wang, R., Ju, G., Zhang, S., & Meng, Z., 2021. Techniques and methods for runway friction measurement: A review of state of the art. *IEEE Transactions on Instrumentation and Measurement*, 70, 1-17. <https://doi.org/10.1109/TIM.2021.3092062>
- Pasindu, H. R., Fwa, T. F., & Ong, G. P., 2016. Analytical evaluation of aircraft operational risks from runway rutting. *International Journal of Pavement Engineering*, 17(9), 810-817. <https://doi.org/10.1080/10298436.2015.1019501>
- Pestana, G., Reis, P., & da Silva, T. R., 2021. Smart Surveillance of Runway Conditions. In *Intelligent Transport Systems, From Research and Development to the Market Uptake: 4th EAI International Conference, INTSYS 2020, Virtual Event, December 3, 2020, Proceedings 4 (pp. 252-270)*. Springer International Publishing.
- Procházka, J., & Kameník, M., 2013. Contaminated Runway Operations-Adverse weather. *MAD-Magazine of Aviation Development*, 1(4), 3-7. <https://doi.org/10.14311/MAD.2013.04.01>
- Sama, D., Gnabahou, D. A., Ouattara, F., Zidouemba, M., Diassibo, O., & Sandwidi, S. A., 2022. Global Reporting Format (GRF) Application Automation for Runway Surface Conditions in West Africa. *Advances in Aerospace Science and Technology*, 7(3), 135-145. <https://doi.org/10.4236/aast.2022.73009>
- Schoenherr, T., Ellram, L. M., & Tate, W. L., 2015. A note on the use of survey research firms to enable empirical data collection. *Journal of Business Logistics*, 36(3), 288-300. <https://doi.org/10.1111/jbl.12092>
- Tabachnick, B.G., & Fidell, L.S., 2019. *Using Multivariate Statistics (Seventh Edition)*. New Jersey: Pearson.
- Tuncal, A., Uslu, S., & Dursun, E., 2021. A Milestone to Enhance Runway Safety: The New Global Reporting Format. *Revista de Investigaciones Universidad del Quindío*, 33(1), 168-178. <https://doi.org/10.33975/riuq.vol33n1.551>
- Van Eekeren, R., Wright, S., & Čokorilo, O., 2018. Early cost safety analysis of runway events. *International Journal for Traffic & Transport Engineering*, 8(3), 261-270. [http://dx.doi.org/10.7708/ijtte.2018.8\(3\).01](http://dx.doi.org/10.7708/ijtte.2018.8(3).01)
- Vorobyeva, O., Bartok, J., Šišán, P., Nechaj, P., Gera, M., Kelemen, M., Polishchuk, V., & Gaál, L., 2020. Assessing the contribution of data mining methods to avoid aircraft run-off from the runway to increase the safety and reduce the negative environmental impacts. *International Journal of Environmental Research and Public Health*, 17(3), 796. <https://doi.org/10.3390/ijerph17030796>



## Wildlife Hazard Management – An Intuitive Web-Based Risk Matrix for Airport Stakeholders

Haoruo Fu<sup>1</sup>, Chien-tsung Lu<sup>2\*</sup>, Ming Cheng<sup>3</sup>, Mengyi Wei<sup>4</sup>

<sup>1</sup> School of Aviation & Transportation Technology, Purdue University, 1401 Aviation Drive, West Lafayette, Indiana, USA  
fu361@purdue.edu - 0009-0003-6790-0230

<sup>2</sup> School of Aviation, Southern Illinois University, 1263 Lincoln Dr, Carbondale, Illinois, USA  
chientsung.lu@siu.edu - 0000-0002-9435-7427

<sup>3</sup> College of Safety Science & Engineering, Civil Aviation University of China, 2898 Jinbei Road, Dongli District, Tianjin, China  
figocm@163.com - 0000-0002-2198-3523

<sup>4</sup> School of Aviation & Transportation Technology, Purdue University, 1401 Aviation Drive, West Lafayette, Indiana, USA  
wei205@purdue.edu - 0009-0004-3043-1415



### Abstract

The purpose of this study is to employ Tableau and R to create a web-based system for early wildlife hazard alerts at airports, addressing the critical need for timely and accurate wildlife risk assessments. The historical data displays specific time, season, altitude, size, and frequency related to wildlife reports in the United States for wildlife management and planning. A user-friendly risk assessment tool, utilizing the Shiny platform, offers airport stakeholders color-coded risk levels by analyzing wildlife hazard report frequencies and sizes. This research distinguishes itself by integrating advanced data visualization techniques and a dynamic risk matrix tool, enhancing proactive wildlife hazard management. The proposed tool is demonstrated through its application at Los Angeles (LAX) and Sacramento (SAC) International Airports, and algorithm is shared to readers for implementation across various airport settings. This paper enhances understanding of wildlife hazard reports, empowering airport stakeholders to make proper decisions for proactive wildlife control, ultimately improving airport safety and sustainability.

### Keywords

Airport Safety  
Wildlife Hazard  
Bird Strike  
Risk Management  
Shiny

### Time Scale of Article

Received 16 February 2024  
Revised until 2 July 2024  
Accepted 12 July 2024  
Online date 28 December 2024

### 1. Introduction

In 2019 alone, there have been reported to be 17,228 wildlife strikes on aircraft and over 227,000 between 1990 and 2019 in the United States (Federal Aviation Administration [FAA], 2021). Wildlife hazards, predominantly associated with avian animals, pose a potential life-threatening issue, especially during takeoff and landing, with a majority of incidents occurring below 2000 ft above ground level (AGL) (Dolbeer, 2013). Noteworthy incidents like the U.S. Airways Flight 1549 in 2009 (“The Miracle on the Hudson”) emphasize the

criticality of wildlife hazard management near busy airports (National Transportation Safety Board [NTSB], 2010). Challenges extend to general aviation airports, exemplified by a 2016 runway incident at Lancaster Airport, Philadelphia, involving a Beechcraft and a deer, resulting in aircraft structural damage and an emergency landing (Kunkle, 2021). This issue is not confined to the United States, affecting other countries, particularly those with emerging economies and increasing airline services (Aircraft Accident Investigation Bureau of India, 2014). The study underscores the necessity of persistent wildlife hazard

\*: Corresponding Author Chien-tsung Lu, [chientsung.lu@siu.edu](mailto:chientsung.lu@siu.edu)  
DOI: [10.23890/IJAST.vm05is02.0205](https://doi.org/10.23890/IJAST.vm05is02.0205)

management for continual and significant benefits to airport safety.

This study introduces an innovative, web-based risk matrix tool to enhance airport wildlife hazard management. This tool uses historical data visualization and risk assessment, offering stakeholders an intuitive and user-friendly platform to understand wildlife risk levels effectively. Building on the fundamental risk assessment methodologies, the developed Shiny application serves as an interface that allows airport operators to dynamically interact with wildlife strike data without requiring extensive coding knowledge.

## 2. Literature review

Airport safety experts believe that initiating a proactively approach to reduce the likelihood and severity of wildlife events around airports is imperative. Believing in this main theory, airports comply with mandatory policies and seek to develop a system or tool that could effectively help operators mitigate wildlife hazards around airports. Per 14 CFR 139.337, Wildlife Hazard Management, it requires airports to report wildlife strikes and implement a wildlife hazard management plan including assessment and controls (14 CFR 139.337, n.d.). Currently, data collection practices are normally conducted via the Form 5200-7 for airports (FAA, 2013) and pilot reports through the FAA web-based reporting system (FAA, n.d.), which enable the Administrator to archive wildlife hazard reports and monitor the potential impact that could arise.

### Airport Wildlife Safety Management System

Clearly, the assurance of airport safety has evolved from a reactive to a proactive fashion. The rationality of a proactive wildlife safety management is to detect hazards or threats and mitigate them before resulting in an accident. To be more proactive in promoting aviation safety, in 2010, the *Airline Safety and Federal Aviation Administration Extension Act 2010* was passed and ratified to mandate airline Safety Management Systems (SMS) implementation including Safety Policy, Safety Risk Management, Safety Assurance and Safety Promotion. Since August 30, 2010, the FAA Order 5200.11 has started to mandate airport Safety Risk Management (SRM) noting that from June 1, 2011, all categories of hub airports, from June 1, 2012, all FAR 139 airports, from June 1, 2013, all towered airports and from June 1, 2014, all National Plan of Integrated Airport Systems (NIPAS) airports must conduct SRM (FAA, August 30, 2010). That said, the SRM process could be used to enable airports to identify wildlife hazards, determine potential risks, and design appropriate risk mitigation strategies in a systemic manner (FAA, 2007, p. 5).

In the Transportation Research Board (TRB) Airport Collaborative Research Program (ACRP) *Synthesis 37 Lessons Learned from Airports Safety Management Systems Pilot Studies* (Transportation Research Board [TRB], 2012), the researchers surveyed on FAA pilot study airports revealed that there are challenges associated with the implementation of SMS such as the usage of risk matrix while available documents and manuals are conceptually simple. While the FAA is maintaining a voluntary wildlife hazard reporting system, the risk matrix is nebulous to the airport managers when deciding the risk level. In 2015, the TRB published a handbook, *Applying an SMS approach to wildlife hazard management*, that promulgates a proactive and risk-based method to manage wildlife (TRB, 2015). The advanced Wildlife Hazard Management Risk Assessment Tool (WHaMRAT) was introduced and the risk severity table was provided to airport operators to calculate severity score (Table 1). However, the likelihood or probability score was up to a subjective assumption.

### Approaches of Wildlife Hazard Management

U.S. Department of Agriculture (USDA) estimates that about thirty-eight wildlife strikes are reported to the FAA every day. Around ninety-seven percent of wildlife strikes involve birds (U.S. Department of Agriculture, [USDA], 2017). DeVault, Blackwell, Seamans, and Belant (2016) extracted wildlife hazard records from the Federal Aviation Administration National Wildlife Strike Database for Interspecific Avian Hazards. Their research presented comprehensive descriptive statistics on wildlife reports, encompassing details such as species involved, seasonal variations, group sizes, corresponding bird masses, and the extent of damage caused by the strikes. The findings underscored the need for prioritized control measures, guided by the severity of wildlife, to enhance aviation safety. ICAO has also identified that certain land uses near airports, such as parking lots, theaters, food outlets, and golf courses, contribute to wildlife hazards. To mitigate wildlife hazards, the advocated strategies include technical and managerial formats. Technical formats such as installing fences, bar wired roofs, perched light poles, ultrasound repellents, wildlife radars, etc. On the managerial side, making the nearby wetlands around airports inhabitable is the key such as cutting grass and trees, draining water, and covering up the storm drainage system (FAA, 2020).

Annex 14 of ICAO focuses on assessing and mitigating wildlife hazards in and around airports, which mandates member states to assess the extent of wildlife hazards, implement wildlife reduction measures, and prevent attraction sites (Blackwell, DeVault, Fernandez-Juricic, and Dolbeer, 2009). Despite the implementation of various wildlife detection and control initiatives, the lingering potential threat persists and intermittently results in damages.

**Table 1.** Advanced-Version WHaMRAT, Severity scores.

	Severity	Guild	Severity	Guild	Severity
Waterbirds		Shorebirds		Rodents	
Waterbirds < 300g	1	If flocks < 20	4	Rodents < 100g	1
Waterbirds 300-999g	2	If flocks ≥ 20	5	Rodents 100-599g	2
Waterbirds 1000-1999g	3	Shorebirds < 300g	1	Rodents 600-1999g	3
Waterbirds 2000-3999g	4	Shorebirds 300-999g	2	Rodents 2000-9999g	4
Waterbirds > 4000g	5	Gulls/Terns		Rodents > 10000g	5
Seabirds		If flocks < 10	4	Lagomorphs	
Seabirds < 300g	1	If flocks ≥ 10	5	Lagomorphs 100-599g	2
Seabirds 300-999g	2	Gulls/Terns < 300g	1	Lagomorphs 2000-9999g	4
Seabirds 1000-1999g	3	Gulls/Terns 300-999g	2	Bats	
Seabirds 2000-3999g	4	Gulls/Terns 1000-1999g	3	Bats < 100g	1
Pelicans/Comorants		Pigeons/Doves		Bats 100-600g	2
Pelicans 1000-1999g	3	If flocks < 20	4	Mesomammals	
Pelicans 2000-3999g	4	If flocks ≥ 20	5	Mesomammals 100-599g	2
Pelicans > 4000g	5	Pigeons/Doves < 300g	1	Mesomammals 600-1999g	3
Waders		Pigeons/Doves 300-999g	2	Mesomammals 2000-9999g	4
If flocks ≥ 5	5	Parrots		Mesomammals > 10000g	5
Waders 300-999g	2	Parrots < 300g	1	Canids	
Waders 1000-1999g	3	Parrots 300-999g	2	Canids 2000-9999g	4
Waders 2000-3999g	4	Parrots 1000-3999g	3	Canids > 10000g	5
Waders > 4000g	5	Aerial Foragers	1	Felids	
Waterfowl		Woodland Birds	1	Felids 600-1999g	3
If flocks < 5	4	Corvids		Felids > 2000g	5
If flocks ≥ 5	5	If flocks < 15	2	Hooved	
Waterfowl 300-999g	2	If flocks ≥ 15	5	Hooved > 10000g	4
Waterfowl 1000-1999g	3	Corvids < 300g	1	Bears	
Waterfowl 2000-3999g	4	Corvids 300-999g	2	Bears > 10000g	5
Waterfowl > 4000g	5	Corvids 1000-1999g	3	Criteria for Score	Severity
Raptors/Vultures/Owls		Grassland Birds	1	0-99g	1
Raptors < 300g	1	Blackbirds/Starlings		100-599g	2
Raptors 300-999g	2	If flocks < 100	4	600-1999g	3
Raptors 1000-1999g	3	If flocks ≥ 100	5	2000-9999g	4
Raptors 2000-3999g	4	Miscellaneous		Greater than 10000g	5
Raptors > 4000g	5	Miscellaneous < 300g	1		
Upland Game Birds		Miscellaneous 300-999g	2		
Upland Game Birds < 300g	1	Miscellaneous 1000-1999g	3		
Upland Game Birds 300-999g	2	Miscellaneous > 4000g	5		
Upland Game Birds 1000-1999g	3	Criteria for Score	Severity		
Upland Game Birds 2000-3999g	4	Less than 300g	1		
Upland Game Birds > 4000g	5	300-999g	2		
Cranes	5	1000-1999g	3		
		2000-3999g	4		
		Greater than 4000g	5		

Note: TRB. (2015). ACRP Report 145, pps. 50-51.

## Aviation Safety Models and the Purpose of the Study

There are leading risk management models often used by aviation researchers and practitioners such as SHELL (Software, Hardware, Environment, and Liveware) (Edwards, 1972), James Reason's Swiss Cheese (Reason, 1990), Bowtie barrier-based risk assessment (FAA, 2017), Heinrich's Safety Pyramid (1959), and Human Factors Analysis and Classification System (HFACS) (Wiegmann & Shappell, 2017), just to name a few. However, tracking wildlife animals such as foxes, raccoons, deer, and various bird species are often challenging until they make an appearance in the vicinity of airport facilities or after the post-strike investigation. Having said that, when formulating strategic plans to address wildlife issues, modern safety researchers strive to identify and mitigate potential hazards at the project's outset using a risk matrix. Lu, Schreckengast and Jia (2011) delivered a low-cost airport hazard reporting system using MySQL and On-Line Analytic Processing (OLAP) data mining skills for the budget-constrained airports. However, the hazard report was simply stored and presented on a map while the corresponding risk was not calculated. Fu, Lu and Ji (2023) applied MATLAB to propose a Risk Assessment Matrix of Operational Safety (RAMOS) for aviation safety enthusiasts. Yet coding and troubleshooting become particularly intricate, especially when updating the two independent variables—probability and severity—in response to new archived reports. Following the aforementioned studies, a study centers on advanced wildlife hazard analytics involving examining independent variables to customize a risk matrix besides presenting data dashboards is imperative.

Our approach enhances proactive risk assessment by leveraging diverse factors, contributing to a more robust system for ensuring airport safety. Thus, to propose another layer of proactive defense, identifying an airport's potential wildlife hazards and preparing countermeasures would be plausible.

To do so, the purpose of this study is twofold: (1) to display descriptive data visualization based on archived wildlife reports between January 1, 2000, and October 17, 2023, and (2) to design and propose a user-friendly wildlife risk matrix tool for stakeholders. Utilizing Tableau and R for data visualization provides a clear and interactive platform for stakeholders (including airport operators, air traffic management, drone pilots, regulatory officials, etc.) to understand the distribution and frequency of wildlife strikes. The risk matrix tool, developed using the Shiny platform, offers an intuitive interface for airport operators to assess risk levels based on historical data. This tool aims to enhance proactive wildlife hazard management by allowing users to interact dynamically with the data, making informed decisions without extensive coding knowledge.

## 3. Technical Methodology

This project serves a dual purpose in shaping a wildlife hazard reference figures/tables and facilitating a wildlife risk matrix exercise. It aims to achieve the following objectives: (1) Utilizing Tableau and R language (Appendix I) to create visualizations of wildlife hazard reports. These visualizations offer vital insights and information crucial for stakeholders, enabling informed decision-making processes. The visualization tools present an intuitive overview of wildlife strike data extracted from the FAA wildlife strike database from January 1, 2000, to October 17, 2023. (2) The Shiny Online (Appendix II) is used to generate coding and risk level for two selected airports, Los Angeles and Sacramento International Airports to showcase the proposed risk matrix tool.

## 4. Result and Finding

To give a holistic view of airport wildlife hazards in the U.S., between January 1, 2000, and October 17, 2023, the total case count of wildlife strike reports in the United States is 258,218, which include 147,282 (57.25 %) near-miss, 2,756 (1.06%) substantial damage 58 (.0224%) destroyed cases and others.

Near miss. The top five airports for receiving near-miss wildlife reports, as indicated in Figure 1 below, are Dallas/Fort Worth (6,930, 4.70%), Austin-Bergstrom (2,588, 1.76%), Houston George Bush (2,280, 1.55%), Dallas Love Field (1,822, 1.24%), and Houston William-Hobby Airports (1,570, 1.07%).

Despite unspecified species, Mourning Doves (2,709, 1.84%) are associated with the highest number of near-miss reports, followed by Rock Pigeons (821, 0.56%), Killdeer (760, 0.51%), and Barn Swallows (646, 0.44%) (Fig. 2).

Figure 3 below illustrates that the majority of near-miss cases occurred during the Approach phase, followed by incidents during Landing Rolls, Climb, and Take-off Run phases.

**Minor damage cases.** For the cumulative count of minor damage, it tallies up to 6,013 (2.328%) from January 1, 2000, to October 17, 2023. To streamline readers' comprehension, the authors focus on airports that contribute a minimum of 30 wildlife hazard reports for the initial data analysis. The findings reveal that within the contiguous United States, California, Florida, and Texas stand out as the states experiencing the most frequent wildlife strikes resulting in minor damages (Fig. 4), with recorded cases of 502, 470, and 339 incidents, respectively. Furthermore, there are two notable peaks in case counts observed during the months of April and October regarding minor damage cases (Fig. 5).

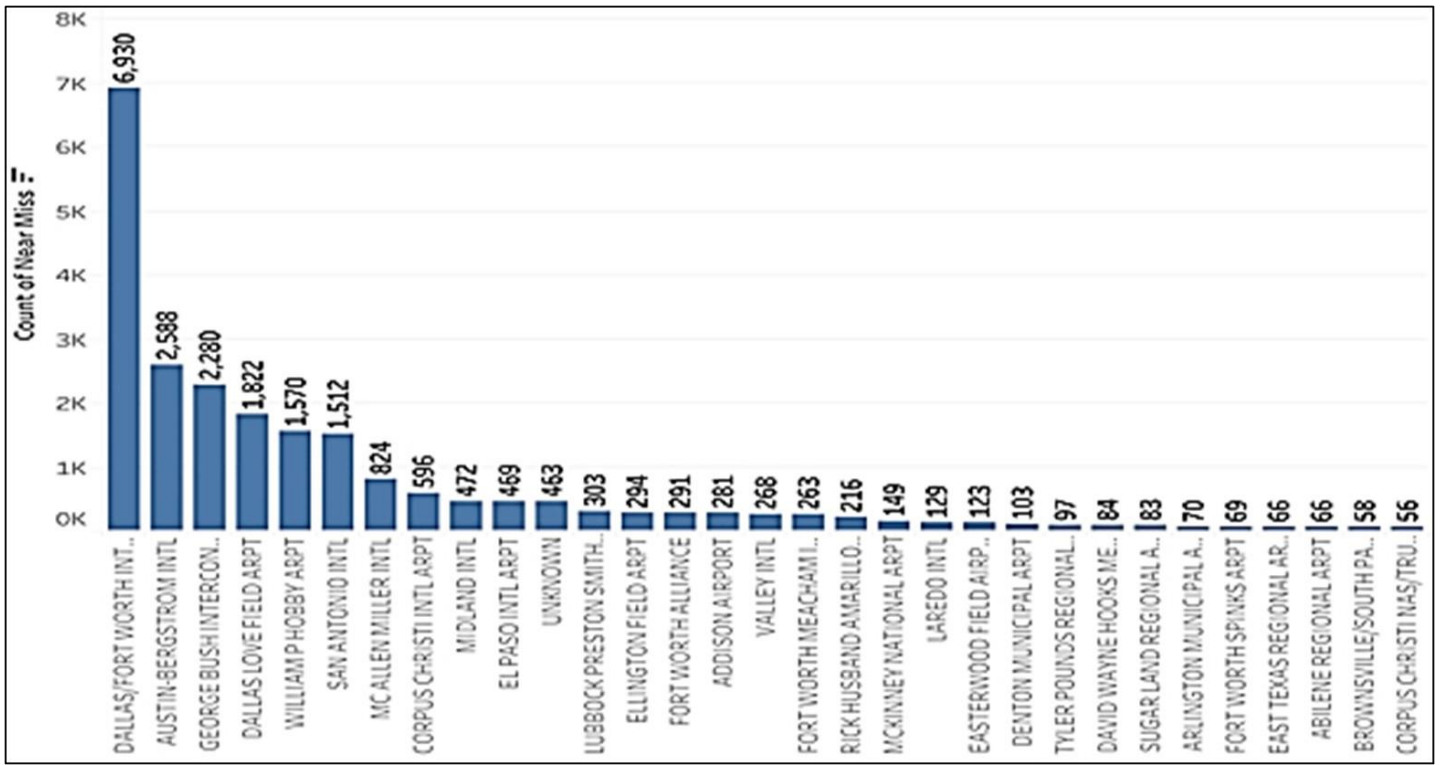


Fig. 1. Near Miss Cases - Airport

Note: Species equal to or more than 50 reports.

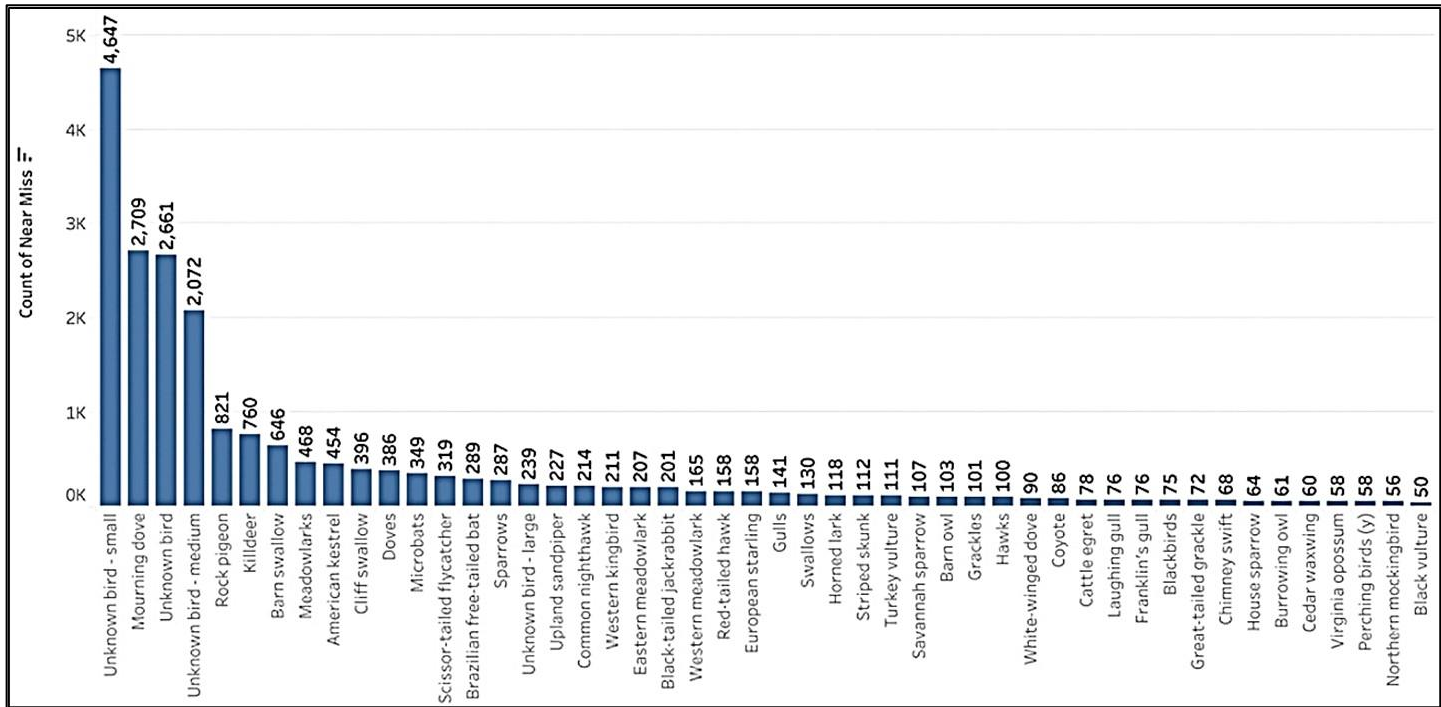
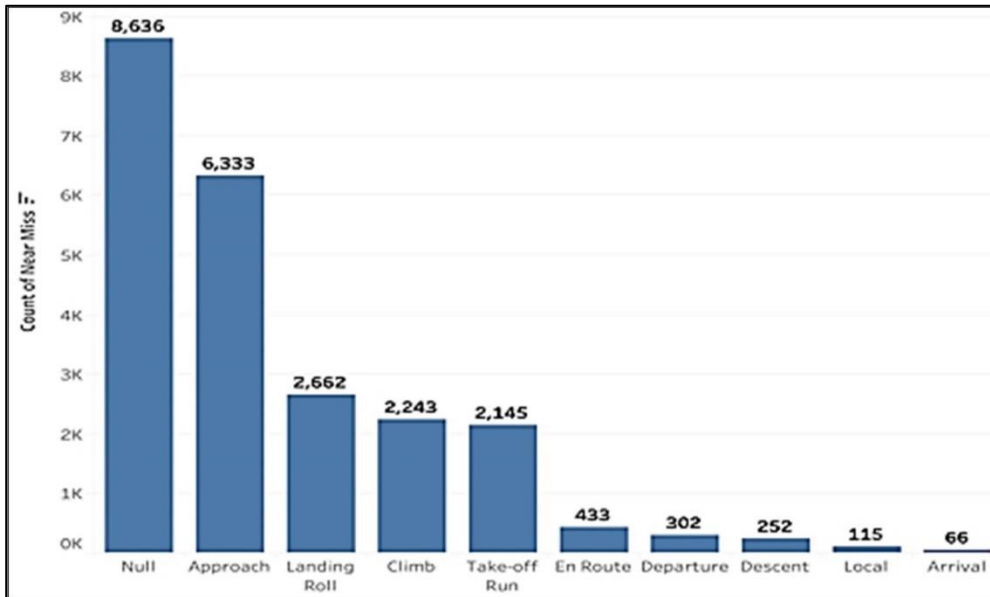


Fig. 2. Near Miss Cases - Species

Note: Species equal to or more than 50 reports.



**Fig. 3.** Near Miss Cases – Flight Phases

Note: This figure excludes “null” data and species equal to or more than 50 reports.

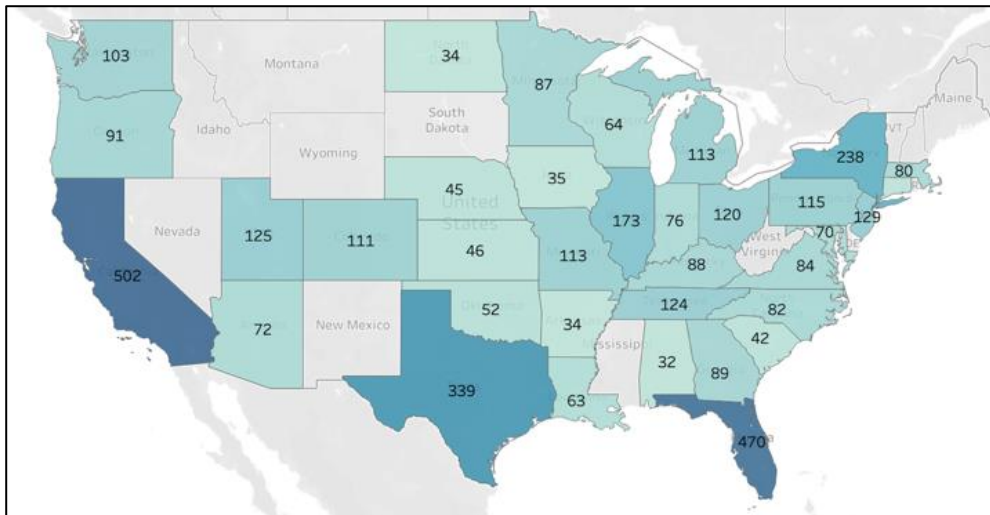


**Fig. 4.** Minor Damage Count – States

Note: This figure exclusively accounts for reports that are equal to or exceed 30 in count.

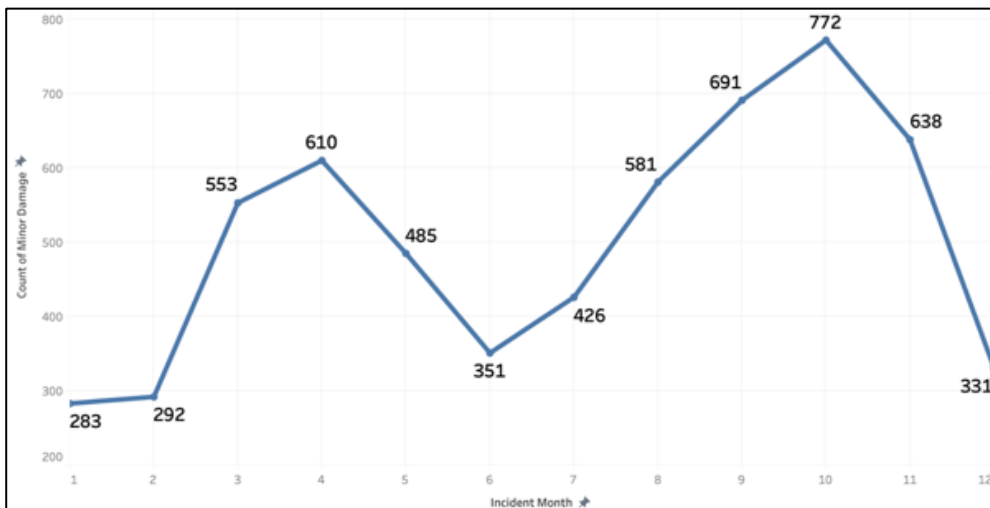


**Fig. 5.** Minor Damage Count – Month

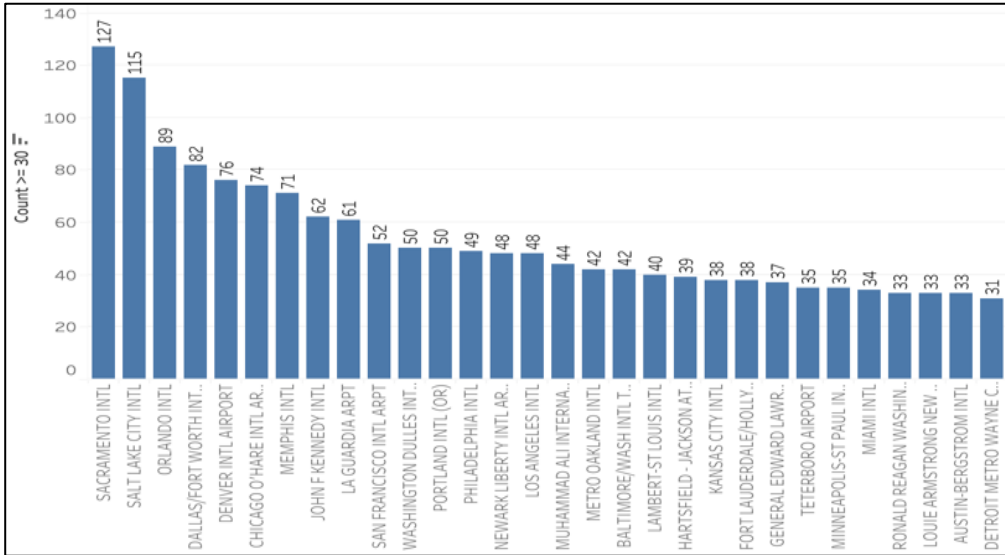


**Fig. 6.** Minor Damage Cases - Airports

Note: This figure exclusively accounts for reports that are equal to or exceed 30 in count.

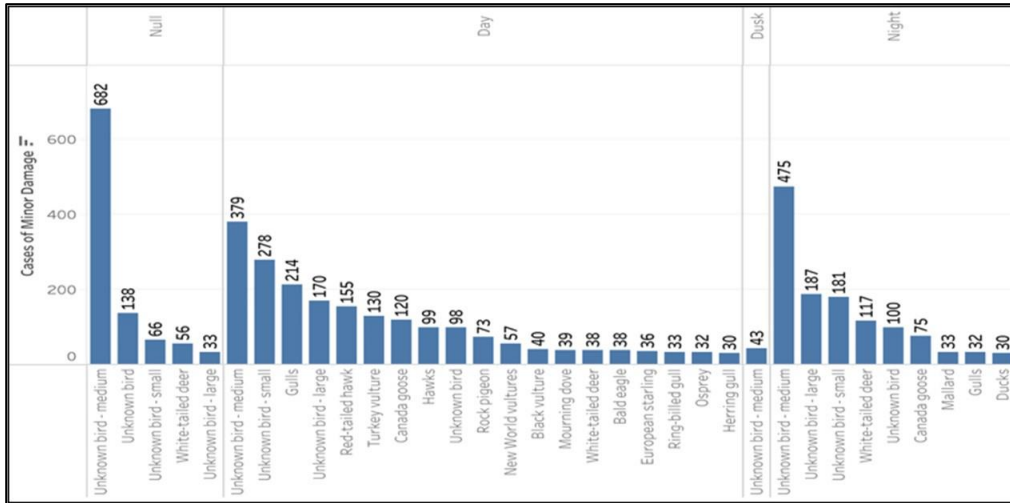


**Fig. 7.** Minor Damage Cases - Time

Note: This figure exclusively accounts for reports that are equal to or exceed 30 in count.

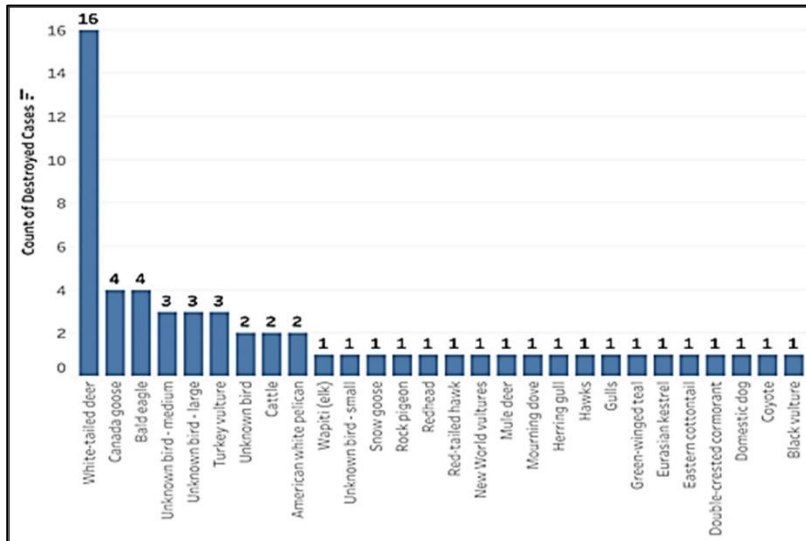


**Fig. 8.** Destroyed Cases - Species

Note: Excluding "unknown" species

In terms of individual airports, Sacramento International Airport stands out with the highest frequency of occurrences, totaling 127 cases. It is closely followed by Salt Lake City, Orlando, Dallas/Fort Worth, Denver, and Chicago, recording 115, 89, 82, 76, and 74 cases, respectively (Fig. 6).

Although some reports do not specify the species of wildlife involved, the majority of wildlife hazard cases are attributed to Gulls, Red-tailed Hawks, Turkey Vultures, and Canada Goose during daylight hours. Interestingly, during nighttime, White-tailed Deer and Canada Goose are identified as the primary causes of most minor damage incidents (Fig. 7).

**Destroyed.** The total count of destroyed cases is 58. In instances resulting in destroyed aircraft, White-tailed Deer are responsible for fourteen (16) cases,

representing 27.58% of the accidents, followed by Canada Goose and Bald Eagle, each accounting for 6.89% of the accidents (Fig. 8). While the height of accidents involving White-tailed Deer is 0~9 ft AGL, collisions happened at altitude of 8,800 ft AGL (Canada Goose) and 2,137 ft AGL (Bald Eagle) (Fig. 9).

For the categories of operations, Business and Privately-Owned operations encountered most destroyed accident due to wildlife collisions (Fig. 10). The data highlights a significant trend where most destroyed accidents occurred during the En Route flight phase, closely followed by Climb, Landing Roll, Take-off Run, and Approach (Fig. 11). Interestingly, there isn't a discernible specific high-risk time of day associated with these severe damage incidents (Fig. 12).

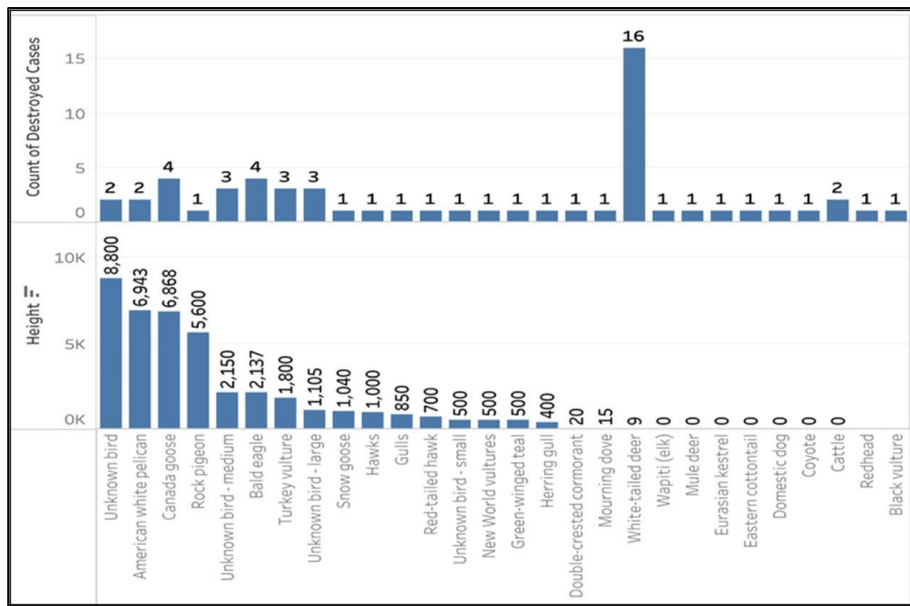


Fig. 9. Destroyed Cases – Heights and Species

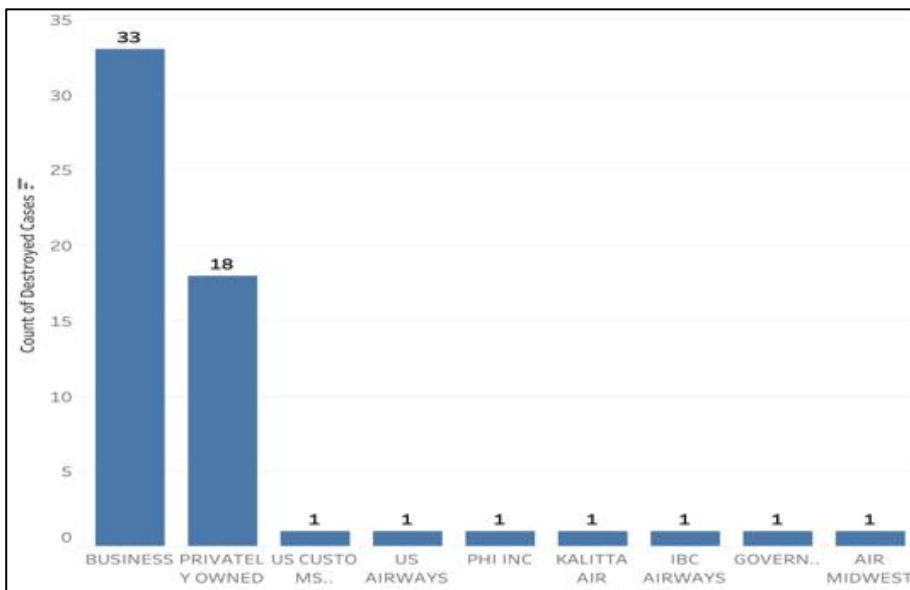
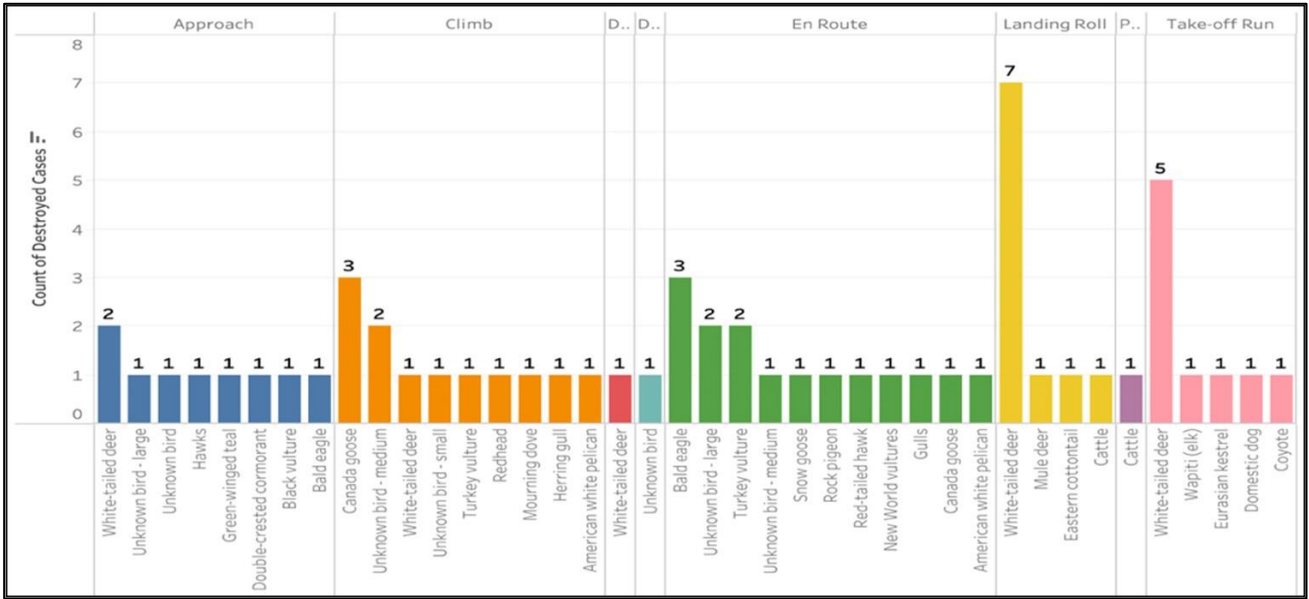


Fig. 10. Destroyed Cases – Operators



**Fig. 11.** Destroyed Cases – Phases of Flight and Species

The most substantial financial impacts from wildlife-related accidents are observed at LaGuardia Airport (KLGA) in New York, incurring costs of \$49.068 million involving Canada Goose. Moreover, significant financial losses of \$15.68 million at Troy Municipal Airport (KTOI) in Troy, Alabama, and \$8.125 million at Astoria Regional Airport (KAST) in Oregon are linked to encounters with White-tailed Deer and Wapiti, respectively (Table 2).

**Probability and Severity of the Risk Matrix**

To demonstrate the convenience and practicality of the designed risk matrix, two Californian airports, Los Angeles International Airport (LAX) and Sacramento International Airport (SAC), are selected for a comparative analysis of wildlife incidents due to the high volume of wildlife hazard reports in California. The similar process can be applied to other interested airport stakeholders.

To identify the probability to estimate risk, Figure 13 shows the hourly cumulative wildlife incidents at Sacramento International Airport (SAC) and Los Angeles International Airport (LAX). It is clear that that both

airports experience the lowest number of incidents during the early hours of the day, from midnight to about 05:00. This is likely due to reduced air traffic during these hours. Starting from 06:00, as air traffic begins to increase, so does the number of wildlife strikes, with a noticeable uptick at both airports. A particularly interesting pattern emerges at SAC, where there is a substantial increase in wildlife strike incidents starting from around 17:00, reaching a peak at midnight. This suggests that wildlife activity around SAC is significantly higher during these hours, which could be due to a variety of factors such as nocturnal wildlife behavior, feeding patterns, or the presence of species that are more active during dusk and the early night hours. LAX exhibits a more evenly spread pattern of wildlife strike incidents over the day, with the most significant peak occurring at 07:00. This morning surge may be attributed to the convergence of heightened airport traffic as flights typically ramp up for the day and the early morning wildlife activities. This observation could suggest that the strategies employed should differ in timing and approach due to the distinct patterns of wildlife activity at each location.

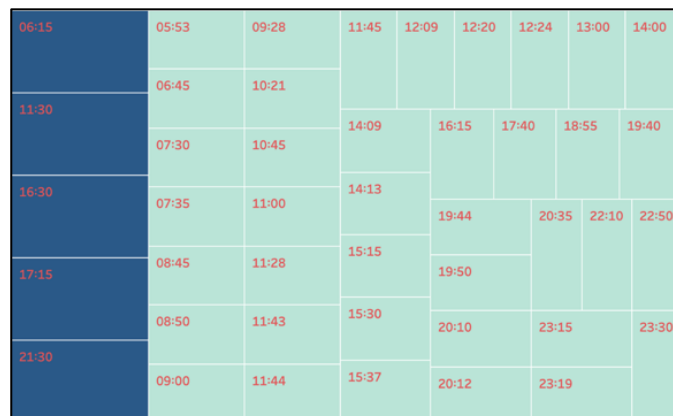


**Fig. 12.** Destroyed Cases – Time of the Flight

**Table 2.** Destroyed cases – Financial Losses

Species	Airport ID	Financial Losses
Canada goose	1C9	85.554
	KLGA	49.068.000
Coyote	KOGS	2.242.500
Eastern cottontail	NC30	113.022
Hawks	O41	35.250
Herring gull	KROC	1.852.500
Mourning dove	KLPR	1.794.000
Unknown bird - large	KCPR	234.000
Unknown bird - medium	4IA2	296.100
Unknown bird - small	KCPS	1.191.000
Wapiti (elk)	KAST	8.125.000
White-tailed deer	KLRO	49.472
	KMBT	47.640
	KOZS	253.575
	KRRT	1.157.000
	KTNT	971.750
	KTOI	15.684.500
	Y96	225.900

Note: KLGA – US Airways flight 1549 accident; KTOI – Ark Air Learjet 60 accident

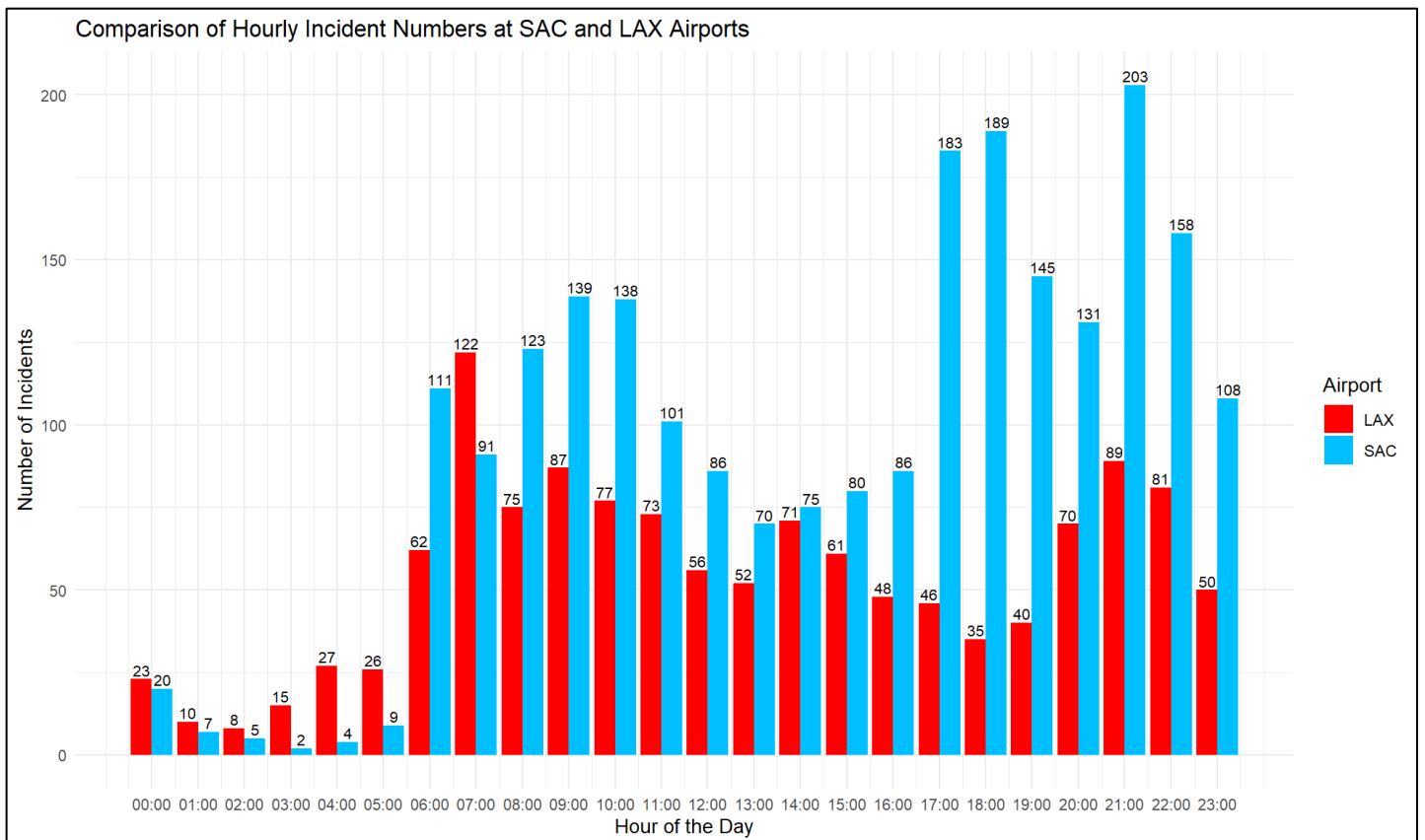


**Fig. 13.** Hourly Incidents – Comparison between LAX and SAC

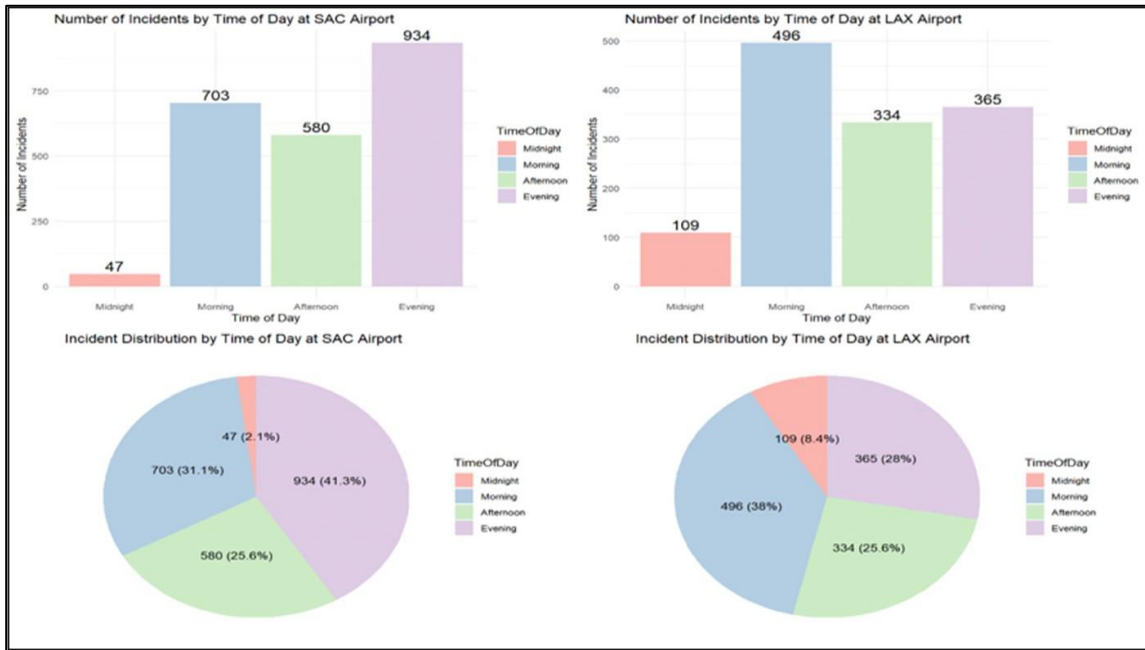


**Fig. 14.** Number of Incidents – Time of Day Comparison between LAX and SAC

To have better understanding of the time distribution of the incidents at these two airports for proper risk calculation, the following analysis split the time into four different sections: Midnight (00:00–05:59), Morning (06:00–11:59), Afternoon (12:00–17:59), and Evening (18:00–23:59). The following charts shows the number and percentage of incidents at two airports (Fig. 14).

To provide better understanding of the time distribution of wildlife strikes, Figure 15 below depicts a multi-dimensional analysis of wildlife strike incidents at LAX, the data for LAX shows a dramatic percentage increase in evening from February to April, followed by a

significant decrease until June (Fig. 15). Midnight incidents at LAX remain consistently low hinting at reduced risks during these hours.

At SAC, Figure 16 presents the percentages of incidents occur within specific time periods (Morning, Afternoon, Evening, and Midnight) across different months of the year. Evening incidents peak notably in April and October, suggesting that these periods have the highest relative occurrence of wildlife strikes during this time of day. This observation plays an important role in deciding wildlife strike probability.

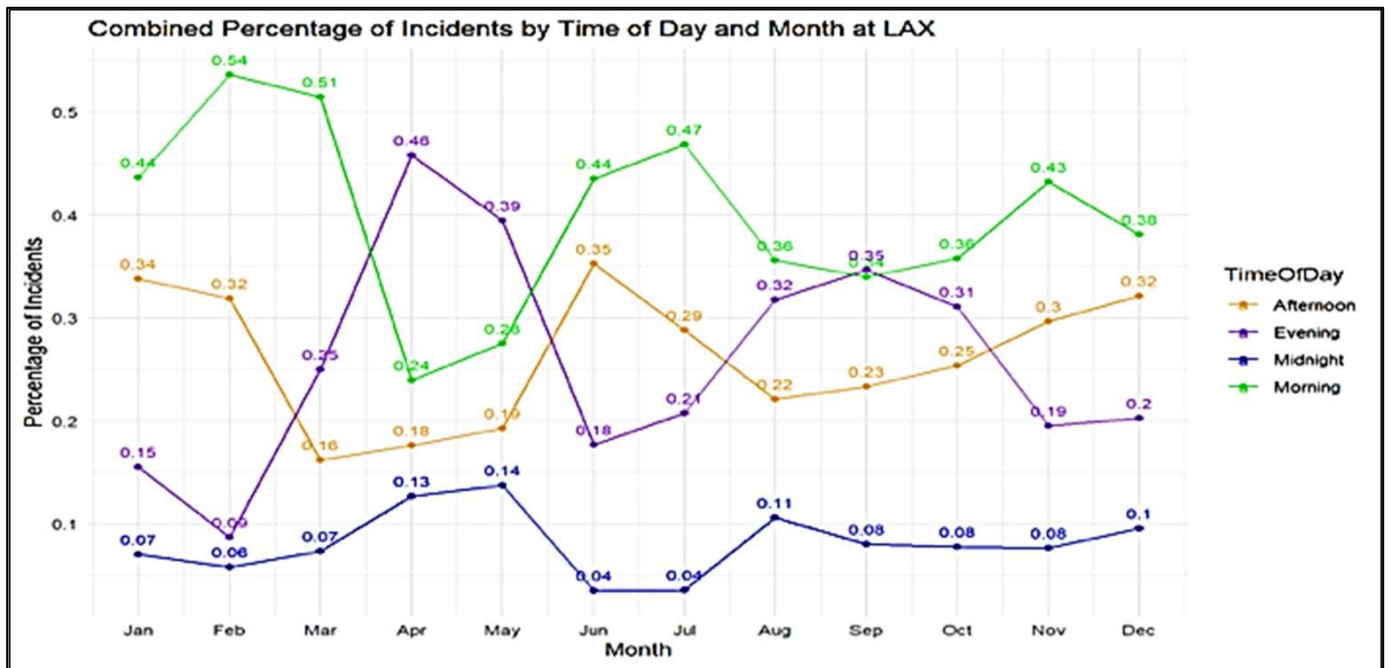


**Fig. 15.** Probability Density of Incidents by Time of Day – LAX

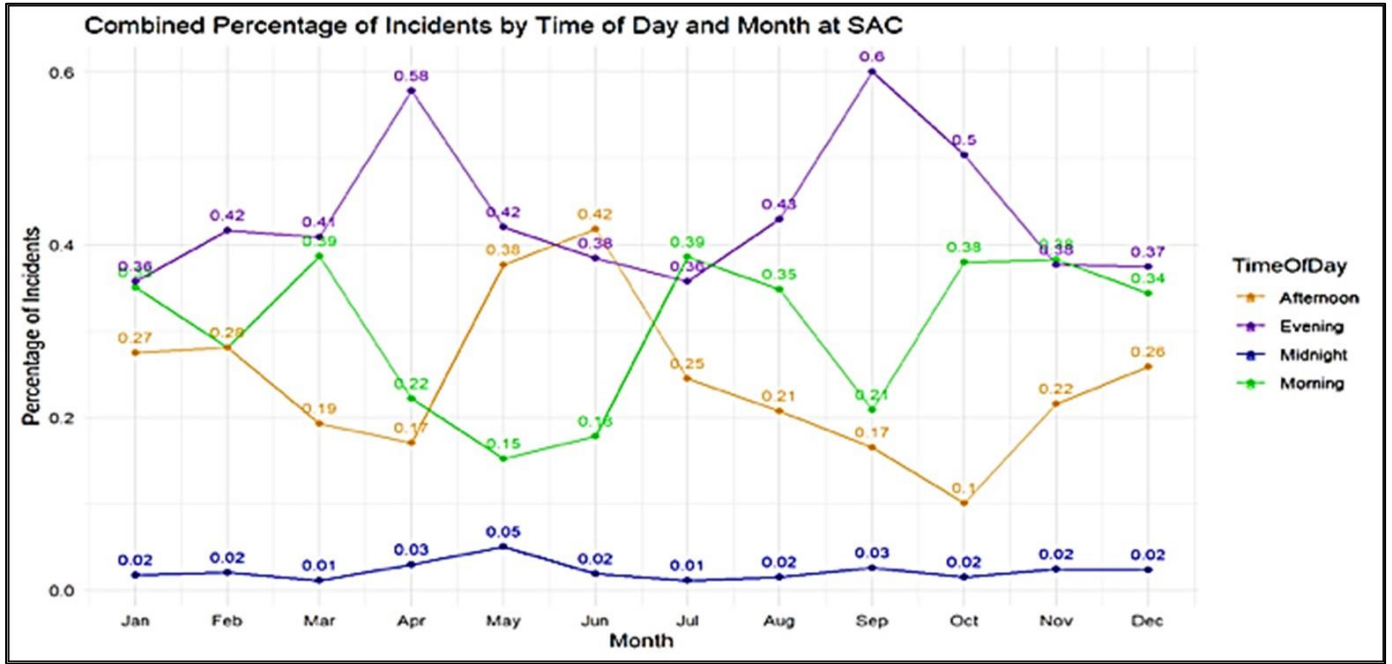


Fig. 16. Probability Density of Incidents by Time of Day – SAC

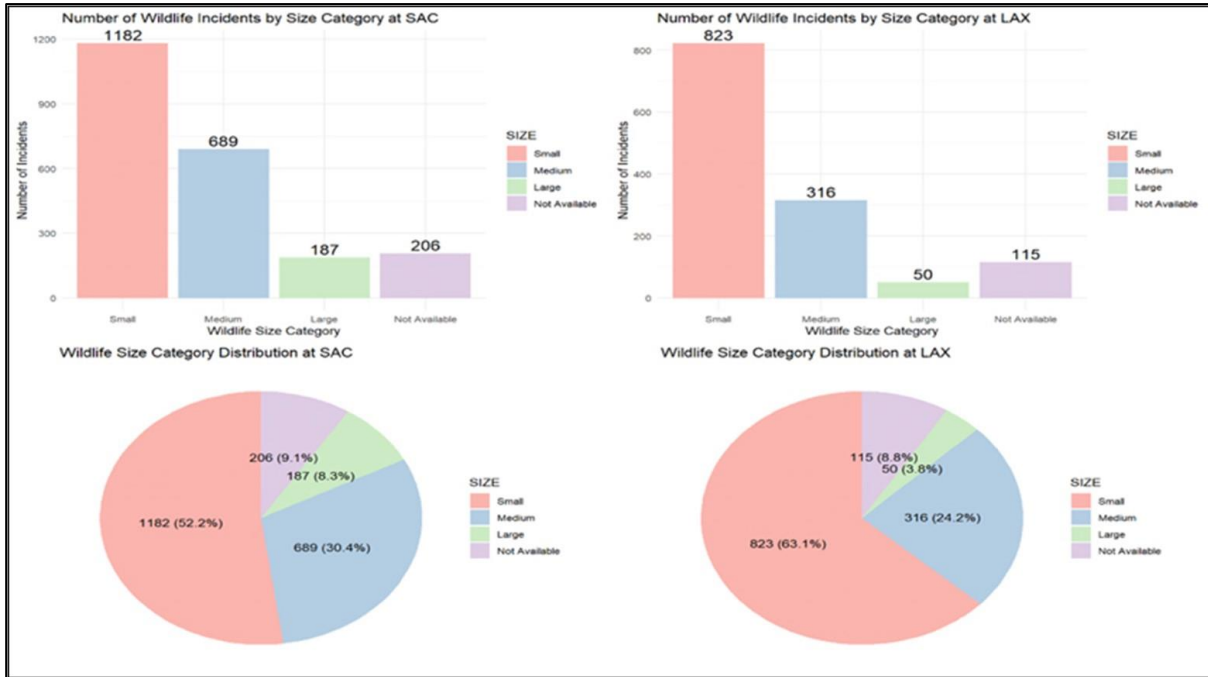


Fig. 17. Incidents by Size – Comparison between LAX and SAC

To decide the severity levels, the size of species is crucial while conducting risk analysis. At SAC, the majority of wildlife incidents involve small-sized animals, with a count of 1,182 incidents representing 52.2% of the total. Notably, SAC has a considerable proportion of medium-sized wildlife strike incidents, accounting for 30.4% with 689 incidents. Large wildlife strike incidents are fewer, with 187 incidents making up 8.3%, and incidents with size not available at 9.1% with 206 incidents. In comparison, LAX also has the highest percentage of incidents involving small-sized avian animals at 63.1%, totaling 823 incidents. However, the percentage of medium-sized wildlife strike incidents is lower than SAC,

at 24.2% with 316 incidents. The data reveals that while both airports have the highest incidence with small-sized avian animals, SAC has a notably higher percentage of incidents involving medium-sized avian animals compared to LAX (Fig. 17).

Finding both probability and severity enables the researchers to estimate risk level as risk (R) is theoretically equal to the product of probability (P) and severity (S). Our approach helps identify risk level where resource can be allocated to initiate preventive measures during times of greater risk. It may also guide decisions beforehand on flight scheduling, maintenance activities, and staffing, all aimed at minimizing the

magnitude of wildlife strikes. This level of process enhances the airport’s risk assessment and management plans, ultimately contributing to safer airport operations and reducing financial losses.

**Risk Analysis Web-based Tool – An Exercise**

In addition to conducting a visualized analysis of wildlife strike incidents, we developed a specialized website using the free Shiny framework to enable airport operators to dynamically interact with the data and assess risk levels (Wildlife Strikes - Risk Analysis, 2024). While a specialized coding algorithm is developed, this demonstrative platform allows users to select an airport (in this paper, we use SAC or LAX) and month to view a tailored risk analysis for different wildlife size categories.

The Shiny application is structured into two sections: the UI, which is the front end that users interact with, and the server function, which processes the data and generates the output. In the UI, dropdown menus facilitate the selection of an airport and month, creating a user experience that is both intuitive and efficient. The

server side uses reactive expressions to filter the data according to these user inputs, ensuring that the displayed information is both relevant and specific to the selected parameters. The codes are presented in Appendices I and II for dissemination among the interested public.

The risk level calculation is a critical feature of the application, providing a quantifiable measure of risk by multiplying the frequency of wildlife strike incidents (probability) by the object’s size (severity), with small being 1, medium being 2, and large being 3). While the frequency and object’s size are both coded into a corresponding risk level, the overall risk scores could fall into three different risk levels—low (Green), moderate (Yellow), and high (Red). Colored bars are represented in an interactive Plotly bar chart on the main panel of the website so stakeholders could take a prompt risk recognition and decide whether a control is required. Figures 18 and 21 exemplifies the color-coded risk level associated with the selected month at LAX and SAC.

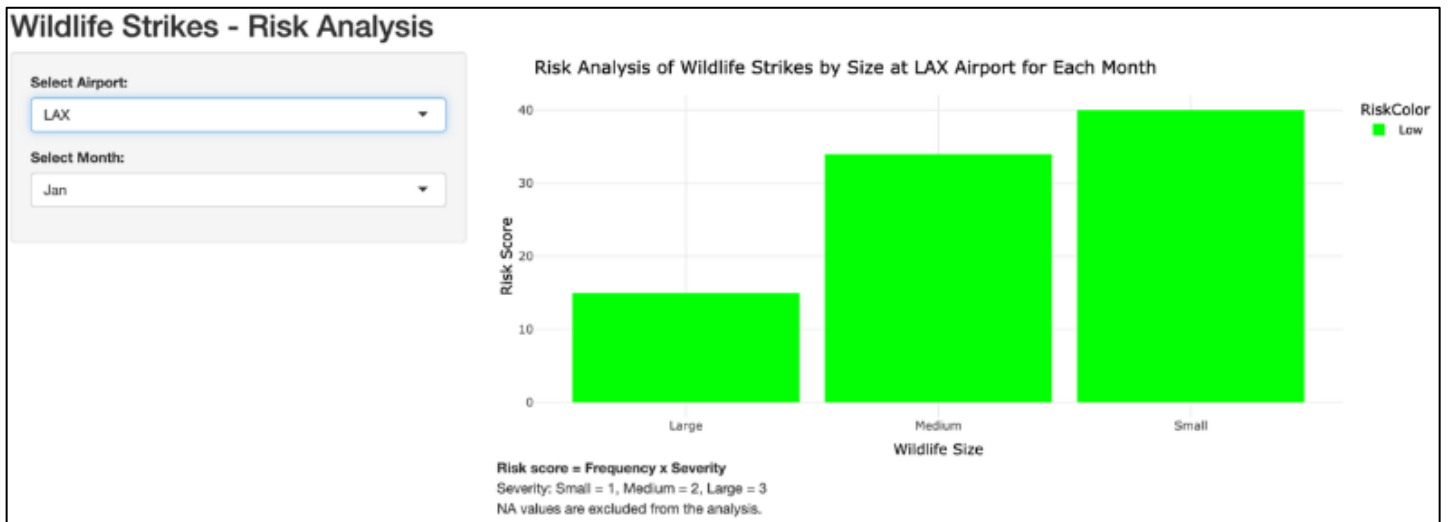


**Fig. 18.** Wildlife Risk Level – LAX in January

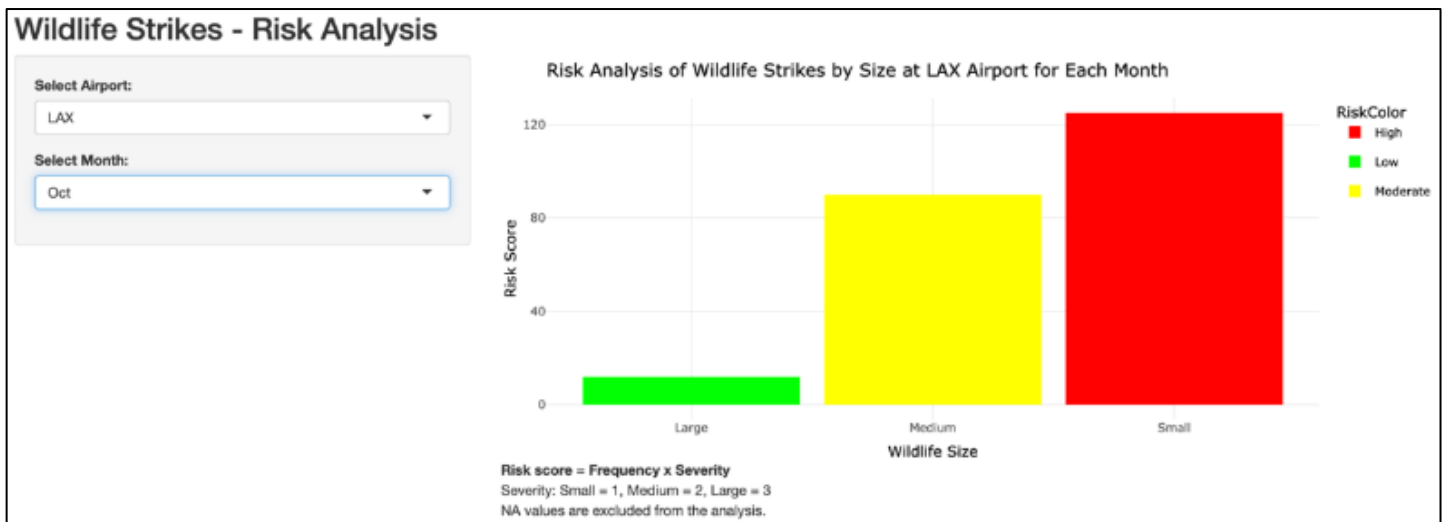


**Fig. 19.** Wildlife Risk Level – LAX in October

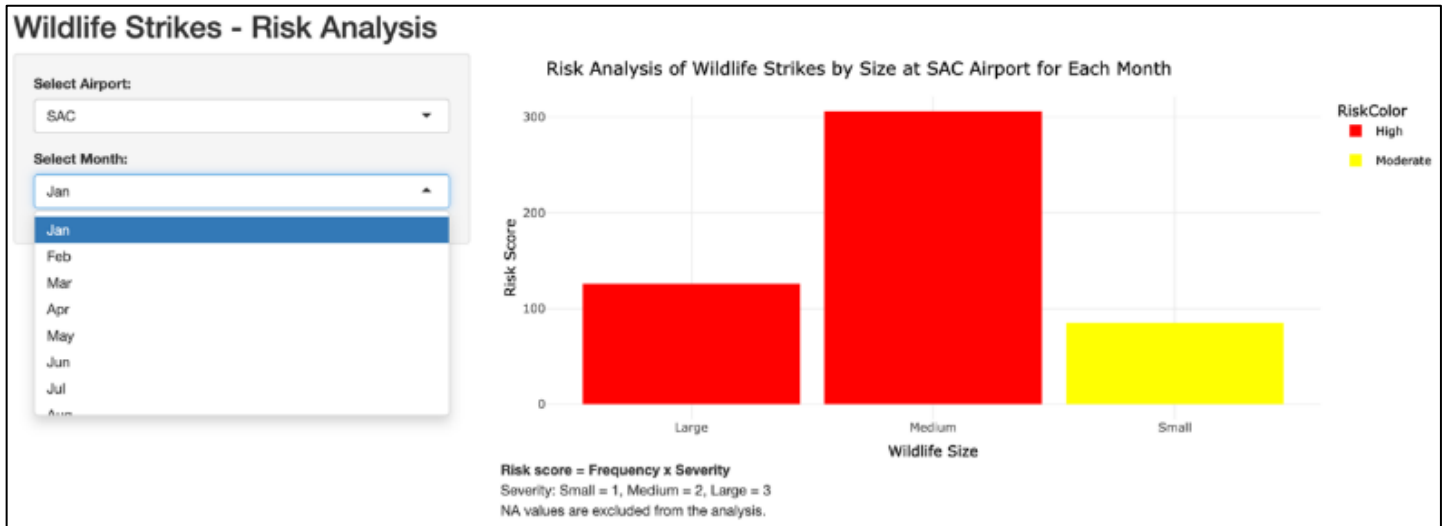


Fig. 20. Wildlife Risk Level – SAC in January

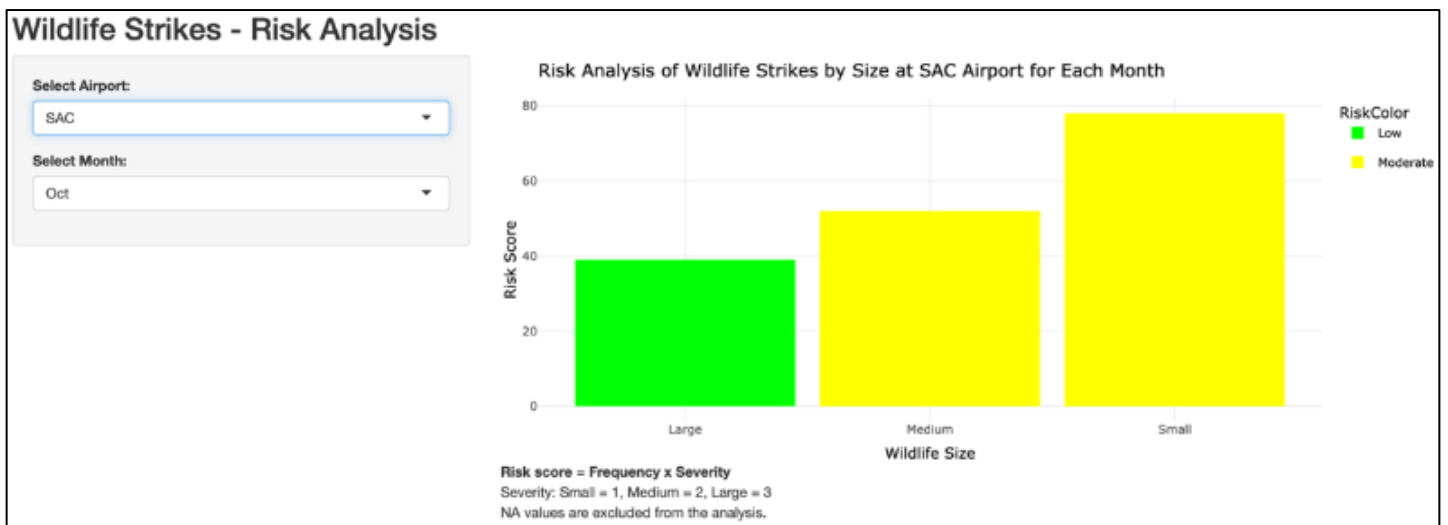


Fig. 21. Wildlife Risk Level – SAC in October

### 5. Conclusion

The completion of this study provides early wildlife alerts to stakeholders: airport operators, traffic controllers, and pilots. We apply Tableau and R for wildlife hazard data visualization to provide a quick reference to airport stakeholder in addition to providing an interactive and customizable risk decision-making tool using Shiny platform. The web-based system empowers airport stakeholders with the ability to promptly identify high-risk periods simply based on the coded report frequencies and wildlife sizes. When the new database is updated, the risk probability will be recalculated simultaneously supporting an accurate risk assessment. This approach not only facilitates a deeper understanding of the hazard report but also enhances the decision-making capabilities of airport operators. In summary, by leveraging advanced technologies to assess and determine risk levels, airport stakeholders not only can take a proactive approach in implementing strategic wildlife controls or measures, but also enhance overall

airport safety and sustainability. While the authors use LAX and SAC airports to showcase the function of the proposed tool, researchers with an interest in the field can apply the codes to other airports by substituting their own wildlife hazard database. Utilizing interactive visualizations guarantees the effective communication of intricate data in a user-friendly manner, facilitating instant interpretation and enabling prompt airport wildlife preventive action.

This paper primarily serves as a demonstration of the potential capabilities of the risk matrix tool, laying the groundwork for future development into a fully operational solution. This study considers probability as the volume of operations and severity as the size of reported wildlife, forming the basic foundation of the risk assessment methodology used. Future iterations will incorporate additional factors such as geographical location, operational times, and wildlife migration patterns to provide a more comprehensive risk assessment framework. Understanding the impact of quiet hours, geographical features, and wildlife

migration patterns is crucial for effective wildlife hazard management. Airports near natural flyways or breeding areas may experience higher wildlife activity during specific times of the year or day. The risk matrix tool is designed to be adaptable, allowing for integrating these critical factors in future updates to provide a more accurate and holistic risk assessment. The developers will develop and integrate these features, allowing stakeholders to select relevant variables without extensive coding. This ensures the tool remains user-friendly while accommodating wildlife hazards' complex and varied nature across different airports.

### Future Study

This paper does not include meteorological information, quiet hours, geography, or airport wildlife movement patterns. Interested researchers or stakeholders can conduct a follow-up study. Specifically, integrating meteorological data could enhance predictive accuracy by accounting for weather-related wildlife behaviors. Investigating the impact of quiet hours on wildlife activity around airports could provide insights into optimal times for implementing control measures.

Further studies could also explore the influence of geographical features and airport wildlife movement patterns to refine risk assessments and improve the tool's adaptability across different airport environments. Future research should focus on incorporating machine learning algorithms to enhance predictive modeling capabilities, enabling more accurate and dynamic risk assessments.

During the development and implementation of the web-based system, several challenges were encountered. Data quality issues, such as inconsistent or incomplete wildlife strike reports, can affect the accuracy and reliability of the risk assessments. Integrating the tool with existing airport management systems posed technical challenges, requiring customized solutions for different airports. Ensuring that airport staff are adequately trained and comfortable using the new tool is critical for its success. The reliance on historical data may limit the tool's predictive accuracy in rapidly changing environments, highlighting the need for continuous data updates and model refinements. Validating the system's scalability and effectiveness across different airport settings remains an ongoing challenge, necessitating further research and testing.

### CRedit Author Statement

**Haoruo Fu:** Data Visualization, Coding, Final Edit. **Chien-tung Lu:** Topic, Literature Review, Contents, Data Visualization, Final Edit. **Ming Cheng:** Topic, Literature

Review, Contents, Data Visualization, Final Edit. **Mengyi Wei:** Data Visualization, Coding, Final Edit.

### Nomenclature

FAA	: Federal Aviation Administration
SMS	: Safety Management Systems
SRM	: Safety Risk Management
WHaM-RAT	: Wildlife Hazard Management Risk Assessment Tool
LAX	: Los Angeles International Airport
SAC	: Sacramento Airport
AGL	: Above Ground Level
R	: Risk level
P	: Probability (wildlife incident frequency)
S	: Severity (wildlife size)
Shiny	: An R-based platform for building interactive web applications
Tableau	: A data visualization software used for interactive reports and dashboards

### References

- 14 CFR 139.337 Wildlife hazard management, n.d. <https://www.ecfr.gov/current/title-14/chapter-I/subchapter-G/part-139/subpart-D/section-139.337>
- Aircraft Accident Investigation Bureau of India (AAIB), 2014. Final investigation report on accident to SpiceJet Boeing B737-800 aircraft VT-SGK at Surat on 06.11.2014. Retrieved from <https://www.skybrary.aero/sites/default/files/bookshelf/4127.pdf>
- Blackwell, B. F., DeVault, T. L., Fernández-Juricic, E., & Dolbeer, R. A., 2009. Wildlife collisions with aircraft: A missing component of land-use planning for airports. *Landscape and Urban Planning*, 93(1), 1-9. <https://doi.org/10.1016/j.landurbplan.2009.07.005>
- Colón, A. M. & Long, M. R., 2023. When can local bird detection radars best complement broad-scale early-warning forecasts of risk potential for bird-aircraft strikes as part of an integrated approach to strike mitigation? *Ecology*, 8. doi: 10.1111/ecog.06772
- DeVault, T. L., Blackwell, B. F., Seamans, T. W., & Belant, J. L., 2016. Identification of Off Airport Interspecific Avian Hazards to Aircraft. *The Journal of Wildlife Management* 80(4):746-752. DOI: 10.1002/jwmg.1041

- Dolbeer, R. A., 2013. The history of wildlife strikes and management at airports. U.S. Department of Agriculture: Animal and Plant Health Inspection Service. Retrieved from: [https://digitalcommons.unl.edu/cgi/viewcontent.cgi?article=2473&context=icwdm\\_usdanwrc](https://digitalcommons.unl.edu/cgi/viewcontent.cgi?article=2473&context=icwdm_usdanwrc)
- Dziak, D. et. al., 2022. Airport Wildlife Hazard Management System - A Sensor Fusion Approach. *Elektronika ir Elektrotechnika*, 28(3), 45–53.
- Edwards, E., November 1972. Man and Machine - Systems for Safety. Outlook on Safety: Proceedings of the 13th Annual Technical Symposium. London: British Air Line Pilots Association, 21–36.
- FAA. (2007). AC 150/5200-37 Introduction to safety management systems for airport operators. Retrieved from [https://www.faa.gov/documentlibrary/media/advisory\\_circular/150-5200-37/150\\_5200\\_37.pdf](https://www.faa.gov/documentlibrary/media/advisory_circular/150-5200-37/150_5200_37.pdf) (Accessed November 5, 2023)
- FAA., August 2010. Order 5200.11 FAA airport (ARP) safety management. Retrieved from [https://www.faa.gov/documentlibrary/media/order/order\\_5200\\_11\\_arp\\_sms.pdf](https://www.faa.gov/documentlibrary/media/order/order_5200_11_arp_sms.pdf) (Accessed: October 28, 2023)
- FAA., 2013. AC 150/5200-32B Reporting wildlife aircraft strikes. [https://www.faa.gov/documentLibrary/media/Advisory\\_Circular/AC\\_150\\_5200-32B.pdf](https://www.faa.gov/documentLibrary/media/Advisory_Circular/AC_150_5200-32B.pdf) (Accessed: November 4, 2023)
- FAA., 2017. Order 8040.4B. Safety risk management policy. Retrieved from [https://www.faa.gov/documentLibrary/media/Order/FAA\\_Order\\_8040.4B.pdf](https://www.faa.gov/documentLibrary/media/Order/FAA_Order_8040.4B.pdf) (Accessed: November 4, 2023)
- FAA., 2020. AC 150/5200-33C Hazardous wildlife attractants on or near airports. Retrieved from [https://www.faa.gov/documentLibrary/media/Advisory\\_Circular/150-5200-33C.pdf](https://www.faa.gov/documentLibrary/media/Advisory_Circular/150-5200-33C.pdf) (Accessed: November 19, 2023)
- FAA., February 2021. Wildlife strikes to civil aviation – 1990 ~ 2019. Retrieved from file:///Users/chien-tunglu/Downloads/Wildlife-Strike-Report-1990-2019.pdf (Accessed: November 13, 2023)
- Federal Aviation Administration (FAA), n.d.. Report a strike. <https://wildlife.faa.gov/add>
- Fu, H, Lu, c-t., & Ji, Z., September 2023. Risk Assessment Matrix of Operational Safety (RAMOS): Aviation Safety with a MATLAB® Design Toolkit, *Journal of Aviation/Aerospace Education & Research*. 32(2). DOI: <https://doi.org/10.58940/2329-258X.1982>
- Heinrich, H. W., 1959. *Industrial Accident Prevention: A Scientific Approach* (4th ed.). New York: McGraw-Hill.
- Kunkle, F., October 28, 2021. Plane Hits Deer. and so begins the annual rut, when lovesick animals collide with vehicles. *The Washington Post*. Retrieved December 8, 2022, from <https://www.washingtonpost.com/news/tripping/wp/2016/10/25/plane-hits-deer-and-so-begins-the-annual-rut-when-lovesick-animals-collide-with-vehicles/>
- Lu, C-t., Schreckengast, S., & Jia, J., 2011. Safety risk management, assurance, and promotion: hazard control system for budget-constrained airports. *Journal of Aviation Technology and Engineering*, 1(1), 1-15. DOI: <https://doi.org/10.5703/1288284314630>
- Mendonca, F. A. C., & Wallace, R., 2021. Utilizing UAS to support wildlife hazard management efforts by airport operators. *Collegiate Aviation Review International*, 39(2), 238-248. Retrieved from <http://ojs.library.okstate.edu/osu/index.php/CARI/article/view/8385/7686>
- Misra, S., Toppo, I., & Mendonca, F., 2022. Assessment of aircraft damage due to bird strikes: a machine learning approach. *International Journal of Sustainable Aviation*, 8(2), 136-151. Retrieved from <https://www.inderscienceonline.com/doi/abs/10.1504/IJSA.2022.122328>
- National Transportation Safety Board (NTSB), October 2010. NTSB/AAR-10/03 Loss of Thrust in Both Engines After Encountering a Flock of Birds and Subsequent Ditching on the Hudson River. Retrieved from <https://www.nts.gov/investigations/AccidentReports/Reports/AAR1003.pdf>
- Reason, J., 1990. *Human Error*. London, U.K.: Cambridge University Press.
- Transportation Research Board (TRB), 2012. Lesson learned from airport safety management systems pilot studies. Retrieved from <https://nap.nationalacademies.org/download/22740>
- TRB., 2015. ACRP Report 145 - Applying an SMS approach to wildlife hazard management. Retrieved from file:///Users/chien-tunglu/Downloads/22091.pdf
- U.S. Department of Agriculture (USDA), 2017, February. *Wildlife Damage Management Technical Series*. USDA APHIS | Wildlife Damage Management Technical Series. [https://www.aphis.usda.gov/aphis/ourfocus/wildlifedamage/sa\\_reports/ct\\_wildlife+damage+management+technical+series](https://www.aphis.usda.gov/aphis/ourfocus/wildlifedamage/sa_reports/ct_wildlife+damage+management+technical+series)

Wiegmann, D. A. & Shappell, S. A., 2017. A Human Error Approach to Aviation Accident Analysis: The Human Factors Analysis and Classification System. London: Taylor and Francis.

Wildlife Strikes - Risk Analysis., (2024). Shinyapps. Available at: [https://hfu2014.shinyapps.io/ca\\_analysis/](https://hfu2014.shinyapps.io/ca_analysis/) (Accessed: 2024).

## Appendix I Code of R Analysis

```

##### California Wildlife Hazard Analysis #####

##### Notice #####
## This is just the analysis used in the paper. Most of the following code ##
## are just used for this analysis. ##
## For Shiny.io part, please refer to the second part of the code ##
## There will be some duplicates in this code, please check carefully ##

# Necessary packages
library(readxl)
library(gdata)
library(ggplot2)
library(dplyr)
library(lubridate)
library(leaflet)
library(tmap)
library(sf)
library(viridis)
library(cluster)
library(spdep)
library(gridExtra)
library(corrplot)

# Import Data We selected LAX and SAC data
# Modify your own file destination
LAX_Event <- read_excel("../LAX/LAX_Event_2002_2022.xlsx")
#LAX_Flight <- read_excel("../LAX/LAX_Flight_2002_2022.xlsx")
SAC_Event <- read_excel("../SAC/SAC_Event_2002_2022.xlsx")
#SAC_Flight <- read_excel("../SAC/SAC_Flight_2002_2022.xlsx")

##### Simply Descriptive Analysis #####
### SAC Airport Analysis
# Calculate the count of incidents per year for SAC
yearly_incidents_SAC <- SAC_Event %>%
  group_by(INCIDENT_YEAR) %>%
  summarise(Incidents = n()) %>%
  arrange(INCIDENT_YEAR)

# Create a bar plot for SAC
ggplot(yearly_incidents_SAC, aes(x = INCIDENT_YEAR, y = Incidents)) +
  geom_bar(stat = "identity", fill = "red") +
  geom_text(aes(label = Incidents), vjust = -0.3, size = 3.5) +
  labs(x = "Year", y = "Number of Incidents",
       title = "Number of Incidents per Year at SAC Airport") +
  theme_minimal()

### LAX Airport Analysis
# Calculate the count of incidents per year for LAX
yearly_incidents_LAX <- LAX_Event %>%
  group_by(INCIDENT_YEAR) %>%
  summarise(Incidents = n()) %>%
  arrange(INCIDENT_YEAR)

# Create a bar plot for LAX
ggplot(yearly_incidents_LAX, aes(x = INCIDENT_YEAR, y = Incidents)) +
  geom_bar(stat = "identity", fill = "deepskyblue") +
  geom_text(aes(label = Incidents), vjust = -0.3, size = 3.5) +
  labs(x = "Year", y = "Number of Incidents",
       title = "Number of Incidents per Year at LAX Airport") +
  theme_minimal()

# Combine these two for better comparison or visualization
yearly_incidents_SAC <- yearly_incidents_SAC %>%
  mutate(Airport = "SAC")

yearly_incidents_LAX <- yearly_incidents_LAX %>%
  mutate(Airport = "LAX")

# Combine the data
combined_data <- rbind(yearly_incidents_SAC, yearly_incidents_LAX)

# Create a grouped bar plot
ggplot(combined_data, aes(x = INCIDENT_YEAR, y = Incidents, fill = Airport)) +
  geom_bar(stat = "identity", position = position_dodge()) +
  geom_text(aes(label = Incidents), vjust = -0.3, position = position_dodge(0.9), size = 3.5) +
  labs(x = "Year", y = "Number of Incidents",
       title = "Comparison of Incident Numbers per Year at SAC and LAX Airports") +
  theme_minimal() +
  scale_fill_manual(values = c("red", "deepskyblue"))

##### Per Month Section #####
# Calculate the count of incidents per month for SAC
monthly_incidents_SAC <- SAC_Event %>%
  group_by(INCIDENT_MONTH) %>%
  summarise(Incidents = n()) %>%
  arrange(INCIDENT_MONTH)

# Create a bar plot for SAC
ggplot(monthly_incidents_SAC, aes(x = INCIDENT_MONTH, y = Incidents)) +
  geom_bar(stat = "identity", fill = "red") +
  geom_text(aes(label = Incidents), vjust = -0.3, size = 3.5) +
  scale_x_continuous(breaks = 1:12, labels = month.abb) +
  labs(x = "Month", y = "Number of Incidents",
       title = "Number of Incidents per Month at SAC Airport") +
  theme_minimal()

# Same for for LAX
monthly_incidents_LAX <- LAX_Event %>%
  group_by(INCIDENT_MONTH) %>%
  summarise(Incidents = n()) %>%
  arrange(INCIDENT_MONTH)

# Create a bar plot for LAX
ggplot(monthly_incidents_LAX, aes(x = INCIDENT_MONTH, y = Incidents)) +
  geom_bar(stat = "identity", fill = "deepskyblue") +
  geom_text(aes(label = Incidents), vjust = -0.3, size = 3.5) +
  scale_x_continuous(breaks = 1:12, labels = month.abb) +
  labs(x = "Month", y = "Number of Incidents",
       title = "Number of Incidents per Month at LAX Airport") +
  theme_minimal()

# Combine the data
monthly_incidents_SAC <- monthly_incidents_SAC %>%
  mutate(Airport = "SAC")

monthly_incidents_LAX <- monthly_incidents_LAX %>%
  mutate(Airport = "LAX")

# Combine the data
combined_monthly_data <- rbind(monthly_incidents_SAC, monthly_incidents_LAX)

# Create a grouped bar plot for comparison and visualization
ggplot(combined_monthly_data, aes(x = INCIDENT_MONTH, y = Incidents, fill = Airport)) +
  geom_bar(stat = "identity", position = position_dodge()) +
  geom_text(aes(label = Incidents), vjust = -0.3, position = position_dodge(0.9), size = 3.5) +
  scale_x_continuous(breaks = 1:12, labels = month.abb) +
  labs(x = "Month", y = "Number of Incidents",
       title = "Comparison of Monthly Incident Numbers at SAC and LAX Airports") +
  theme_minimal() +
  scale_fill_manual(values = c("red", "deepskyblue"))

##### Hour Analysis #####
# Extract hour and clean NA for SAC ( The NAs need to be careful), some
# can use NAs and some may not.
SAC_Event$Hour <- as.integer(sub("^(\\d{2}):.*", "\\1", SAC_Event$TIME))
SAC_Event <- SAC_Event[!is.na(SAC_Event$Hour), ]

# Count incidents by hour for SAC
hourly_incidents_SAC <- SAC_Event %>%
  group_by(Hour) %>%
  summarise(Incidents = n()) %>%
  arrange(Hour)

# Create a bar plot for SAC
hourly_bar_chart_SAC <- ggplot(hourly_incidents_SAC, aes(x = Hour, y = Incidents)) +
  geom_bar(stat = "identity", fill = "red") +
  geom_text(aes(label = Incidents), vjust = -0.3, size = 3) +
  scale_x_continuous(breaks = 0:23, labels = sprintf("%02d:00", 0:23)) +
  labs(x = "Hour of the Day", y = "Number of Incidents", title = "Number of Incidents by Hour
of the Day at SAC Airport") +
  theme_minimal()
hourly_bar_chart_SAC

# Extract hour and clean NA for LAX (same as the SAC)
LAX_Event$Hour <- as.integer(sub("^(\\d{2}):.*", "\\1", LAX_Event$TIME))
LAX_Event <- LAX_Event[!is.na(LAX_Event$Hour), ]

# Count incidents by hour for LAX
hourly_incidents_LAX <- LAX_Event %>%
  group_by(Hour) %>%
  summarise(Incidents = n()) %>%
  arrange(Hour)

# Create a bar plot for LAX
hourly_bar_chart_LAX <- ggplot(hourly_incidents_LAX, aes(x = Hour, y = Incidents)) +
  geom_bar(stat = "identity", fill = "deepskyblue") +
  geom_text(aes(label = Incidents), vjust = -0.3, size = 3) +
  scale_x_continuous(breaks = 0:23, labels = sprintf("%02d:00", 0:23)) +
  labs(x = "Hour of the Day", y = "Number of Incidents", title = "Number of Incidents by Hour
of the Day at LAX Airport") +
  theme_minimal()
hourly_bar_chart_LAX

# Add an airport column to each dataset
hourly_incidents_SAC <- hourly_incidents_SAC %>%
  mutate(Airport = "SAC")

hourly_incidents_LAX <- hourly_incidents_LAX %>%
  mutate(Airport = "LAX")

# Combine the data
combined_hourly_data <- rbind(hourly_incidents_SAC, hourly_incidents_LAX)

# Create a grouped bar plot for comparison and visualization
combined_hourly_chart <- ggplot(combined_hourly_data, aes(x = Hour, y = Incidents, fill =
Airport)) +
  geom_bar(stat = "identity", position = position_dodge()) +
  geom_text(aes(label = Incidents), vjust = -0.3, position = position_dodge(0.9), size = 3) +
  scale_x_continuous(breaks = 0:23, labels = sprintf("%02d:00", 0:23)) +
  labs(x = "Hour of the Day", y = "Number of Incidents",
       title = "Comparison of Hourly Incident Numbers at SAC and LAX Airports") +
  theme_minimal() +
  scale_fill_manual(values = c("red", "deepskyblue"))

# Print the combined chart
combined_hourly_chart

##### Time Section Analysis #####
# Create Function to categorize time into sections
# So for this we splitted them into four time sections
# Midnight 0000-0559 Morning 0600-1159 Afternoon 1200-1759 Evening 1800-2359
categorize_time <- function(data) {
  data$TimeObj <- as.POSIXct(data$TIME, format = "%H:%M", tz = "UTC")
  data$TimeOfDay <- cut(data$TimeObj,
                        breaks = c(as.POSIXct('00:00', format='%H:%M', tz='UTC'),
                                  as.POSIXct('06:00', format='%H:%M', tz='UTC'),
                                  as.POSIXct('12:00', format='%H:%M', tz='UTC'),
                                  as.POSIXct('18:00', format='%H:%M', tz='UTC'),
                                  as.POSIXct('23:59', format='%H:%M', tz='UTC')),
                        labels = c('Midnight', 'Morning', 'Afternoon', 'Evening'),
                        include.lowest = TRUE)
  data <- data[!is.na(data$TimeOfDay), ]
  return(data)
}

# Apply the function to LAX and SAC datasets
LAX_Event <- categorize_time(LAX_Event)
SAC_Event <- categorize_time(SAC_Event)

# Function to create time section analysis plots
create_time_section_plots <- function(data, airport_name) {
  # Count the number of incidents in each time section
  time_section_incidents <- data %>%
    group_by(TimeOfDay) %>%
    summarise(Incidents = n())

  # Create a bar chart
  bar_chart <- ggplot(time_section_incidents, aes(x = TimeOfDay, y = Incidents, fill =
TimeOfDay)) +
    geom_bar(stat = "identity") +
    geom_text(aes(label = Incidents), vjust = -0.3, size = 5) +
    labs(x = "Time of Day", y = "Number of Incidents", title = paste("Number of Incidents by
Time of Day at", airport_name, "Airport")) +
    theme_minimal() +
    scale_fill_brewer(palette="Pastell")

  # Calculate the percentage for the pie chart labels
  time_section_incidents$Percentage <- (time_section_incidents$Incidents /
sum(time_section_incidents$Incidents)) * 100

  # Pie chart with numbers and percentages
  pie_chart <- ggplot(time_section_incidents, aes(x = "", y = Incidents, fill = TimeOfDay)) +
    geom_bar(width = 1, stat = "identity") +
    coord_polar("y", start = 0) +

```

```

geom_text(aes(label = paste(Incidents, " (", round(Percentage, 1), "%)", sep = "")),
  position = position_stack(vjust = 0.5)) +
  labs(x = "", y = "", title = paste("Incident Distribution by Time of Day at", airport_name,
"Airport")) +
  theme_void() +
  scale_fill_brewer(palette="Pastell1")

# Print the bar chart and the pie chart
print(bar_chart)
print(pie_chart)
}

# Apply the function to LAX and SAC
create_time_section_plots(LAX_Event, "LAX")
create_time_section_plots(SAC_Event, "SAC")

# Comparison we made plot place in the same chart for easier comparison
# There are a lot of duplicates down, you can modify them.
# Function to Create Time Section Analysis Plots
create_time_section_plots <- function(data, airport_name) {
  # Count the number of incidents in each time section
  time_section_incidents <- data %>%
    group_by(TimeOfDay) %>%
    summarise(Incidents = n())

  # Create a bar chart
  bar_chart <- ggplot(time_section_incidents, aes(x = TimeOfDay, y = Incidents, fill =
TimeOfDay)) +
    geom_bar(stat = "identity") +
    geom_text(aes(label = Incidents, vjust = -0.3, size = 5) +
  labs(x = "Time of Day", y = "Number of Incidents", title = paste("Number of Incidents by
Time of Day at", airport_name, "Airport")) +
  theme_minimal() +
  scale_fill_brewer(palette="Pastell1")

  # Calculate the percentage for the pie chart labels
  time_section_incidents$Percentage <- (time_section_incidents$Incidents /
sum(time_section_incidents$Incidents)) * 100

  # Pie chart with numbers and percentages
  pie_chart <- ggplot(time_section_incidents, aes(x = "", y = Incidents, fill = TimeOfDay)) +
    geom_bar(width = 1, stat = "identity") +
    coord_polar("y", start = 0) +
    geom_text(aes(label = paste(Incidents, " (", round(Percentage, 1), "%)", sep = "")),
  position = position_stack(vjust = 0.5)) +
  labs(x = "", y = "", title = paste("Incident Distribution by Time of Day at", airport_name,
"Airport")) +
  theme_void() +
  scale_fill_brewer(palette="Pastell1")

  # Return the plots
  return(list(bar_chart = bar_chart, pie_chart = pie_chart))
}

# Apply the categorize_time function to LAX and SAC datasets
LAX_Event <- categorize_time(LAX_Event)
SAC_Event <- categorize_time(SAC_Event)

# Generate the plots for each airport
plots_LAX <- create_time_section_plots(LAX_Event, "LAX")
plots_SAC <- create_time_section_plots(SAC_Event, "SAC")

# Arrange the plots in a 2x2 grid
combined_plot <- grid.arrange(
  plots_SAC$bar_chart, plots_LAX$bar_chart,
  plots_SAC$pie_chart, plots_LAX$pie_chart,
  ncol = 2
)

##### Size Distribution #####
## There are small medium and large in the data
## There are also species in the data. you can do them in either way
## We used NA in this part
# Function to process and plot data
process_and_plot <- function(data, airport_name) {
  # Replace NA or empty entries with "Not Available"
  data$SIZE <- as.character(data$SIZE)
  data$SIZE[is.na(data$SIZE) | data$SIZE == "" ] <- "Not Available"

  # Convert back to factor with all levels
  data$SIZE <- factor(data$SIZE, levels = c("Small", "Medium", "Large", "Not Available"))

  # Count the number of incidents by wildlife size
  size_distribution <- data %>%
    group_by(SIZE) %>%
    summarise(Incidents = n())

  # Bar chart
  size_chart <- ggplot(size_distribution, aes(x = SIZE, y = Incidents, fill = SIZE)) +
    geom_bar(stat = "identity") +
    geom_text(aes(label = Incidents, vjust = -0.3, size = 5) +
  labs(x = "Wildlife Size Category", y = "Number of Incidents",
  title = paste("Number of Wildlife Incidents by Size Category at", airport_name)) +
  theme_minimal() +
  scale_fill_brewer(palette="Pastell1")

  # Percentage for pie chart labels
  size_distribution$Percentage <- (size_distribution$Incidents /
sum(size_distribution$Incidents)) * 100

  # Pie chart
  pie_chart <- ggplot(size_distribution, aes(x = "", y = Incidents, fill = SIZE)) +
    geom_bar(width = 1, stat = "identity") +
    coord_polar("y", start = 0) +
    geom_text(aes(label = paste(Incidents, " (", round(Percentage, 1), "%)", sep = "")),
  position = position_stack(vjust = 0.5)) +
  labs(x = "", y = "",
  title = paste("Wildlife Size Category Distribution at", airport_name)) +
  theme_void() +
  scale_fill_brewer(palette="Pastell1")

  # Print the charts
  list(BarChart = size_chart, PieChart = pie_chart)
}

# Process and plot for LAX
lax_charts <- process_and_plot(LAX_Event, "LAX")
lax_charts$BarChart
lax_charts$PieChart

# Process and plot for SAC
sac_charts <- process_and_plot(SAC_Event, "SAC")
sac_charts$BarChart
sac_charts$PieChart

##### Total number of incidents per month for LAX #####
## This is to provide operator with the understand of the distribution of

# Generate the charts for LAX and SAC
lax_charts <- process_and_plot(LAX_Event, "LAX")
sac_charts <- process_and_plot(SAC_Event, "SAC")

# Arrange the charts into a 2x2 grid
combined_chart <- grid.arrange(
  sac_charts$BarChart, lax_charts$BarChart,
  sac_charts$PieChart, lax_charts$PieChart,
  ncol = 2, nrow = 2
)

# Print the combined chart
combined_chart

# Percentage
# Function to create pie chart for a given dataset
create_pie_chart <- function(data, airport_name) {
  # Replace NA or empty entries with "Not Available"
  data$SIZE <- as.character(data$SIZE) | data$SIZE == "" ] <- "Not Available"
  data$SIZE <- factor(data$SIZE, levels = c("Small", "Medium", "Large", "Not Available"))

  # Count the number of incidents by wildlife size
  size_distribution <- data %>%
    group_by(SIZE) %>%
    summarise(Incidents = n())

  # Calculate the percentage for the pie chart labels
  size_distribution$Percentage <- (size_distribution$Incidents /
sum(size_distribution$Incidents)) * 100

  # Pie chart with numbers and percentages
  pie_chart <- ggplot(size_distribution, aes(x = "", y = Incidents, fill = SIZE)) +
    geom_bar(width = 1, stat = "identity") +
    coord_polar("y", start = 0) +
    geom_text(aes(label = paste(Incidents, " (", round(Percentage, 1), "%)", sep = "")),
  position = position_stack(vjust = 0.5)) +
  labs(x = "", y = "",
  title = paste("Wildlife Size Category Distribution at", airport_name)) +
  theme_void() +
  scale_fill_brewer(palette="Pastell1")

  return(pie_chart)
}

# Create pie chart for LAX
lax_pie_chart <- create_pie_chart(LAX_Event, "LAX")

# Create pie chart for SAC
sac_pie_chart <- create_pie_chart(SAC_Event, "SAC")

# Print the pie charts
lax_pie_chart
sac_pie_chart

##### Section 02 Event Categories #####
# Load required libraries
library(ggplot2)
library(dplyr)
library(gridExtra)

# In case the time slot is missing we did it again here.
# Function to categorize time into sections
categorize_time <- function(data) {
  data$TimeObj <- as.POSIXct(data$TIME, format = "%H:%M", tz = "UTC")
  data$TimeOfDay <- cut(data$TimeObj,
    breaks = c(as.POSIXct('00:00', format='%H:%M', tz='UTC'),
    as.POSIXct('06:00', format='%H:%M', tz='UTC'),
    as.POSIXct('12:00', format='%H:%M', tz='UTC'),
    as.POSIXct('18:00', format='%H:%M', tz='UTC'),
    as.POSIXct('23:59', format='%H:%M', tz='UTC')),
    labels = c("Midnight", "Morning", "Afternoon", "Evening"),
    include.lowest = TRUE)
  data <- data[!is.na(data$TimeOfDay), ]
  return(data)
}

# Function to create time and size distribution plots
create_time_size_plots <- function(data, airport_name) {
  # Count the number of incidents by wildlife size for each time of day
  size_time_distribution <- data %>%
    group_by(TimeOfDay, SIZE) %>%
    summarise(Incidents = n(), .groups = 'drop') %>%
    mutate(Percentage = (Incidents / sum(Incidents)) * 100)

  # Bar chart with size distribution for each time of day
  bar_chart_time_size <- ggplot(size_time_distribution, aes(x = SIZE, y = Incidents, fill =
SIZE)) +
    geom_bar(stat = "identity") +
    geom_text(aes(label = Incidents, vjust = -0.3, size = 3) +
  facet_wrap(~TimeOfDay, scales = "free.y") +
  labs(x = "Wildlife Size Category", y = "Number of Incidents",
  title = paste("Wildlife Size Distribution for Each Time of Day at", airport_name)) +
  theme_minimal() +
  scale_fill_brewer(palette="Pastell1")

  # Pie charts for each time of day
  pie_charts_time_size <- lapply(unique(size_time_distribution$TimeOfDay),
function(time_section) {
  data_section <- size_time_distribution[size_time_distribution$TimeOfDay == time_section, ]
  ggplot(data_section, aes(x = "", y = Incidents, fill = SIZE)) +
    geom_bar(width = 1, stat = "identity") +
    coord_polar("y", start = 0) +
    geom_text(aes(label = paste(Incidents, " (", round(Percentage, 1), "%)", sep = "")),
  position = position_stack(vjust = 0.5)) +
  labs(title = paste("Size Distribution at", airport_name, "-", time_section), x = "", y =
"")) +
  theme_void() +
  scale_fill_brewer(palette="Pastell1")
})

# Print the bar chart and arrange the individual pie charts
print(bar_chart_time_size)
do.call(grid.arrange, pie_charts_time_size)
}

# Apply the function to LAX and SAC datasets
LAX_Event <- categorize_time(LAX_Event)
SAC_Event <- categorize_time(SAC_Event)

```

```

## the incident every month
total_incidents_per_month_lax <- LAX_Event %>%
  group_by(INCIDENT_MONTH) %>%
  summarise(TotalIncidents = n())

# Function to calculate and plot time of day incidents
plot_time_of_day_incidents <- function(data, time_of_day, color, label) {
  incidents_per_month <- data %>%
    filter(TimeOfDay == time_of_day) %>%
    group_by(INCIDENT_MONTH) %>%
    summarise(Incidents = n())

# Merge with total incidents to calculate the percentage
percentage_incidents <- merge(total_incidents_per_month_lax, incidents_per_month, by =
"INCIDENT_MONTH", all = TRUE)
percentage_incidents$Incidents[is.na(percentage_incidents$Incidents)] <- 0
percentage_incidents$Percentage <- (percentage_incidents$Incidents /
percentage_incidents$TotalIncidents)

# Plot the percentages by month as a line plot
percentage_plot <- ggplot(percentage_incidents, aes(x = INCIDENT_MONTH, y = Percentage)) +
  geom_line(group=1, colour=colour) +
  geom_point(colour=colour) +
  scale_x_continuous(breaks = 1:12, labels = month.abb) +
  labs(x = "Month", y = "Percentage", title = paste("Percentage of Incidents in the", label,
"by Month at LAX")) +
  theme_minimal()

return(percentage_plot)
}

# Plot for each time of day for LAX
midnight_plot_lax <- plot_time_of_day_incidents(LAX_Event, "Midnight", "blue", "Midnight")
morning_plot_lax <- plot_time_of_day_incidents(LAX_Event, "Morning", "green", "Morning")
afternoon_plot_lax <- plot_time_of_day_incidents(LAX_Event, "Afternoon", "orange", "Afternoon")
evening_plot_lax <- plot_time_of_day_incidents(LAX_Event, "Evening", "purple", "Evening")

# Print the plots
midnight_plot_lax
morning_plot_lax
afternoon_plot_lax
evening_plot_lax

# Function to calculate percentages for a given time of day for LAX
calculate_percentages_lax <- function(data, time_of_day, color) {
  incidents_per_month <- data %>%
    filter(TimeOfDay == time_of_day) %>%
    group_by(INCIDENT_MONTH) %>%
    summarise(Count = n()) %>%
    merge(total_incidents_per_month_lax, by = "INCIDENT_MONTH", all = TRUE) %>%
    mutate(Percentage = Count / TotalIncidents,
           TimeOfDay = time_of_day,
           Color = color)

# Replace NA with 0
incidents_per_month$Count[is.na(incidents_per_month$Count)] <- 0
incidents_per_month$Percentage[is.na(incidents_per_month$Percentage)] <- 0

return(incidents_per_month)
}

# Calculate percentages for each time of day for LAX
midnight_data_lax <- calculate_percentages_lax(LAX_Event, "Midnight", "blue")
morning_data_lax <- calculate_percentages_lax(LAX_Event, "Morning", "green")
afternoon_data_lax <- calculate_percentages_lax(LAX_Event, "Afternoon", "orange")
evening_data_lax <- calculate_percentages_lax(LAX_Event, "Evening", "purple")

# Combine all data into one dataframe
combined_data_lax <- rbind(midnight_data_lax, morning_data_lax, afternoon_data_lax,
evening_data_lax)

# Create one combined line plot for LAX
combined_line_plot_lax <- ggplot(combined_data_lax, aes(x = INCIDENT_MONTH, y = Percentage, group
= TimeOfDay, color = TimeOfDay)) +
  geom_line() +
  geom_point() +
  geom_text(aes(label = round(Percentage, 2)), vjust = -1, size = 3) +
  scale_x_continuous(breaks = 1:12, labels = month.abb) +
  labs(x = "Month", y = "Percentage of Incidents",
       title = "Combined Percentage of Incidents by Time of Day and Month at LAX") +
  theme_minimal() +
  scale_color_manual(values = c("Midnight" = "blue", "Morning" = "green", "Afternoon" = "orange",
"Evening" = "purple"))

# Print the combined line plot for LAX
combined_line_plot_lax

##### Total number of incidents per month for SAC #####
## Basically it is the same as LAX
# Total number of incidents per month for SAC
total_incidents_per_month_sac <- SAC_Event %>%
  group_by(INCIDENT_MONTH) %>%
  summarise(TotalIncidents = n())

# Function to calculate percentages for a given time of day for SAC
calculate_percentages_sac <- function(data, time_of_day, color) {
  incidents_per_month <- data %>%
    filter(TimeOfDay == time_of_day) %>%
    group_by(INCIDENT_MONTH) %>%
    summarise(Count = n()) %>%
    merge(total_incidents_per_month_sac, by = "INCIDENT_MONTH", all = TRUE) %>%
    mutate(Percentage = Count / TotalIncidents,
           TimeOfDay = time_of_day,
           Color = color)

# Replace NA with 0
incidents_per_month$Count[is.na(incidents_per_month$Count)] <- 0
incidents_per_month$Percentage[is.na(incidents_per_month$Percentage)] <- 0

return(incidents_per_month)
}

# Calculate percentages for each time of day for SAC
midnight_data_sac <- calculate_percentages_sac(SAC_Event, "Midnight", "blue")
morning_data_sac <- calculate_percentages_sac(SAC_Event, "Morning", "green")
afternoon_data_sac <- calculate_percentages_sac(SAC_Event, "Afternoon", "orange")
evening_data_sac <- calculate_percentages_sac(SAC_Event, "Evening", "purple")

# Combine all data into one dataframe
combined_data_sac <- rbind(midnight_data_sac, morning_data_sac, afternoon_data_sac,
evening_data_sac)

# Create one combined line plot for SAC
combined_line_plot_sac <- ggplot(combined_data_sac, aes(x = INCIDENT_MONTH, y = Percentage, group
= TimeOfDay, color = TimeOfDay)) +
  geom_line() +
  geom_point() +
  geom_text(aes(label = round(Percentage, 2)), vjust = -1, size = 3) +
  scale_x_continuous(breaks = 1:12, labels = month.abb) +
  labs(x = "Month", y = "Percentage of Incidents",
       title = "Combined Percentage of Incidents by Time of Day and Month at SAC") +
  theme_minimal() +
  scale_color_manual(values = c("Midnight" = "blue", "Morning" = "green", "Afternoon" = "orange",
"Evening" = "purple"))

# Print the combined line plot for SAC
combined_line_plot_sac

# GitHub: hf2014
# This Code focus on LAX and SAC.

# Packages
library(shiny)
library(ggplot2)
library(dplyr)
library(lubridate)
library(plotly)

# UI Set up
ui <- fluidPage(
  titlePanel("Wildlife Strikes - Risk Analysis"),
  sidebarLayout(
    sidebarPanel(
      selectInput("airportInput", "Select Airport:", choices = c("SAC", "LAX")),
      selectInput("monthInput", "Select Month:", choices = setNames(1:12, month.abb))
    ),
    mainPanel(
      plotlyOutput("timeOfDayPlot"),
      HTML("<strong>Risk score = Frequency x Severity</strong><br/>
Severity: Small = 1, Medium = 2, Large = 3<br/>
NA values are excluded from the analysis.")
    )
  )
)

# Server Set up
server <- function(input, output, session) {

# Reactive expression for the data filtered by the selected airport and month
# Same as the paper we did SAC and LAX
# Can also be used in other airport
filtered_data <- reactive({
  airport_data <- switch(input$airportInput,
    "SAC" = SAC_Event,
    "LAX" = LAX_Event)

# Clean out Not Available for sizes
processed_data <- airport_data %>%
  filter(!is.na(SIZE), SIZE %in% c('Small', 'Medium', 'Large'),
         INCIDENT_MONTH == as.integer(input$monthInput))

processed_data
})

# Generate the bar chart based on the filtered data
output$timeOfDayPlot <- renderPlotly({
  data <- filtered_data()

  if (nrow(data) == 0) {
    return()
  }

# Calculate the risk score and determine the risk color
size_risk <- data %>%
  group_by(SIZE) %>%
  summarise(Frequency = n(), .groups = 'drop') %>%
  mutate(
    Score = case_when(
      SIZE == 'Small' ~ 1,
      SIZE == 'Medium' ~ 2,
      SIZE == 'Large' ~ 3
    ),
    RiskScore = Frequency * Score
  ) %>%
  arrange(desc(RiskScore))

# Add the risk color outside of the mutate function
size_risk$RiskColor <- with(size_risk, case_when(
  RiskScore <= 50 ~ 'Low',
  RiskScore > 50 & RiskScore <= 100 ~ 'Moderate',
  RiskScore > 100 ~ 'High'
))

# Plot the data with the correct colors for the risk levels
p <- ggplot(size_risk, aes(x = SIZE, y = RiskScore, fill = RiskColor, text = paste("Frequency:
", Frequency, "\nSeverity: ", Score, "\nRisk Score: ", RiskScore))) +
  geom_bar(stat = "identity") +
  scale_fill_manual(values = c('Low' = 'green', 'Moderate' = 'yellow', 'High' = 'red')) +
  labs(title = paste("Risk Analysis of Wildlife Strikes by Size at", input$airportInput,
"Airport for Each Month"),
       x = "Wildlife Size", y = "Risk Score") +
  theme_minimal()

ggplotly(p, tooltip = "text") # Enable tooltips
})

# Run the Shiny app
shinyApp(ui = ui, server = server)

### Notes: This is just three levels of risk matrix, total flight is not used.
### Please follow us for the update.

```

## Appendix II Code of Shiny.io Website